INOTROPIC ACTIONS OF PHENAMIL

AN EPITHELIAL SODIUM CHANNEL BLOCKER

BY

ANTONIO GUIA

A Thesis
Submitted to the Faculty of Graduate Studies
in Partial Fulfillment of the Requirements
for the Degree of

DOCTOR OF PHILOSOPHY

Department of Pharmacology and Therapeutics
University of Manitoba
Winnipeg, Manitoba

ISBN 0-612-13159-9

Name Antonio Guia

Dissertation Abstracts International is arranged by broad, general subject categories. Please select the one subject which most nearly describes the content of your dissertation. Enter the corresponding four-digit code in the spaces provided.

Pharmacology

SUBJECT TERM

0	4	1	9

SUBJECT CODE

U·M·I

Subject Categories

THE HUMANITIES AND SOCIAL SCIENCES

COMMUNICATIONS AND THE ARTS
Architecture 0729
Art History 0377
Cinema 0900
Dance 0378
Fine Arts 0357
Information Science 0723
Journalism 0391
Library Science 0399
Mass Communications 0708
Music 0413
Speech Communication 0459
Theater 0465

EDUCATION
General 0515
Administration 0514
Adult and Continuing 0516
Agricultural 0517
Art 0273
Bilingual and Multicultural 0282
Business 0688
Community College 0275
Curriculum and Instruction 0727
Early Childhood 0518
Elementary 0524
Finance 0277
Guidance and Counseling 0519
Health 0680
Higher 0745
History of 0520
Home Economics 0278
Industrial 0521
Language and Literature 0279
Mathematics 0280
Music 0522
Philosophy of 0998
Physical 0523
Psychology 0525
Reading 0535
Religious 0527
Sciences 0714
Secondary 0533
Social Sciences 0534
Sociology of 0340
Special 0529
Teacher Training 0530
Technology 0710
Tests and Measurements 0288
Vocational 0747

LANGUAGE, LITERATURE AND LINGUISTICS
Language
- General 0679
- Ancient 0289
- Linguistics 0290
- Modern 0291

Literature
- General 0401
- Classical 0294
- Comparative 0295
- Medieval 0297
- Modern 0298
- African 0316
- American 0591
- Asian 0305
- Canadian (English) 0352
- Canadian (French) 0355
- English 0593
- Germanic 0311
- Latin American 0312
- Middle Eastern 0315
- Romance 0313
- Slavic and East European 0314

PHILOSOPHY, RELIGION AND THEOLOGY
Philosophy 0422
Religion
- General 0318
- Biblical Studies 0321
- Clergy 0319
- History of 0320
- Philosophy of 0322

Theology 0469

SOCIAL SCIENCES
American Studies 0323
Anthropology
- Archaeology 0324
- Cultural 0326
- Physical 0327

Business Administration
- General 0310
- Accounting 0272
- Banking 0770
- Management 0454
- Marketing 0338

Canadian Studies 0385
Economics
- General 0501
- Agricultural 0503
- Commerce-Business 0505
- Finance 0508
- History 0509
- Labor 0510
- Theory 0511

Folklore 0358
Geography 0366
Gerontology 0351
History
- General 0578
- Ancient 0579
- Medieval 0581
- Modern 0582
- Black 0328
- African 0331
- Asia, Australia and Oceania 0332
- Canadian 0334
- European 0335
- Latin American 0336
- Middle Eastern 0333
- United States 0337

History of Science 0585
Law 0398
Political Science
- General 0615
- International Law and Relations 0616
- Public Administration 0617

Recreation 0814
Social Work 0452
Sociology
- General 0626
- Criminology and Penology 0627
- Demography 0938
- Ethnic and Racial Studies 0631
- Individual and Family Studies 0628
- Industrial and Labor Relations 0629
- Public and Social Welfare 0630
- Social Structure and Development 0700
- Theory and Methods 0344

Transportation 0709
Urban and Regional Planning 0999
Women's Studies 0453

THE SCIENCES AND ENGINEERING

BIOLOGICAL SCIENCES
Agriculture
- General 0473
- Agronomy 0285
- Animal Culture and Nutrition 0475
- Animal Pathology 0476
- Food Science and Technology 0359
- Forestry and Wildlife 0478
- Plant Culture 0479
- Plant Pathology 0480
- Plant Physiology 0817
- Range Management 0777
- Wood Technology 0746

Biology
- General 0306
- Anatomy 0287
- Biostatistics 0308
- Botany 0309
- Cell 0379
- Ecology 0329
- Entomology 0353
- Genetics 0369
- Limnology 0793
- Microbiology 0410
- Molecular 0307
- Neuroscience 0317
- Oceanography 0416
- Physiology 0433
- Radiation 0821
- Veterinary Science 0778
- Zoology 0472

Biophysics
- General 0786
- Medical 0760

EARTH SCIENCES
Biogeochemistry 0425
Geochemistry 0996
Geodesy 0370
Geology 0372
Geophysics 0373
Hydrology 0388
Mineralogy 0411
Paleobotany 0345
Paleoecology 0426
Paleontology 0418
Paleozoology 0985
Palynology 0427
Physical Geography 0368
Physical Oceanography 0415

HEALTH AND ENVIRONMENTAL SCIENCES
Environmental Sciences 0768
Health Sciences
- General 0566
- Audiology 0300
- Chemotherapy 0992
- Dentistry 0567
- Education 0350
- Hospital Management 0769
- Human Development 0758
- Immunology 0982
- Medicine and Surgery 0564
- Mental Health 0347
- Nursing 0569
- Nutrition 0570
- Obstetrics and Gynecology 0380
- Occupational Health and Therapy 0354
- Ophthalmology 0381
- Pathology 0571
- Pharmacology 0419
- Pharmacy 0572
- Physical Therapy 0382
- Public Health 0573
- Radiology 0574
- Recreation 0575
- Speech Pathology 0460
- Toxicology 0383

Home Economics 0386

PHYSICAL SCIENCES
Pure Sciences
Chemistry
- General 0485
- Agricultural 0749
- Analytical 0486
- Biochemistry 0487
- Inorganic 0488
- Nuclear 0738
- Organic 0490
- Pharmaceutical 0491
- Physical 0494
- Polymer 0495
- Radiation 0754

Mathematics 0405
Physics
- General 0605
- Acoustics 0986
- Astronomy and Astrophysics 0606
- Atmospheric Science 0608
- Atomic 0748
- Electronics and Electricity 0607
- Elementary Particles and High Energy 0798
- Fluid and Plasma 0759
- Molecular 0609
- Nuclear 0610
- Optics 0752
- Radiation 0756
- Solid State 0611

Statistics 0463

Applied Sciences
Applied Mechanics 0346
Computer Science 0984
Engineering
- General 0537
- Aerospace 0538
- Agricultural 0539
- Automotive 0540
- Biomedical 0541
- Chemical 0542
- Civil 0543
- Electronics and Electrical 0544
- Heat and Thermodynamics 0348
- Hydraulic 0545
- Industrial 0546
- Marine 0547
- Materials Science 0794
- Mechanical 0548
- Metallurgy 0743
- Mining 0551
- Nuclear 0552
- Packaging 0549
- Petroleum 0765
- Sanitary and Municipal 0554
- System Science 0790

Geotechnology 0428
Operations Research 0796
Plastics Technology 0795
Textile Technology 0994

PSYCHOLOGY
General 0621
Behavioral 0384
Clinical 0622
Developmental 0620
Experimental 0623
Industrial 0624
Personality 0625
Physiological 0989
Psychobiology 0349
Psychometrics 0632
Social 0451

INOTROPIC ACTIONS OF PHENAMIL

AN EPITHELIAL SODIUM CHANNEL BLOCKER

BY

ANTONIO GUIA

A Thesis submitted to the Faculty of Graduate Studies of the University of Manitoba in partial fulfillment of the requirements of the degree of

DOCTOR OF PHILOSOPHY

Em homenagem ao meu sobrinho,
Dr. António José Guerreiro Guia

Tó-Zé. Neste feliz período da tua vida, cumpre-me o dever de expressar a minha grande admiração e apreço pelo brilhante exame da tua graduação, o que nos encheu de grande satisfação, pela maneira descontraída e pronta com que sempre usaste responder a todas as perguntas que te eram dirigidas, mostrando a grande capacidade duma preparação bem cuidada e eficaz para um excelente exame. Obrigado Tó-Zé, por seres tu o primeiro doutor da nossa geração mais próxima. Todos os teus familiares estão de paragens, e todas as pessoas que te estimam. As tuas qualidades pessoais tão distintas bem lhe assenta tão nobre profissão, oxalá o destino te reserve grandes sucessos. Todo o teu sacrifício bem merece o prazer com que nos contagias a todos nós, os muitos anos de estudo, as muitas horas diárias esse grande desejo de realizar o teu sonho te fez afastar dos divertimentos próprios da tua idade tendo sempre em vista o fim a alcançar. Valeu a pena Tó-Zé, o teu sacrifício, valeu a vitoria, que ambicionas-te hoje é motivo de orgulho para todos nós e para ti principalmente, o prémio do teu trabalho. Obrigado senhor doutor António J.G. Guia.

-José Guerreiro Raposo

Ao meu sobrinho e amigo
Venho prestar homenagem
E me sinto Muito honrado,
Acabou o teu castigo
Essa dura aprendizagem
Dum brilhante doutorado.

Hoje es um homem feliz
Por teres realizado
Um sonho da tua vida,
Que nasceu em ti em petiz
E agora que estas formado
É recompensa merecida.

Ingressas-te na Universidade
Cheio de fé e vontade
No curso que preferiste,
Hoje te sentes satisfeito
Por tudo o que já tens feito
No caminho que seguiste.

Quase todos os teus descendentes
Tem vindo a ser doentes
De doenças do coração,
E já porque assim tem sido
Te levou a teres escolhido
essa tão nobre missão.

Darás por bem empregado
O tempo de teres estudado
Se um dia tiveres a sorte,
Que agradável recompensa
Puderes curar a doença
Que hoje causa tanta morte.

Já tanto se tem estudado
Muito se tem avançado
Mas muito mais ha para fazer,
Nessa luta que não cansa
Tenham a fé e esperança
De que um dia Há de vencer.

Mal me ficaria min
Neste memorável dia
Senão escrevesse por fim
Para ti uma poesia.

-O Tio,
-J.G.R., Aug., 1995.

This thesis is in honor of those who never had the opportunity

and especially in honor of those who have granted me this opportunity.

They are the same: my family.

ACKNOWLEDGMENTS

I am indebted to many people who have made this work possible. In particular Dr. Ratna Bose who always had so many interesting and useful suggestions as to leave my head spinning. I eventually came to understand the suggestions. I thank her for her patience as well as for her occasional lack of patience.

Drs. Deepak Bose and Normand Leblanc have also provided me with a small sample of their learning; it is to me a great deal of knowledge. I gratefully acknowledge the excellent technical assistance of the following people: Krika Duke for assisting in the execution of *in vivo* dog experiments; Shubra Sharma and Jenny Yu for assisting with smooth muscle *in vitro* preparations; Christopher Fyfe for assisting with the preparation of solutions and with microelectrode experiments; Pak Leung, Yijing Chen and Marie-Andrée Lupien for technical assistance in the preparation of cardiac myocytes. Thanks go out as well to those who have shared their animals and ours in an attempt to spare the lives of many animals, or at least to spare my own conscience. Teresa Chau deserves special mention for her excellent technical assistance with cardiac tension preparations and with microelectrode experiments, and especially for lending some of her skill and experience to my learning. Her enthusiasm will not be forgotten. Finally none of this work would have been accomplished without the funding awarded from the following organizations: Canadian Heart and Stroke Foundation, Manitoba Health Research Council, Medical Research Council of Canada, Canadian Lung Association, and the department of Pharmacology, Therapeutics of the University of Manitoba, and occasionally the "Barbara Guia fund".

Finally, the patience of friends and family deserves mention, if at least for just putting up with my dinner-time conversation.

My inspiration came from Barbara Guia, my mother, for, among many other things, teaching me to not give up: she always wanted to get a university degree, she started while in her 40's and got her degree 7 years ago! I hope to have at least a portion of her determination at that age. Never say never.

SUMMARY

Phenamil, an amiloride derivative, is 17 times more potent than the parent compound in inhibiting epithelial type sodium channels in gut epithelia. Epithelial sodium channel blockers have been found to relax smooth muscle. Phenamil is a potent relaxant of smooth muscle strips. In contrast, it was found to be a cardiac stimulant in canine ventricular trabeculae (EC_{50}=59 μM). Cardiac tissue does not contain epithelial type sodium channels, hence the positive inotropy is due to the unmasking of other effects of phenamil. A knowledge of these other effects will further elucidate the pharmacological profile of phenamil. The mechanism of phenamil-induced positive inotropy was determined through mechanical and electrophysiological studies in cardiac tissue from dog, rat, and guinea pig. Phenamil produced a prolongation of the twitch duration, which was accompanied by a prolongation of the action potential. The sarcoplasmic reticulum of cardiac tissue may be compromized by the presence of cyclopiazonic acid, which inhibits calcium uptake into the longitudinal tubules, or ryanodine, which prevents calcium accumulation into the transverse tubules. Positive inotropy by phenamil is not abolished by compromising the sarcoplasmic reticulum hence calcium uptake, storage, or release from the sarcoplasmic reticulum are not affected. In voltage clamp experiments, the prolongation of the action potential was shown to be due to inhibition of the inwardly rectifying potassium current. Neither of the calcium entry pathways through the

sarcolemma (calcium channels or sodium-calcium exchange) were significantly affected by phenamil, however in biphasic experiments we found that positive inotropy is the result of interference with a sarcolemmal event. The prolongation of the action potential occurrs specifically during phase 3. During this stage the forward mode of sodium-calcium exchange is driven by the membrane potential to remove calcium from the cytosol. It is concluded that the inhibition of the inwardly rectifying potassium current by phenamil results in depolarization of the terminal part of the action potential, thereby reducing the driving force for the forward mode of sodium-calcium exchange. The reduced activity of the sodium-calcium exchanger slows the extrusion of calcium from the cell at the end of the action potential, slowing the twitch duration and causing a gradual development of positive inotropy.

TABLE OF CONTENTS

LIST OF FIGURES AND TABLES

LIST OF ABBREVIATIONS

4AP	4-aminopyridine
APD	Action potential duration.
BCECF	2',7'-bis(carboxyethyl)-5,6-carboxyfluorescein
BCECF-AM	2',7'-bis(carboxyethyl)-5,6-carboxyfluorescein acetoxy methyl ester
CBDMB	5-(4-chlorobenzyl)-2',4'-dimethylbenzamil
CPA	Cyclopiazonic acid
DCB	3',4'-dichlorobenzamil
DMSO	dimethyl sulfoxide
EGTA	Ethylene glycol tetraacetic acid
EIPA	5-(N-ethyl-N-isopropyl)-amiloride
FI_{440}	Fluorescent Intensity with 440 nm excitation, 540 nm emission
FI_{500}	Fluorescent Intensity with 500 nm excitation, 540 nm emission
HEPES	6-N-2-hydroxyethylpiperazine-N'-2-ethanesulfonic acid

HP	Holding potential
I_{CaL}	L-type calcium current
I_K	Outwardly rectifying potassium current
I_{K1}	Inwardly rectifying potassium current
P1	First phase of a biphasic contraction
P2	second phase of a biphasic contraction
pH_i	cytosolic pH
pH_o	pH of bathing medium
PRC	Post-rest contraction(s)
RCC	Rapid Cooling Contracture
RMP	Resting membrane potential
SR	Sarcoplasmic reticulum

INTRODUCTION

PREAMBLE

At the start of my research in Dr. Ratna Bose's laboratory my initial mission was to assess the effectiveness of amiloride in relaxing tracheal smooth muscle (Guia and Bose, 1990) in an animal model of asthma (Kepron, *et al*, 1977). We showed that amiloride is useful in reducing airway resistance in *in vivo* allergic reactions of the airway (Yu *et al*, 1993) and that it relaxes tracheal smooth muscle strips contracted with the antigen or with histamine. At about the same time a long-term study commenced in North Carolina based on work done by Knowles and coworkers (Waltner *et al*, 1987; Henkin, 1990; Gallo, 1990; Knowles *et al*, 1990). The studies were quite promising with the finding that in children with cystic fibrosis the amiloride-induced inhibition of sodium channels in the lung epithelium will also prevent the accumulation of chloride from the lung fluids. This results in an osmotic dilution of the lung fluids so that these can be more easily mobilized resulting in reduced airway blockade (Collins, 1992). In future, amiloride or a mixture containing amiloride may prove to be a valuable agent for the therapy of cystic fibrosis, and its smooth muscle relaxant effect may prove to be useful in the management of obstructive lung disorders.

Amiloride affects many cell membrane events including several ion channels, and some intracellular enzymes (as reviewed in Kleyman and Cragoe, 1988). Phenamil is relatively more potent and specific than amiloride for inhibiting the epithelial sodium channels. This indicates that phenamil may be better than amiloride in reducing airway resistance and in mobilizing lung fluids. This knowledge and the experiments ongoing in the laboratory led to my interest in phenamil.

The potency of phenamil for inhibiting epithelial-type sodium channels makes it difficult to study the pharmacological profile of this drug in tissues that contain this type of channel. Adult cardiac muscle contains many channels that are found in smooth muscle and in endothelium. However it has not been shown to express epithelial type sodium channels. In order to address the specificity of phenamil and further elucidate its pharmacological profile, I chose to work with cardiac tissue in the hope to unmask any other effect(s) of phenamil, unrelated to inhibition of sodium channels. Interestingly, I found that in spite of it being a potent smooth muscle relaxant, in cardiac tissue it is a positive inotrope. This initiated the work to be presented in this thesis.

AMILORIDE

Amiloride is used clinically as a mild, potassium-sparing diuretic (Weiner and Mudge, 1985). Inhibition of epithelial-type sodium channels has been observed in the various tissues, for example: amphibian epithelium, human and rabbit kidneys, toad and turtle urinary bladder (reviewed in Benos, 1982; Benos, 1988). The pharmacological

profiles of this drug and many of its analogs were extensively studied in the 1980's. In addition to sodium channels, amiloride has been shown to also inhibit a variety of other cell membrane-linked processes, namely sodium-calcium exchange, sodium-hydrogen exchange, calcium channels, sodium pump, and potassium channels. This variety of processes modulated by amiloride reduces its usefulness as a pharmacological tool when the objective is to use it as a specific compound to inhibit a sodium-dependent process.

THE ANALOGS AND THEIR SELECTIVITY

Considering the obvious overlap of the effects of amiloride on various membrane events, it is preferable to use the more selective analogs of amiloride as tools for the study of specific membrane events. The relative specificities of the derivatives on membrane ionic channels and other cellular events are reviewed in detail by Kleyman and Cragoe (1988). The majority of the amiloride derivatives can be divided roughly into three categories: sodium channel blockers, sodium-calcium exchanger blockers, and sodium-hydrogen exchanger blockers. The more specific derivatives in each of these categories are: phenamil for inhibiting sodium channels, 5-(4-chlorobenzyl)-2',4'-dimethylbenzamil (CBDMB) for inhibiting sodium-calcium exchange, and 5-(N-ethyl-N-isopropyl)-amiloride (EIPA) or 5-(N-methyl-N-guanidocarbonylmethyl)amiloride (MGCMA) for inhibiting sodium-hydrogen exchange. The more commonly used compounds are listed in table 1 with their specificities for the three processes. This table is limited to only these three classes of action and intentionally does not attempt to include all possible effects of these compounds since they are not the main focus of this study.

Table 1: K_d for analogs of amiloride[1]

Drug	Na-H exchange	Na-Ca exchange	Na channels
Amiloride	83.8	1100	0.34
Phenamil	>500	>400[3]	0.020[1,2]
CBDMB	>500	7.3	>400
DCB	>400	29	0.085
HMA	0.16	100	>400
EIPA	0.05-0.38	130	>400
MGCMA	1.35	1600	>400

Data expressed in μM, extracted from [1]Kleyman and Cragoe, 1988, [2]Armstrong *et al*, 1992; [3]Frelin *et al*, 1988.

The sodium-hydrogen exchange inhibitors have better selectivity for the sodium-hydrogen exchanger than for the other two transport processes. Many studies have used and continue to use 3',4'-dichlorobenzamil (DCB) to inhibit sodium-calcium exchange (e.g.: Harrison and Lancaster, 1994). Unfortunately this compound is a better inhibitor of sodium channels (50% inhibition with 29 μM for sodium-calcium exchange, and 0.085 μM for sodium channels, Kleyman and Cragoe, 1988). In cardiac tissue it has also been shown to interfere with SR calcium ATP-ase, sodium pump, cAMP-dependent phosphodiesterase, voltage-gated calcium channels, and mitochondrial oxidative phosphorylation in the same or lower concentration range as that which inhibits sodium-calcium exchange (Floreani *et al*, 1987; Bielefeld *et al*, 1986). Its isomer, 2',4'-dichloro-

benzamil, different only in the position of the chlorine atoms, is a more potent inhibitor of sodium-calcium exchange (12 μM for sodium-calcium exchange, and 0.136 μM for sodium channels) than DCB. It also has a greater affinity for sodium channels. Several compounds that are potent inhibitors of sodium-calcium exchange are more specific for sodium channel inhibition. CBDMB is chemically similar to DCB but with an aryl group on the pyrazine ring, conferring specificity for inhibiting the sodium-calcium exchanger. This indicates a role of the charged guanyl nitrogen in the inhibition of sodium channels (see figure 4). In fact it is believed that the charged portion of the molecule is involved in the inhibition of channels by inserting into a sodium binding site (Cuthbert and Shum, 1976; Rossier *et al*, 1994). On the other hand, phenamil is much more potent than amiloride in inhibiting sodium channels, yet it is very hydrophobic at physiological pH, implying that the charged form of the molecule is not necessary for inhibiting sodium channels. It has also been proposed that amiloride acts at an allosteric site on the channel (Benos, 1982).

Phenamil is a lipophilic amiloride derivative which is a very potent and selective sodium channel blocker in epithelial cells. Since phenamil blocks epithelial sodium channels in the nanomolar range, it has proven useful in the isolation and purification of renal epithelial-type sodium channels (Benos *et al*, 1986; Benos *et al*, 1987; Barbry *et al*, 1990; Frelin *et al*, 1988). The potency of phenamil for inhibiting sodium channels has been misquoted a few times in the literature (3 nM, Raijman *et al*, 1992; 86 nM, Schiffman *et al*, 1990). Concentrations in the range of 20 to 30 nM phenamil produce 50% inhibition of the epithelial type sodium channels (Vigne *et al*, 1989). Although binding

studies in thyroid cells show 50% specific binding by phenamil with 20 nM (Verrier *et al*, 1989), in other cell types specific binding studies have shown binding to membrane proteins that are not sodium dependent (Goldstein *et al*, 1993). This sodium independent protein is believed to be diamine oxidase (Lingueglia *et al*, 1993; Chassande *et al*, 1994). Functional studies have shown that phenamil inhibits diamine oxidase in kidney epithelium at similar concentrations to those required for inhibiting epithelial sodium channels (Kd = 47 nM, Novotny *et al*, 1994). This same study also showed inhibition of diamine oxidase by amiloride (Kd = 5.1 μM), and by EIPA (Kd = 1.75 μM). These concentrations do not correlate with the concentrations required for inhibiting epithelial type sodium channels, hence inhibition of diamine oxidase by phenamil is independent of sodium channel inhibition. Much higher concentrations of phenamil are required to inhibit cardiac or epithelial sodium-hydrogen and sodium-calcium exchangers (K_I>500 μM and K_I=200 μM, respectively; reviewed in Kleyman and Cragoe, 1988). As compared to amiloride, phenamil is 17 times more potent in blocking sodium channels in the epithelium (Kleyman and Cragoe, 1988). Since phenamil is a potent blocker of slow sodium channels, it's effects on other membrane channels may be masked in tissues containing slow sodium channels.

EPITHELIAL-TYPE SODIUM CHANNELS

Epithelial-type sodium channels (reviewed in Smith and Benos, 1991; Palmer, 1992; Horisberger *et al*, 1993; Garty, 1994) have voltage-independent gating. These are

receptor-operated channels (e.g., controlled by aldosterone, vasopressin, cAMP, ANP, G-proteins, protein kinase C, sodium, calcium, pH_i, etc.) that allow passage of small monovalent cations (Na^+, Li^+, K^+, H^+). The relative permeabilities of sodium and potassium depend on the tissue and species and can vary from 2 to 19 times greater permeability for sodium than for potassium ions. The channel density and distribution on the cell membrane also depends on tissue type and species, ranging from 130 to 400 sites/μm^2. The distribution or density can vary within a cell or within a tissue (e.g.: renal cells have more sodium channels on the apical cell membrane, and it is believed that many cells in lung epithelium have very low channel densities while others within the same tissue have high channel densities).

These ion channels were originally separated into two groups: high affinity amiloride-sensitive sodium channels, and low affinity amiloride-sensitive sodium channels. High affinity sodium channels are inhibited by less than 1 μM amiloride but are not inhibited by EIPA. The high affinity epithelial sodium channel has been isolated from a toad kidney cell line revealing a 700 KD heteromultimeric protein (Sariban-Sohraby and Benos, 1986; Oh and Benos, 1993; Benos *et al*, 1987). Covalent bonds of this protein were reduced to produce 5 proteins with molecular weights of 315, 150, 95, 71, 55, and 40KD (Benos *et al*, 1987). The 150KD protein appears to be sufficient for sodium transport. The 95KD segment is believed to be linked to a G-protein and the 71KD segment contains the aldosterone receptor. The three larger segments are glycosylated. The three smaller segments are believed to be proteolytic products (71 and 55KD from the 150KD segment, and 40KD from the 95KD segment). Single channel conductance for

these channels varies from 4pS to 28pS. Highly sodium-selective channels have lower single channel conductance (reviewed in Rossier *et al*, 1994).

A high affinity sodium channel has recently been sequenced. The channel's sequence reveals that the epithelial sodium channels form part of a gene superfamily that includes other monovalent cation channels such as the P_{2X} receptor, channels involved in mechanosensitivity and neurodegeneration in *C. elegans*, voltage-gated potassium channels, epithelial K channels, inwardly rectifying potassium channels (MB-IRK1, MB-IRK2), and cyclic nucleotide-gated cation channels (Ashford *et al*, 1994; Driscoll, 1992; Takahashi *et al*, 1994; Valera *et al*, 1994; Wible *et al*, 1995; Zhou *et al*, 1994). The channel is a polymer of three units: α (79KD, Canessa *et al*, 1993), β (72KD), and γ (75KD) (Rossier *et al*, 1994). The subunits share 35% homology and span the plasma membrane twice with both terminals in the cytoplasmic side (see figure 1). The α subunit is glycosylated at 4 to 6 sites on the large (400 residues) extracellular loop. Due to homology between subunits, it is likely that the other two subunits are glycosylated similarly.

Amiloride has been shown to inhibit sodium-permitting channels that are activated by glutamate in neurons under certain diseased states and thereby reduce the amount of calcium entering through sodium-calcium exchange (Guiramand *et al*, 1991; Stys *et al*, 1991). It is possible that these non-specific cation channels may be of the P2X type as has been shown in pheochromocytoma PC12 cells (Brake *et al*, 1994), rat vas deferens

A

```
001                                                  050
MMLDHTRAPELNIDLDLHASNSPKGSMKGNQFKEQDPCPPQPMQGLGKGD  α
.....................................MPVKKYLLKC  β
.....................................MAPGEKIKAKI  γ

051                                                  100
KREEQGLGPEPSAPRQPTEEEEALIEFHRSYRELFQFFCNNTTIHGAIRL  α
LHRLQ.KGP.GYT.................YKELLVWYCNNTNTHGPKRI  β
KKNLPVRGPQAPT.................IKDLMHWYCMNTNTHGCRRI  γ

101                                                  150
VCSKHNRMKTAFWAVLWLCTFGMMYWQFALLFEEYLSYPVSLNINLNSDK  α
.ICE.GPKKKAMWFLLTLLFACLVCWQWGVFIQTYLSWEVSVSLSMGFKT  β
VVSR.GRLRPLLWIAFTLTAVALIIWQCALLVFSF..YTVSVSIKVHFQK  γ
                    M1                   H1

151                                                  200
LVFPAVTVCTLNPYRYTEIKEELEELDRITEQTLFDLYKYNSSYTRQAGA  α
MNFPAVTVCNSSPFQYSKVKHLLKDLYKLMEAVLDKILAPKSSH....T  β
LDFPAVTICNINPYKYSAVSDLLTDLDSETKQALLSLYGVKESRKRREAG  γ

201                                                  250
RRRSSRD.....LLGAFPHPLQRLRTPPPP....YSGRTARSGSSSVRD.  α
NTTSTLNFT...IWNHTPLVLIDERNPDHPVVLNLFGDSHNSSNPAPGST  β
SMPSTLEGTPPRFFKLIPLLVFNENEKGKARDF.FTGRKRKISGKIIHKA  γ

251                                                  300
.NNPQVDRKDWKIGFQLCNQNKSDCFYQTYSSGVDAVREWYRFHYINILS  α
CN...AQGCK..VAMRLCSANGTVCTFRNFTSATQAVTEWYILQATNIFS  β
SNVMHVHESKKLVGFQLCSNDTSDCATYTFSSGINAIQEWYKLHYMNIMA  γ

301                                                  350
RLSDTSPALEEEALGNFIFTCRFNQAPCNQANYSKFHHPMYGNCYTFNDK  α
QVLPQDLVGMGYAPDRIILACLFGTEPCSHRNFTPIFYPDYGNCYIFNWG  β
QVPLEKKINMSYSAEELLVTCFFDGMSCDARNFTLFHHPMYGNCYTFNNK  γ

351                                                  400
NNSNLWMSSMPGVNNGLSLTLRTEQNDFIPLLSTVTGARVMVHGQDEPAF  α
MTEKALPSANPGTEFGLKLILDIGQEDYVPFLASTAGARLMLHEQRTYPF  β
ENATILSTSMGGSEYGLQVILYINEDEYNPFLVSSTGAKVLIHQQNEYPF  γ

401                                                  450
MDDGGFNLRPGVETSISMRKEALDSLGGNYGDCTENGSDVPVKNL...YP  α
IREEGIYAMAGTETSIGVLLDKLQGKGEPYSPCTMNGSDVAIQNLYSDYN  β
IEDVGMEIETAMSTSIGMHLTESFKLSEPYSQCTEDGSDVPVTNI...YN  γ

451                                                  500
SKYTQQVCIHSCFQENMIKKCGCAYIFYPKPKGVEFCDYRKQSSWGYCYY  α
TTYSIQACLHSCFQDHMIHNCSCGHYLYPLPAGEKYCNNRDFPDWAYCYL  β
AAYSLQICLYSCFQTKMVEKCGCAQYSQPLPPAANYCNYQQHPNWMYCYY  γ

501                                                  550
KLQGAFSLDSLGCFSKCRKPCSVINYKLSAGYSRWPSVKSQDWIFEMLSL  α
SLQMSVVQRE.TCLSMCKESCNDTQYKMTISMADWPSEASEDWILHVLSQ  β
QLYQAFVREELGCQSVCKQSCSFKEWTLTTSLAQWPSEASEKWLLNVLTW  γ

551                                                  600
QNNYTINNK..RNGVAKLNIFFKELNYKTNSESPSVTMVSLLSNLGSQWS  α
ERDQSSNITLSRKGIVKLNIYFQEFNYRTIEESPANNIVWLLSNLGGQFG  β
DQSQQINKKLNKTDLAKLLIFYKDLNQRSIMESPANSTEMLLSNFGGQLG  γ
                                                H2

601                                                  650
LWFGSSVLSVVEHADV.IFDLLVITLLMLLRRFRSRYWSPGRGARGAREV  α
FWMGGSVLCLIEFGEI.IIDFIWITVIKLVAS........CKGLRRRR..  β
LWMSCSVVCVIEIIEVFFIDFFSIIARRQWHK.........AKDCWARR..  γ
                        M2

651                                                  700
ASTPASSFPSRFCPHPTSPPPSLPQQGMTPPLALTAPPPAYATLGPSAPP  α
.........PQRPYTGPPPTVAELVEAHTNCVFQPDTT.SCRPNAEVYPDQ  β
.........QTPPSTETPSS....RQGQDNPALDTDDDLPTFTSAMRLPPA  γ

701
LDSAAPDCSACALAAL  α
QTLPIPGTPPPNYDSLRLQPLDTMESDSEVEAI  β
PGSTVPGTPPPRYNTLRLDRAFSSQLTDTQLTNEL  γ
```

B

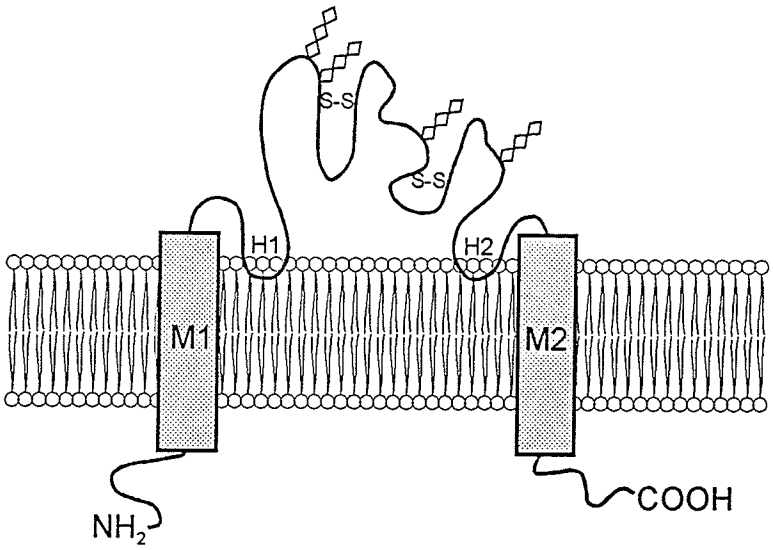

Figure 1

The epithelial sodium channel from rat epithelial tissue. **A**. Amino acid sequence for the three subunits (α, β, and γ) of the epithelial sodium channel (Canessa *et al*, 1984) arranged from N terminus to C terminus. Sequence was deduced from cDNA code. The two transmembrane segments are indicated by underscore and labelled **M1** and **M2**. Two hydrophobic regions in the loop region, close to the transmembrane regions, are also indicated by underscore and labelled **H1** and **H2**. There is 35% identity between α and β chains, 34% between α and γ chains, and 37% between β and γ chains. **B**. Model depicting a proposed transmembrane topology for the α subunit of the epithelial sodium channel. At least 4 N-linked glycosylation sites are indicated. Highly conserved cysteine positions in the loop region indicate some degree of disulfide bridging.

(Valera *et al*, 1994) and other cell types. These are high affinity amiloride-binding sodium channels.

Low amiloride-binding affinity sodium channels are inhibited by 6 to 10 μM amiloride. Barbry *et al* (1989; 1990) have found two phenamil binding sites in renal epithelium, at least one of which was a sodium channel. Unfortunately what they thought was the low affinity sodium channel (a 180KD protein made of two subunits of 90-105KD) was likely to be diamine oxidase (Lingueglia *et al*, 1993; Novotny *et al*, 1994; Chassande *et al*, 1994). Another low affinity sodium channel has been described in lung epithelium (Garty and Benos, 1988) which may be the channel inhibited in the therapy of cystic fibrosis (Collins, 1992). It is possible that this low affinity channel is a subset of the high affinity channels described above, with the lower affinity being due to different isoforms of the α, β, or γ subunits. An epithelial-like sodium channel with very low amiloride affinity has been described in rat aortic cells (Van Renterghem and Lazdunski, 1991). This channel is sensitive to higher concentrations of phenamil (greater than 10 μM). Single channel measurements revealed an open state conductance of 10.7pS with a selectivity 11 times greater for sodium than for potassium ions. A channel with similar properties was found in rabbit renal proximal convoluted tubules (Goegelein and Greger, 1986). It is expected therefore that smooth muscle also contains sodium channels which fall into the family of epithelial-type sodium channels.

SMOOTH MUSCLE

Amiloride itself has attracted much attention as a sodium-hydrogen antiport blocker and a sodium channel blocker. Sodium is important in excitation-contraction coupling in smooth muscle (Brading *et al*, 1980; Bose *et al*, 1989). The usefulness of amiloride as a smooth muscle relaxant of airway smooth muscle (Souhrada *et al*, 1988; Krampetz and Bose, 1988) and other smooth muscle preparations has been demonstrated (Akhtar-Khavari *et al*, 1981). Krampetz and Bose (1988) described the biphasic nature of smooth muscle relaxation produced by amiloride when the log of the effect was plotted as a function of time. The rapid phase of the amiloride-induced relaxation is due to inhibition of sodium-hydrogen exchange, and the slower component is due to inhibition of sodium channels (Krampetz and Bose, 1988). Phenamil has proven to be a potent smooth muscle relaxant showing only one phase of relaxation in the same range of concentrations that block epithelial sodium channels (Yu *et al*, 1989). The relaxant effects in smooth muscle are greater with analogs possessing an epithelial sodium channel inhibitory property. Phenamil and amiloride both produce relaxation of smooth muscle and reduce sodium uptake into smooth muscle cells, whereas neither MGCMA nor CBDMB produced significant relaxation, nor significantly reduced sodium uptake into the smooth muscle cells (Yu *et al*, 1993).

The relaxant properties of amiloride on the tracheal smooth muscle and, implicitly, on the smooth muscle of the respiratory system has aroused the possibility that amiloride could be used in the treatment of not only cystic fibrosis (Waltner *et al*, 1987; Collins, 1992), but also of asthma, or other obstructive pulmonary diseases. A few of the major

complications associated with asthma include airway smooth muscle hyperexcitability, excessive mucus production, tissue thickening, and acidosis (Iafrate, *et al*, 1986). Smooth muscle hyperexcitability is due to histamine-induced contraction of the smooth muscle and antigen-induced contraction of sensitized muscle. The thick mucus produced is difficult to be mobilized by the airway and results in an accumulation which eventually produces plugs that can block the small airways.

It has been shown that amiloride effectively relaxes airway smooth muscle *in vitro* using carbachol (figure 2A; Guia and Bose, 1990) or other smooth muscle stimulants (Figure 2B; Krampetz and Bose, 1988; Souhrada *et al*, 1988; Yu *et al*, 1993; Pinon and Fabre, 1985) as well as *in vivo* using carbachol (Krampetz and Bose, 1987), ragweed antigen (figure 2C; Yu *et al*, 1993), or ovalbumin antigen (Souhrada *et al*, 1988). Ragweed-sensitized dogs are similar to humans during anaphylactic response i.e. the response in airway smooth muscle is mediated by IgE (Ishizaka, 1976; Kepron *et al*, 1977). By inhibiting sodium channels (Haddy *et al*, 1985; Krampetz and Bose, 1988; Souhrada and Souhrada, 1988; Yu *et al*, 1990), it is likely to cause calcium to be extruded by indirectly enhancing forward mode or decreasing reverse mode of sodium-calcium exchange. Pinon and Fabre (1985) have proposed that reverse sodium-calcium exchange is inhibited by amiloride. In addition, in other tissues sodium is required for the production of IP_3 (Kimura *et al*, 1994; Guiramand *et al*, 1991), hence it is likely that the relaxation of smooth muscle is due to an increase in forward mode of the exchanger, as well as a decrease in IP_3 production.

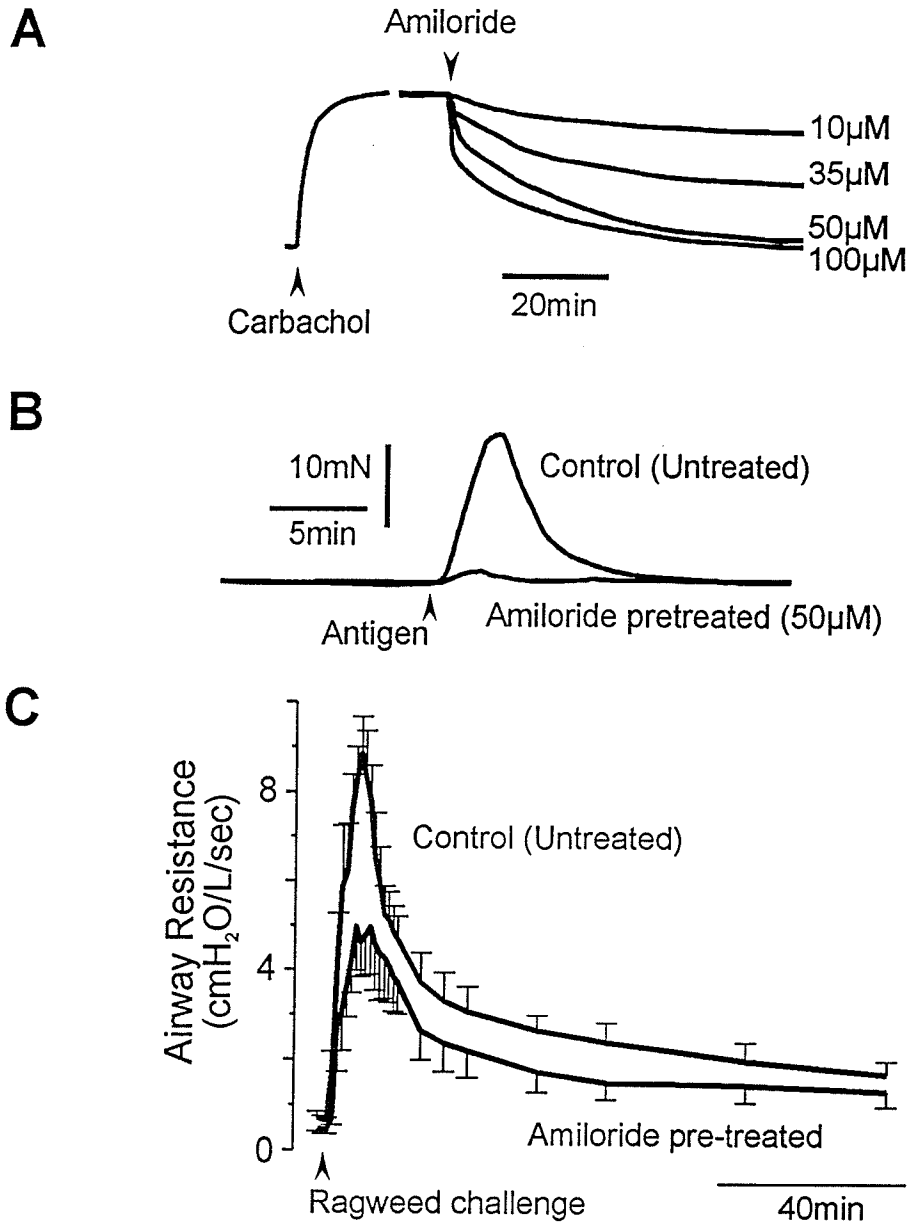

Figure 2

The relaxant effect of amiloride on smooth muscle. **A**. Typical *in vitro* tension-time traces of 1μM carbachol-contracted canine tracheal smooth muscle showing relaxation by amiloride (10 to 100μM) (adapted from Krampetz,I.: PhD Thesis, University of Manitoba, Winnipeg, Canada). Traces are aligned so as to illustrate the concentration-dependence of amiloride-induced relaxation. **B**. *In vitro* time-tension curve showing relaxation of ragweed (25μg/ml) antigen-contracted smooth muscle by 50μM amiloride pretreatment. Amiloride was added 5 minutes before the ragweed challenge. Amiloride did not change the resting tension upon addition. Tissue was isolated from ragweed-sensitized dogs, or passively sensitized with blood plasma from ragweed-sensitized dogs (from Yu *et al*, 1993). **C**. *In vivo* time-response curve of measurements of ragweed-sensitized canine ventilated airway resistance in response to an insult with ragweed antigen. Data shown for ragweed challenge to untreated controls and to dogs pretreated with a nebulized form of amiloride (10μM for 5 minutes) (from Yu *et al*, 1993).

Epithelium has been shown to be a potent modifier of the smooth muscle contraction, especially in the upper respiratory tract (Farmer *et al*, 1986; Vanhoutte, 1989). Although the *in vitro* traces shown in figure 2A are from tissues with the epithelium removed, the relaxant effect of amiloride was found to be unmodified by the epithelium (Guia and Bose, 1990). The involvement of epithelium-derived factors in the contraction of smooth muscle may only be of any concern in the larger airways and would be negligible in the smaller airways (Stuart-Smith and Vanhoutte, 1987). Amiloride proved to be effective in decreasing mucus viscosity and mobilizing airway fluid by blocking excess salt (sodium) uptake through the epithelium in patients with cystic fibrosis. It allows a build-up of sodium, and chloride, its counterion, in the airway fluid (Waltner *et al*, 1987). This allows cilliary action and coughing responses to clear the airways because of the thinning of the secretion.

Amiloride will therefore alleviate at least two of the complications of asthma: smooth muscle hyperexcitability, and the airway lumen blockade due to thick mucus production. Amiloride was found to have a long lasting effect in isolated tissues, eventually bringing about a complete relaxation of canine tracheal smooth muscle for as long as it was present in the bathing solution (Guia and Bose, 1990). *In vivo*, amiloride was observed to be active in the dog for up to four hours. In contrast, the relaxant potency of salbutamol, a common anti-asthmatic agent, slowly declined *in vitro* so that no relaxation was seen after 15 to 40 minutes. Maximum relaxation *in vitro* occurred in less than 10 minutes after the addition of salbutamol and resulted in only a 35% decrease in maximum tension (60 μM). This degree of relaxation was achieved by the same

concentration of amiloride in only five minutes, and a 70% decrease in tension was observed after 20 minutes exposure to amiloride (Guia and Bose, 1990). Due to down-regulation of beta receptors by salbutamol, multiple applications of the drug are not feasible. Amiloride does not down-regulate its receptors. Furthermore, salbutamol does not increase fluid motion in the airways (Robinson *et al*, 1989). These facts further favor the use of phenamil for the treatment of asthma due to it's inhibitory properties on the epithelial-type sodium channels.

Phenamil is 17 times more potent than amiloride at inhibiting the epithelial-type sodium channels, but only 5.5 times more potent than amiloride at inhibiting sodium-calcium exchange. It has no effect on sodium-hydrogen exchange (Frelin *et al*, 1988; Kleyman and Cragoe, 1988; Bridges *et al*, 1989; Barbry *et al*, 1990). In smooth muscle and gut epithelia, phenamil blocks sodium and calcium entry (Ki<50 nM, Voilley *et al*, 1994; Bridges *et al*, 1989; Barbry *et al*, 1990; Yu *et al*, 1989) and is a very potent smooth muscle relaxant (Yu *et al*, 1993). This may make it a better candidate for the therapy of cystic fibrosis, asthma, or COPD.

EFFECT OF PHENAMIL ON SMOOTH MUSCLE

Phenamil has been used as a tool to inhibit voltage independent sodium channels in *bacilli* bacteria (Atsumi *et al*, 1990), where it was shown to have more specificity for all slow sodium channels than amiloride, to various mammalian tissues including white blood cells (Kraut *et al*, 1993; de Moraes, 1993), intestinal epithelium (Sellin and Dubinsky, 1994), human colonic membrane vesicles (Dudeja *et al*, 1994), thyroid epithelium

(Armstrong *et al*, 1992; Yap *et al*, 1993), renal tubules (Merot *et al*, 1989; Parenti *et al*, 1992; Barbry *et al*, 1990), vascular smooth muscle (Van Renterghem and Lazdunski, 1991), vascular endothelium (Vigne *et al*, 1989), tongue epithelium (Schiffman *et al*, 1990), etc.

Phenamil produces fast and complete relaxation of tracheal smooth muscle more potently than that observed with amiloride (figure 3; Yu *et al*, 1993). Phenamil also impairs sodium uptake from airway fluids (O'Brodovich *et al*, 1991) therefore it would be expected to liquefy the airway mucus and alleviate the symptoms of cystic fibrosis by the same mechanism as amiloride (Collins, 1992). The mechanism by which phenamil produces relaxation of smooth muscle is by inhibition of sodium channels (Van Renterghem and Lazdunski, 1991; Yu *et al*; 1989; Yu *et al*, 1993).

The relative benefits of the use of phenamil in place of amiloride in a clinical situation seem convincing. It is known that phenamil inhibits epithelial-type sodium channels in systems that contain such channels, and in those systems, the sodium channel inhibition is the dominant role of phenamil, masking any other effects it may have. Aside from inhibition of sodium channels, little else is known about phenamil. In order to elucidate other pharmacological effects of phenamil on membrane ionic events, and on cell function, it must be tested in tissues that do not contain epithelial-type sodium channels.

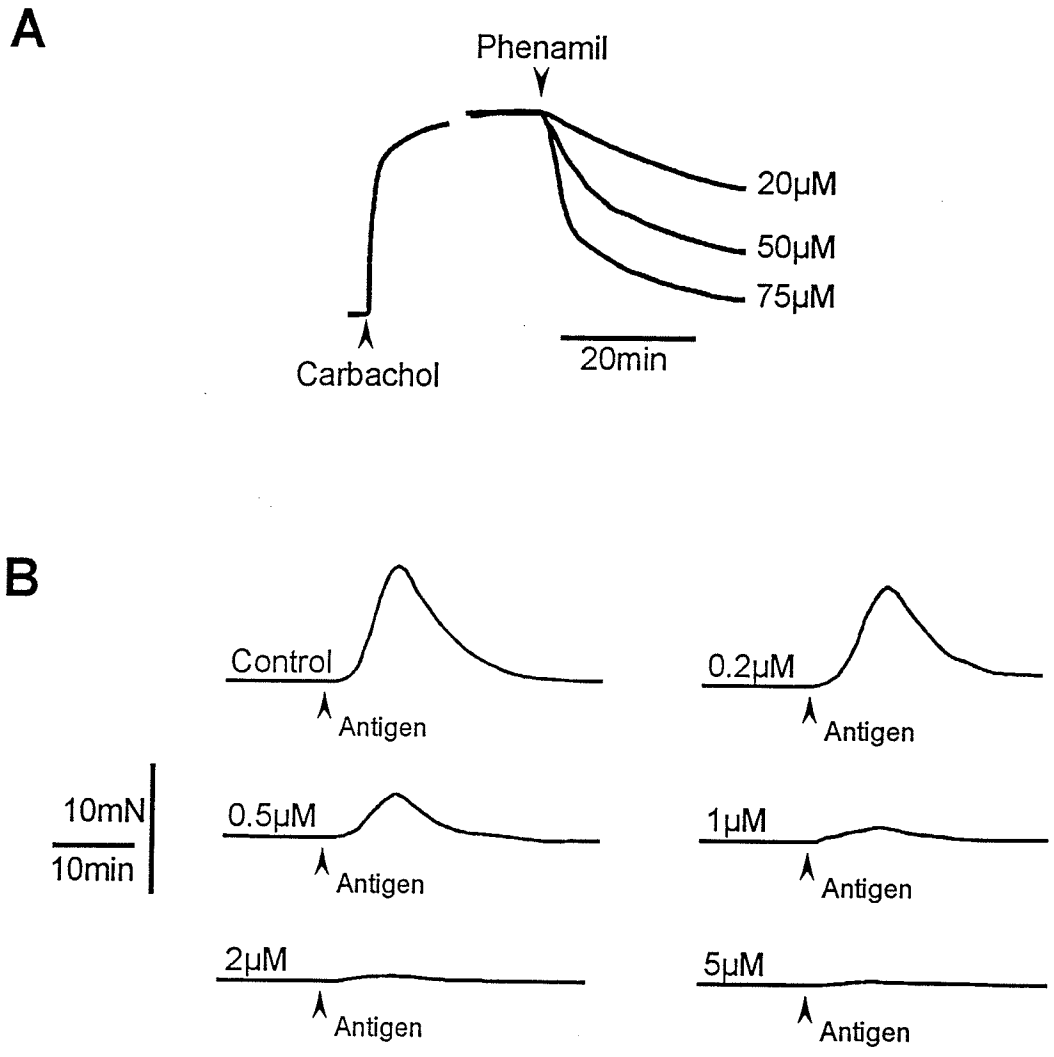

Figure 3
The relaxant effect of phenamil on isolated smooth muscle. **A.** Typical tension-time traces of 1μM carbachol-contracted canine tracheal smooth muscle showing relaxation by phenamil (20 to 75μM) (from Yu *et al*, 1993). Traces are aligned so as to illustrate the concentration-dependence of the phenamil-dependent relaxation. **B.** Tension-time curves showing relaxation of ragweed (25μg/ml) antigen-contracted smooth muscle by phenamil pretreatment. Phenamil was added 5 to 10 minutes before the antigen. Ragweed pollen was added at the time indicated by an arrow. Since there is no resting tension in canine tracheal smooth muscle, phenamil had no effect on the tension of uncontracted tissue. Tissue strips were different from those in figure 2 but from the same ragweed-sensitized dogs, or passively sensitized with blood plasma from ragweed-sensitized dogs (from Yu *et al*, 1993).

EFFECTS ON CARDIAC MUSCLE

The tetrodotoxin-insensitive slow sodium channels, which are found in epithelial and smooth muscle tissues, are believed not to be present in measurable amounts in healthy adult cardiac tissue, which has tetrodotoxin-sensitive fast sodium channels (Reuter, 1979; Colatsky, 1980; Fozzard *et al*, 1985). A study of the effects of phenamil on cardiac tissue will therefore unmask any other effects that phenamil may have on cell function and will provide valuable information towards elucidating the pharmacological profile of phenamil.

Amiloride has been shown to produce either positive inotropy or negative inotropy (Yamashita *et al*, 1981; Duff *et al*, 1991; Brown *et al*, 1991) or both in guinea pig tissue (Pousti and Khoyi, 1979; Kennedy *et al*, 1986; Cargnelli *et al*, 1989). The appearance of both positive inotropy and negative inotropy in guinea pig heart was linked to the stimulation rate (Pousti and Khoyi, 1979). Amiloride inhibits sodium-calcium exchange in guinea pig and beef cardiac membrane vesicles (Siegl *et al*, 1984). Inotropy by amiloride and its analogs has been proposed to be due to inhibition of sodium-calcium exchange in guinea pig tissue (Floreani and Luciani, 1984; Altschuld *et al*, 1984; Cargnelli *et al*, 1989). This conclusion appears to be supported by data in rat ventricular tissue (Brown *et al*, 1991). Micromolar concentrations of amiloride are required to produce positive inotropy, however inhibition of sodium-calcium exchange is only achieved with much higher concentrations of amiloride (>0.35 mM; Siegl *et al*, 1984; Floreani and Luciani, 1984; Smith *et al*, 1982) or more (Ki=1.0 mM; Kleyman and Cragoe, 1988), and at these

concentrations a number of other processes are also inhibited by amiloride (Frelin *et al*, 1984; Kleyman and Cragoe, 1988). Several derivatives of amiloride have been shown to produce positive inotropy in cardiac tissue (Floreani *et al*, 1987; Brown *et al*, 1991; Siegl *et al*, 1984). Negative chronotropy has also been associated with inhibition of the sodium-calcium exchanger (Brown *et al*, 1991; Satoh and Hashimoto, 1986; Yamashita *et al*, 1981).

In rat right ventricular papillary muscle, both amiloride and EIPA produced negative inotropy whereas derivatives more specific for inhibition of sodium-calcium exchange produced positive inotropy (Brown *et al*, 1991). EIPA is relatively specific for inhibition of sodium-hydrogen exchange. Amiloride inhibits sodium-hydrogen exchange at much lower concentrations (EC_{50}=83 to 87 μM, Kleyman and Cragoe, 1988) than those that inhibit sodium-calcium exchange. The rank order of potency of amiloride and its derivatives for producing positive inotropy in rat ventricular papillae does not match their rank order of potency for inhibiting the sodium-calcium exchanger (Brown *et al*, 1991; Kleyman and Cragoe, 1988). The direct inhibition of this exchanger does not offer a good explanation for the inotropic effects of amiloride.

Calcium channel inhibition by amiloride has been demonstrated for L-type calcium channels in rabbit SA node (87 μM; Satoh and Hashimoto, 1986). Derivatives that inhibit sodium-calcium exchange also inhibit L-type calcium channels in cardiac tissue (5 μM; Bielefeld *et al*, 1986). Amiloride blocks low threshold T-type calcium channels in mouse neuroblastoma cells and chick dorsal root ganglion (30 μM, Tang *et al*, 1988) and in

cardiac tissue (Tytgat *et al*, 1990). However, its usefulness as a pharmacological tool to study these channels has been limited due to other effects of amiloride on cell membrane proteins, and due to the small currents elicited by these channels. T-type calcium channels were recorded with high calcium and low sodium concentrations in the extracellular solutions and were not inhibited by lidocaine or by tetrodotoxin. These channels are inhibited by nickel and amiloride whereas the tetrodotoxin-sensitive sodium channels are not inhibited by nickel, or by lower concentrations of amiloride (<1 mM). Garcia *et al* (1990) generalized that inhibition of calcium channels by amiloride and its derivatives is related to the hydrophobicity of the compounds. Inhibition of calcium channels cannot be a predominant effect of amiloride or of derivatives which produce positive inotropy in cardiac tissue.

Inhibition of the sodium pump results in elevated cytosolic sodium levels. These elevated levels of sodium can reduce or even reverse sodium-calcium exchange in cardiac tissue, resulting in positive inotropy and eventual tissue damage (Lazdunski *et al*, 1985). The sodium pump in guinea pig left atria and ventricular papillary muscle is inhibited only with high concentrations of amiloride (0.3 mM to 2 mM; Kennedy *et al*, 1986; 6 mM; Floreani *et al*, 1987) and derivatives specific for inhibiting sodium-calcium exchange (68 μM DCB; Floreani *et al*, 1987). In other tissues as well, high concentrations of amiloride are required to observe inhibition of the sodium pump (Soltoff and Mandel, 1983). It has long been known that amiloride protects the heart from arrhythmias brought about by sodium pump inhibitors (Seller *et al*, 1975; Waldorff *et al*, 1981; Rabkin, 1989). It appears therefore that inhibition of the sodium pump is not responsible for positive

inotropy otherwise this effect would be additive with the effects of sodium pump inhibitors and would promote arrhythmias.

Inhibition of potassium channels can slow the repolarization process and secondarily enhance calcium entry into the myocytes. Amiloride has been shown to inhibit I_K in rabbit SA node (Satoh and Hashimoto, 1986) and possibly I_{K1} in human ventricles (Duff *et al*, 1991). The conclusion that I_{K1} was inhibited in human tissue was made from its antiarrhythmic actions and is yet unclear. Inhibition of I_K has also been observed in frog right atria using a derivative of amiloride that is specific for inhibition of sodium-calcium exchange (Bielefeld *et al*, 1986). Although not entirely carried by potassium, the potassium portion of I_{to} that is sensitive to 4AP is enhanced by another amiloride derivative. Tedisamil slows the inactivation of I_{to}, thereby prolonging and promoting I_{to} (30 μM; Dukes and Morad, 1989). Inhibition of I_{to} results in positive inotropy, therefore potentiation of I_{to} would likely result in negative inotropy. The potentiation of I_{to} may not be considered a dominant effect of amiloride and its derivatives in cardiac tissue.

pH_i directly affects the force of contraction by interaction of H^+ with binding sites for calcium on troponin C (Fabiato and Fabiato, 1978; Orchard and Kentish, 1990) and by more indirect effects such as on SR calcium release sites (Rousseau and Pinkos, 1990), potassium channels (Harvey and Ten Eick, 1989b), calcium channels (Irisawa and Sato, 1986), and other mechanisms (Kaila *et al*, 1987; Orchard and Kentish, 1990). The relationship between pH_i and cell or muscle contraction has been described in detail

elsewhere (MacLeod and Harding, 1991; Vaughan-Jones *et al*, 1987). Activation of sodium-hydrogen exchange could alkalinize the cytosol and produce positive inotropy.

EFFECT OF AMILORIDE ANALOGS ON POST-ISCHEMIC CONTRACTILE DYSFUNCTION

Ischemia involves many simultaneous events (Hearse, 1988), one of which is cytosolic acidosis resulting from the hydrolysis of high energy phosphates and anaerobic glycolysis during ischemia (Lazdunski *et al*, 1985; Karmazyn, 1988; Meng and Pierce, 1990). Upon reperfusion the extracellular pH increases, thereby increasing the driving force for the sodium-hydrogen exchanger. Lazdunski *et al* (1985) proposed that ischemia-reperfusion damage was due to calcium overload resulting from enhanced sodium-calcium exchange activity in response to a cytosolic sodium overload. The sodium overload was proposed to be due to the activity of sodium-hydrogen exchange (Lazdunski *et al* 1985; Karmazyn, 1988; Meng and Pierce, 1990). Thirty minutes of *in vitro* ischemia, by stopped flow, suffices to produce damage during reperfusion (Cobbe and Poole-Wilson, 1980; Karmazyn, 1988). Amiloride was found to protect the heart from post-ischemic reperfusion-induced damage (Karmazyn, 1988; Meng and Pierce, 1990), thus interpreted as inhibiting sodium-hydrogen exchange.

Sodium levels were found to increase during acidosis (Bielen *et al*, 1990; Kaila and Vaughan-Jones, 1987), due to the activity of sodium-hydrogen exchange. Manipulation of the cytosolic pH alone should therefore produce tissue damage similar to that produced by ischemia. Simulated metabolic acidosis, with lactic acid, has been shown to histologically damage endocardium and cardiac cells in multicellular preparations (Carter and Gavin, 1989). Simulated respiratory acidosis, with CO_2, did not result in myocardial damage upon restoration of pH_o (Cobbe and Poole-Wilson, 1980). The sodium-hydrogen exchanger was also found not to contribute to increased cytosolic calcium concentrations

in single cells (Hayashi *et al*, 1992) nor to play a role in low-flow ischemic conditions since more specific inhibition of the exchanger did not alter pH_i during the ischemia (Imai *et al*, 1991). It therefore appears that sodium-hydrogen exchange does not directly contribute to tissue damage under low-flow ischemic conditions. The driving force for the sodium-hydrogen exchanger is reduced by the increased extracellular H^+ during acidification, hence the sodium-hydrogen exchanger is not a significant contributor to the increased sodium levels during acidification (Imai *et al*, 1991). Sodium loading through the exchanger will therefore only occur during reperfusion (Karmazyn, 1988; Meng and Pierce, 1990; Vaughan-Jones and Wu, 1990). Amiloride and some of its analogs are cardioprotective only if present during reperfusion (Meng and Pierce, 1990). However since acidification alone is not sufficient to produce ischemic damage (Imai *et al*, 1991; Kohmoto *et al*, 1990; Mohabir *et al*, 1991), it seems more likely that amiloride has some other effects that are protective for the tissue. Further, many of the studies showing cardioprotective effects of amiloride have used higher concentrations than those required to inhibit sodium-hydrogen exchange (Murphy *et al*, 1991).

Both amiloride and EIPA, a sodium-hydrogen exchange specific blocker, slowed the sodium accumulation in the perfused hearts during hypoxia and removal of KCl (Anderson *et al*, 1990). Unfortunately Anderson *et al* (1990) did not show an increase in cytosolic sodium during restoration of potassium and normoxia but instead showed a decrease in cytosolic calcium upon restoration of potassium to the perfusate and during removal of acidosis. In spite of the slowed sodium accumulation during hypoxia, a recent study showed that amiloride protects the heart from post-ischemic reperfusion damage to the contractile function, but EIPA does not (Harrison and Lancaster, 1994). Amiloride also inhibits sodium-calcium exchange in the millimolar concentrations used to prevent post-ischemic contractile dysfunction. Other sodium-calcium exchange blockers prevent reperfusion-induced damage (Harrison and Lancaster, 1994). These data suggest some

mechanism other than sodium-hydrogen exchange and hence it is difficult to implicate the sodium-hydrogen exchanger for explaining the increase in cytosolic calcium during acidosis (Orchard and Kentish, 1990).

Increased calcium results in further cytosolic acidification (Kaila *et al*, 1987) and in cell damage (Lazdunski *et al*, 1985). Excess cytosolic calcium increases ATP hydrolysis. With limited substrate, such as during ischemia or hypoxia, ATP hydrolysis causes further intracellular acidification (Cobbe and Poole-Wilson, 1980). It is possible therefore that cytosolic acidification is a product of elevated cytosolic calcium levels. Increased ATP hydrolysis produces adenosine and other byproducts. Metabolism of adenosine involves an oxygen-requiring step for the activation of xanthine oxidase. Reperfusion after hypoxia induces free radical formation (from the activation of xanthine oxidase) which can directly produce tissue damage (Allen and Orchard, 1987; McCord, 1985). It is therefore more likely that the reintroduction of oxygen may produce tissue damage by the liberation of free radicals (McCord, 1985).

EFFECT OF PHENAMIL ON CARDIAC MUSCLE

Blockade of the epithelial sodium channels by phenamil occurs in the nanomolar range (K_i=0.086 μM; Kleyman and Cragoe, 1988) or micromolar range (Smith and Benos, 1991) depending upon the type of epithelial channel. Amiloride also causes positive inotropy (Cargnelli *et al*, 1989; Floreani, and Luciani, 1984) in concentrations which inhibit epithelial sodium channels (Kleyman and Cragoe, 1988; Smith and Benos, 1991). One would expect a shortened action potential duration and negative inotropy following inhibition of sodium channels. It is therefore unlikely that blockade of sodium channels is responsible for producing positive inotropy.

Phenamil produces positive inotropy in rat right ventricular trabeculae (Brown *et al*, 1991). In the heart, pharmacological studies revealed that amiloride and some of its derivatives inhibit L-type calcium and delayed rectifier potassium channels (Bielefeld *et al*, 1986; Kleyman and Cragoe, 1988; Pierce *et al*, 1993), sodium/calcium exchange, and sodium/hydrogen exchange (Frelin *et al*, 1988). Inhibition of potassium channels could account for the increased tension development in the presence of phenamil. Inhibition of sodium/calcium exchange has been suggested to explain the positive inotropic effect of high concentrations of amiloride (1.6 mM, Pousti and Khoyi, 1979; 0.7 mM, Floreani and Luciani, 1984) and some of its analogs such as DCB (20 μM, Floreani *et al*, 1987). Brown *et al* (1991) concluded that positive inotropy by phenamil (10 to 100 μM) and other derivatives in rat ventricular papillary muscle was due to inhibition of sodium-calcium exchange. Their conclusion was based on the similarity of the inotropic actions of phenamil and CBDMB in their preparation. Much higher concentrations of phenamil are required to block the exchanger (Kleyman and Cragoe, 1988) as compared to concentrations that produced positive inotropy. Other compounds in their study produced positive inotropy at similar concentrations in spite of being more potent inhibitors of sodium-calcium exchange than phenamil. The rank order of potency of these compounds for producing positive inotropy does not correlate with their rank order of potency for inhibiting sodium-calcium exchange. The mechanism of positive inotropy by phenamil is therefore not clearly understood.

PHENAMIL: PHYSICAL PROPERTIES

Phenamil (figure 4) has the chemical composition of N-phenylamidino-3,5-diamino-6-chloropyrazinecarboxamide (compound #64, Cragoe *et al*, 1967) resulting from the introduction of a phenyl group on the terminal nitrogen of the carboxylguanidino moiety amiloride (N-amidino-3,5-diamino-6-chloropyrazinecarboxamide). Phenamil crystallizes in methanesulfonate (CH_3SO_2OH, 96 g/mol) as a yellow powder (272°C melting point) with the formula $C_{12}H_{12}N_7OCl$ (305.727 g/mol). The 8 conjugated double bonds in the molecule may result in interference with fluorescence measurements. Under physiological conditions phenamil exists in a protonated or unprotonated form (pK_a 7.8 in an aqueous solution of 30% ethanol) (Kleyman and Cragoe, 1988) and is expected to attain a higher steady state concentration in the cytosol (pH_i ~7.2) as compared to extracellular medium (pH_o 7.4). It distributes 98.7% into octanol or chloroform when equilibrated between equal volumes of the solvent and 0.1M aqueous phosphate buffer (pH 7.4) or water making phenamil difficult to wash out of biological preparations (Kleyman and Cragoe, 1988; O'Brodovich *et al*, 1991).

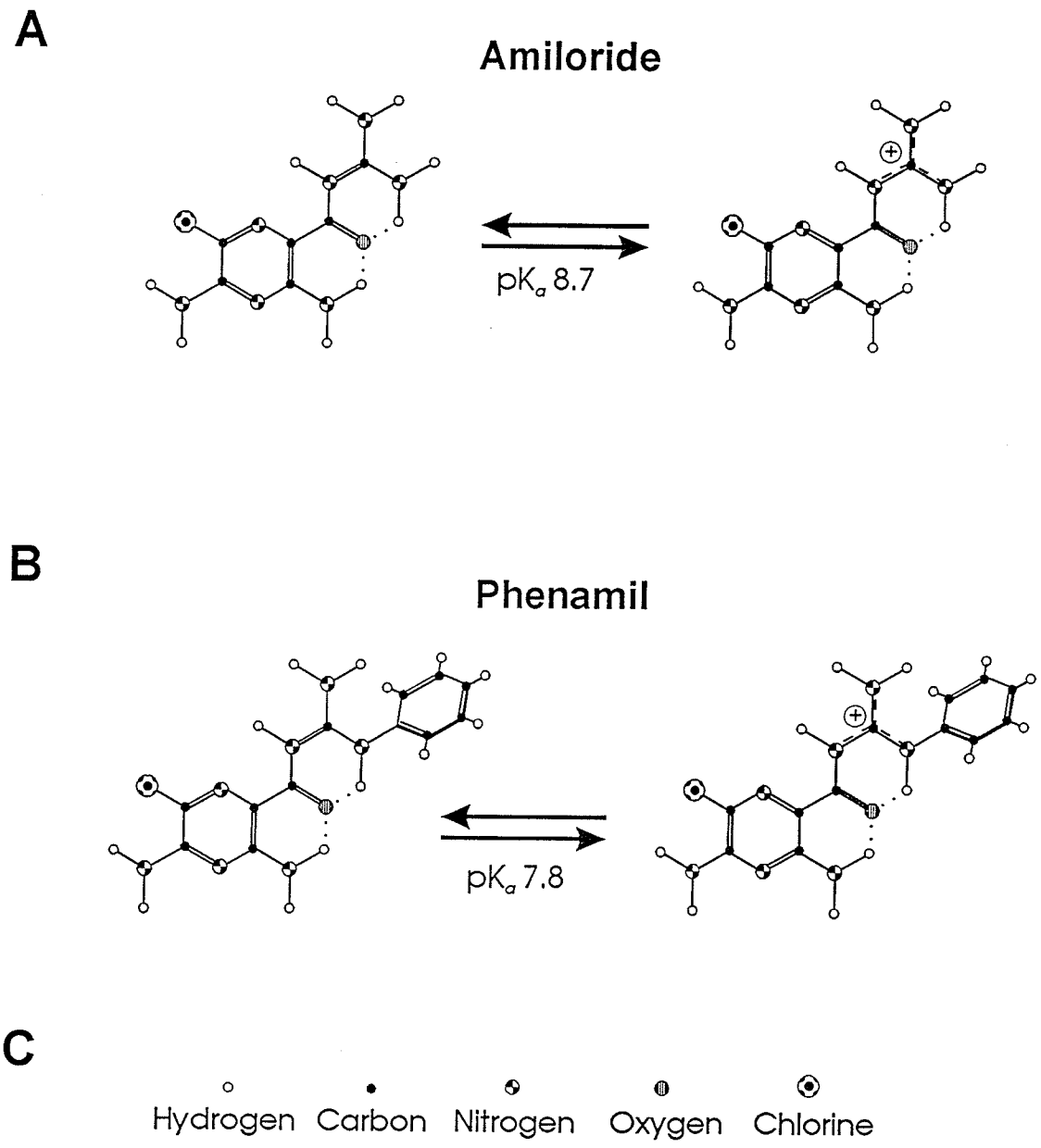

Figure 4
The chemical structure of amiloride and phenamil. **A.** Amiloride, N-amidino-3,5-diamino-6-chloropyrazine carboxamide, is a weak acid in aqueous solutions. Due to the sp2 hybrid orientation of the chemical bonds, both species exist as planar molecules. **B.** Phenamil, N-phenylamidino-3,5-diamino-6-chloropyrazine carboxamide, is similar in structure to amiloride, however with a phenyl group on one of the guanyl amines. Due to repulsion between hydrogens, the phenyl group extends above and below the plane of the molecule. **C.** Designation of atoms.

CELLULAR ELECTROPHYSIOLOGY

ELECTROCHEMISTRY

To understand ion channels, some basic principles of electrochemistry must be understood. Hille (1992) reviews the concepts of electrochemistry that are relevant to biological systems.

All matter is made up of charged particles that are usually in equal numbers of opposite charges, hence most bodies are electrically neutral, meaning that a mole of NaCl completely dissolved in water becomes 6.02×10^{23} positive charges, and the same number of negative charges (Avogadro's constant for the number of particles in a mole of substance). Every charged particle, whether a cation or an anion, contains the same amount of charge per valence. This quantum is measured in Coulombs, with each charged particle having 1.6×10^{-19} Coulombs. The Faraday constant describes the charge per valence of a mole of cations or of anions: 9.648×10^{4} Coulombs per mole per valence. These charges in a solution balance out to give neutrality at steady state. Energy is required to move a body away from neutrality. This energy is conserved as electrical potential energy, which represents the quantity of charge in a body.

Selectively permeable membranes can exclude the passage of certain charges or ions. There is a measurable difference in electrical potential energies of the solutions on either side of the membrane. This difference in potential energies is called the membrane potential, and is measured in Volts. Electrical charges moving across a membrane

produce a current, measured in Amperes where one Ampere is equal to the movement of one Coulomb of charge per second. The current produced by ion movement across a membrane is therefore directly proportional to the number of charges moving across that membrane. Ionic current across a membrane will move the membrane potential towards the equilibrium potential of the ion. The currents of ions that move across the membrane are additive. The movement of ions across a membrane is also dependent on the relative concentrations of the ion on either side of the membrane. The Nernst equation may be used to predict the equilibrium potential across a membrane for each ion that exists in the solutions at steady state. An equilibrium potential is the membrane potential that produces no net movement of that ion across the membrane. More specifically, it is where the electrochemical driving force for the movement of that ion is exactly equal in magnitude to the driving force created by the transmembrane concentration gradient of that ion. The difference between the steady state equilibrium potential, or reversal potential, for an ion and the membrane potential determines the electrochemical driving force for that ion to cross the membrane.

The strategy of current clamp involves injecting a known quantity of current into a cell, and measuring the resulting changes in the membrane potential. Voltage clamping involves measuring how much current needs to be injected into the cell in order to force the membrane potential to the desired value and holding it there. By convention, the current and voltage measurements are reported as measurements on the cytosolic side of the membrane with reference to the matrix outside the cell. A negative current trace therefore means that negative current had to be applied to clamp the cell voltage, meaning

that the net ion movement across the membrane carried a positive charge into the cell. Negative applied currents are therefore called "inward currents" since they represent inward movement of positive charge or outward movement of negative charge. Biological systems contain channels on their membranes that are usually selectively permeable to a particular ion or group of ions. Permeability is usually presented as a ratio of permeabilities between two permeant ions.

In the cytosol there is a higher concentration of potassium and a lower concentration of sodium than in the extracellular space. Cell membranes, at rest, are more permeable to potassium than to sodium, hence the outward movement of potassium produces a resting membrane potential that is polarized in a negative direction. Changes in membrane potential are either hyperpolarizing (in a negative direction from the resting membrane potential) or depolarizing (in a positive direction). The movement of positive charges into the cell, or of negative charges out of the cell produces a membrane depolarization while outward movement of positive charges or inward movement of negative charges repolarizes the membrane.

CARDIAC ELECTROPHYSIOLOGY

With an electrode inserted into a cardiac cell it is possible to measure electrical events, of which the action potential is the most important. The electrical properties of the cardiac action potential have been extensively reviewed (e.g.: Katz, 1977; Surawicz, 1992). The action potential (AP) is made up of four phases, with the resting state being the fifth phase. At rest the membrane potential is always in phase 4, with a resting

membrane potential (RMP) typically between -70 mV and -85 mV. Phase 0 is the upstroke of the AP. The rate of the upstroke during phase 0 depends on I_{Na} and is a determinant of the tissue conduction velocity or the rate of travel of the electrical stimulus within the tissue (from cell to cell, and along the cell membrane). An area of tissue where there is a decreased rate of upstroke will have a smaller conduction velocity, and hence be a potential site for reentrant arrhythmias. The "peak" of the AP is the maximum voltage of the AP, typically reaching +20 mV to +45 mV. Since this value is greater than 0 mV, it is also called the "overshoot". Phase 1 is the "notch" after the peak of the AP. In some tissues the notch is barely noticeable (e.g.: guinea pig ventricle) whereas in others it is prominent (e.g.: canine ventricle). The notch has been shown to be deeper in epicardial cells than in endocardial cells (Lukas and Antzelevitch, 1993). Phase 2 is the "plateau" of the AP where most of the calcium enters the cells. Phase 3, the repolarization phase, terminates the action potential.

The action potential is initiated by a small deflection of the membrane potential which is sufficient to open fast tetrodotoxin-sensitive sodium channels (I_{Na}). These channels are responsible for phase 0 of the ventricular action potential (Trautwein, 1973). The notch of the action potential is caused by the action of transient outward currents (I_{to}), the plateau by calcium current (I_{Ca}), termination of phase 2 and initiation of phase 3 is accomplished by the delayed outwardly rectifying potassium currents (I_K) and the final repolarization in phase 3 as well as the resting membrane potential are brought about by the inwardly rectifying potassium current (I_{K1}).

The voltage-gated channels carrying inward current (I_{Ca} and I_{Na}) have more than one gate, each operating at different speeds. The sodium current offers an ideal example of this, containing an "m" gate and an "h" gate. The h gate is open while the m gate is closed at rest. Upon depolarization to -70 mV or more positive, the m gate opens quickly (within 0.1 to 0.2 ms), allowing entry of sodium. Sodium channels have a low threshold for activation. The h gate closes slowly (2 ms) at higher voltages (>-100 mV) therefore there is an eventual inactivation of the channel. These gating kinetics produce a sodium current that turns on and off quickly and, for the most part, the event is over within 5 ms. All of the h gates are opened at a membrane potential of -100 mV and closed at a voltage of -50 mV. Closing of this gate is accelerated by more positive potentials hence inactivation of sodium channels is accelerated by more positive membrane potentials. Opening of this gate is also accelerated by more negative potentials, however at physiological membrane potential, the opening of this gate is slow hence the sodium channel remains refractory to activation for a short time after repolarization of the membrane. The large number of sodium channels on the membrane, combined with their simultaneous openings and rapid activation, produces a very fast and strong inward sodium current. In spite of the amplitude of the current, the rapid inactivation does not allow much sodium to enter the cell. The strong current brings about the fast upstroke (phase 0) of the action potential (Stühmer *et al*, 1989).

I_{to} brings about a quick repolarizing current during the notch or initial fast repolarization (phase 1) of the action potential. This current is outwardly rectifying and activates at a much more depolarized potential (-45 mV), hence it does not appear until

after the membrane potential is already depolarized in phase 0 of the action potential. It activates within 10 milliseconds and inactivates after 80 to 100 ms (Josephson *et al*, 1984; Shimoni and Severson, 1995; Wang *et al*, 1993). Besides its activation after depolarization, this current is also increased because the reversal potential of potassium channels is negative to the membrane potential. Rat ventricular myocytes possess a strong I_{to} component. The abundance of these channels in the myocardial sarcolemma varies from endocardium, to mesocardium, to epicardium and is dependent on the age of the animal (Wahler *et al*, 1994; Walker *et al*, 1993; Lukas and Antzelevitch, 1993; Tande *et al*, 1991; Wang *et al*, 1991). This current is comprised of multiple components (Wang *et al*, 1993). It results predominantly from potassium currents, but there is also chloride current associated with this outward current. The role of the chloride currents in the action potential of healthy cardiac tissue is not well understood. The notch of the action potential is shaped by the turning off of I_{Na}, by the profile of I_{to}, and by the turning on of I_{Ca}.

There are two varieties of calcium currents: L-type and T-type. I_{CaL} turns on within 20 to 50 ms and becomes partially inactivated after 120 to 160 ms. Inactivation of this current is calcium-dependent (Kass and Sanguinetti, 1984). L-type calcium channels are activated at voltages positive to -35 mV and maximum current occurs with the membrane potential near 0 to +10 mV. T-type calcium channels have been described in cardiac tissue (Tytgat *et al*, 1990) but their role is as yet not well understood. They activate and inactivate quickly (within 100ms) and carry a small current. These low threshold channels are activated by voltages positive to -55 mV. Inactivation of these channels is accelerated

by higher membrane potentials such that the peak current of these channels occurs at around -30 to -40 mV. It has been suggested that I_{CaT} is involved in initiating the release of calcium from the SR (Mitra and Morad, 1986; Sham *et al*, 1992).

Towards the middle of the plateau (phase 2) of the action potential, the voltage starts to repolarize. This repolarization is due in part to the inactivating calcium channels, and to the activation of the delayed outwardly rectifying potassium currents (I_K). I_K activates very slowly (in about 250 to 400 ms), but is significant in contributing to the repolarization of the membrane. I_K is potentiated by the presence of small amounts of calcium (Tohse, 1990). Due to its time dependence, a longer action potential will elicit progressively more I_K. This provides a safety to the cells so that a prolonged action potential cannot continue to render the cells inexcitable for long periods of time.. This current does not inactivate with time. One component of the current is inhibited at higher membrane potentials (I_{Kr}, is completely inhibited by +60 mV), but this may not be considered an inactivation since upon repolarization it possesses deactivation kinetics similar to the other component of I_K: I_{Ks} (Sanguinetti and Jurkiewicz, 1990). This current also has a high threshold of activation, opening only at potentials more positive than -40 mV. The deactivation rate is slow so that a small decaying current is present during repolarization to voltages below -40 mV. The deactivation does not allow this current to fully repolarize the membrane potential during phase 3 hence there is another current that predominates in the tail of the action potential, and maintains the resting membrane potential: I_{K_1}.

I_{K1} is the inwardly rectifying potassium current. Although it has been postulated to be inhibited by magnesium at voltages positive to -20 mV (Biermans *et al*, 1987; Matsuda, 1988), it is now believed that this is temperature and species dependent (Martin *et al*, 1995). In the range of voltage in the action potential, this current activates and deactivates quickly without significantly inactivating. The inwardly rectifying potassium current increases to a maximum at -60 mV then decreases toward the reversal potential for potassium channels. The relative strength of I_{K1}, I_{Na} and other inward leak currents together determine the threshold voltage for an action potential. A small deflection of membrane voltage may not open enough sodium channels to oppose I_{K1}, whereas a larger deflection will open enough sodium channels so that I_{Na} is larger than I_{K1}, which will initiate an AP.

EXCITATION-CONTRACTION COUPLING

Contractile tension is proportional to the cytosolic free calcium concentration. Mechanisms by which calcium may be released into the cytosol will therefore regulate contraction (Fabiato, 1983). There are two such mechanisms: transsarcolemmal calcium entry, and calcium release from the SR. Trans sarcolemmal calcium entry occurs through two main entry pathways: calcium channels and sodium-calcium exchange. Calcium channels are active from the end of phase 1 to the beginning of phase 3 of the action potential as discussed above. T-type calcium channels probably open during the upstroke of the action potential (phase 0) and inactivate by the plateau phase, bringing calcium into the sub-sarcolemmal space early during the action potential. The overall amount of

sodium that enters through sodium channels during the upstroke of the action potential is small, but because it happens within a couple of milliseconds, and because there is a diffusion barrier just inside the membrane to create a "fuzzy space" (Lederer *et al*, 1990), most of the sodium that enters the cell remains near the sub-sarcolemmal space. This high concentration of sodium just inside the membrane stimulates the reverse mode of the sodium-calcium exchanger. This event as well brings calcium into the sub-sarcolemmal space. The reason that this should be an important issue is that the small amount of calcium that enters produces calcium release through ryanodine receptors in the SR membrane. Opinions in the literature at present appear unresolved as to whether cytosolic calcium release is triggered by sodium-calcium exchange (Leblanc and Hume, 1990; Levesque *et al*, 1991; Levesque *et al*, 1994), calcium channels (Lederer *et al*, 1990; Cannell *et al*; 1995; López-López *et al*, 1995).

The calcium release channel in the SR (ryanodine receptors) has been found in the terminal cisternae, juxtaposed to the T-tubules of cardiac myocytes. They are presumably connected to the membrane through a "foot protein" which links them to dihydropyridine receptors and to the sodium-calcium exchanger (Frank *et al*, 1992). Although 50% linkage with sodium-calcium exchange and 50% linkage with dihydropyridine receptors has been described, the ryanodine receptor may be linked with more than one membrane channel. It is possible therefore that other channel types are also linked with the ryanodine receptors. The small amount of calcium that enters through the sarcolemma either via reverse mode sodium-calcium exchange or via T-type calcium channels is sufficient to

produce calcium induced calcium release from the SR (Leblanc and Hume, 1990; Lipp and Niggli, 1994). The released calcium produces contraction in the tissue.

During phase 2 of the action potential, calcium enters the cells through L-type calcium channels. This continues to increase twitch tension and prevents calcium accumulation in the SR by maintaining the release channels open. The relative contribution of calcium release from the SR versus transsarcolemmal calcium entry to the contraction may be determined by a variety of interventions that compromise the SR. A common method is by the use of ryanodine or caffeine to deplete the SR calcium pool by opening the calcium release channels on the SR and thus determine the contribution of just transsarcolemmal calcium movement to contraction as compared to control where both are present. By this method it is known that some species, such as frog, do not rely on calcium release from the SR for the production of a ventricular contraction, whereas other species, such as rat, are strongly dependent on calcium release from the SR for their contraction (Bers, 1989; Bers, 1991).

Equal in importance to contraction is the relaxation of cardiac muscle. Relaxation begins at the end of phase 2 of the action potential when calcium channels inactivate with time or deactivate with voltage. The free cytosolic calcium is removed by several mechanisms. SR calcium ATP-ase is known to sequester calcium from the cytosol and into the longitudinal section of the SR (Ebashi and Lipmann, 1962). In the absence of transsarcolemmal calcium entry, the sequestered calcium will accumulate in the terminal cisternae of the SR and allow the muscle to relax. Another mechanism of calcium removal

from the cytosol is through sarcolemmal calcium ATP-ase however this is probably not fast enough to explain the fast relaxation times (Bers *et al*, 1993). A final mechanism is via forward mode sodium-calcium exchange. During the repolarization phase, the sodium-calcium exchanger has been shown to play a role in promoting an inward current during phase 3 in rat ventricular muscle (Schouten and Ter Keurs, 1985), slowing the repolarization of the action potential. Inward current is produced by the inward movement of three sodium atoms per atom of calcium removed from the cytosol, causing a net inward current during forward mode. The result is the removal of calcium from the cytosol. At the end of the action potential the cytosolic calcium concentration should be at least high enough to promote further calcium release from the SR via stimulation of the ryanodine receptors. In spite of this, the muscle is able to relax. It is likely that due to the clustering of ryanodine receptors and sodium-calcium exchange sites, sodium-calcium exchange plays an important role in preventing calcium induced calcium release at the end of the action potential by removing calcium from the vicinity of the ryanodine receptors.

MECHANISMS FOR POSITIVE INOTROPY: PLAN OF WORK

Contraction is the end result of an interaction between calcium and troponin C (Katz, 1977). To produce positive inotropy a compound must either increase the amount of calcium bound to troponin C, or increase the force of contraction brought about by a given amount of calcium bound to troponin C. The mechanisms of inotropy may be grouped into those of intracellular origin, and those of sarcolemmal origin.

INTRACELLULAR SOURCES

Several mechanisms produce positive inotropy without increasing the amount of calcium entering through the sarcolemma. An increase in the affinity of the binding of calcium to troponin C or a decrease in calcium buffering in the vicinity of the myofilament (such as with caffeine, Wendt and Stephenson, 1983; or with cytosolic pH changes, Fabiato and Fabiato, 1978), will both increase the number of sites with calcium bound to them and result in positive inotropy. Saponification or permeabilization of the tissue allows one to clamp calcium concentration in the cytosol and prevent contributions from SR calcium release or from sarcolemmal calcium entry. In permeabilized canine ventricular trabeculae (With 0.1% Triton-x100) it was determined that phenamil does not change the sensitivity of the myofibrils to calcium (unpublished results). Whether phenamil changes cytosolic pH to modulate the binding affinity of troponin C to calcium has not been previously tested.

Tissues can be made to contract biphasically by replacing 95% of the calcium with strontium (King and Bose, 1983). Strontium can enter the cells through the sarcolemmal calcium channels but it does not inactivate these channels. The 5% calcium that enters during the long action potentials is not sufficient to inactivate calcium channels. However, it partially replenishes the SR calcium pools and provides a trigger for the release of calcium from the SR. This results in two phases of contraction. The first phase comes from release of calcium from the SR which is induced by the small amount of calcium entering the cell during the action potential. The second phase results from the eventual transsarcolemmal accumulation of strontium. Compounds that can increase calcium

storage in the SR will preferentially increase the first phase of contraction. Compounds that can increase endogenous sensitivity to calcium and strontium will increase both phases equally. Compounds that can potentiate or prolong calcium entry through the sarcolemma, or reduce calcium removal from the cells will preferentially increase the second phase of contraction.

Drugs that increase calcium release from or increase calcium uptake into cytosolic stores (SR) are capable of producing inotropy by increasing the amount of calcium released into the cytosol upon stimulation. Calcium uptake into the SR is accomplished by a calcium ATP-ase in the SR membrane. This calcium pump is inhibited by cyclopiazonic acid (CPA) (Baudet *et al*, 1993) and thapsigargin (Kijima *et al*, 1991). In the presence of inhibitors of the SR calcium ATP-ase, compounds that enhance calcium accumulation into the SR will no longer be capable of producing inotropy. Calcium release sites are controlled by a number of agonists and antagonists. Ryanodine is capable of maintaining these release channels open and eventually depletes the SR of calcium. In the presence of ryanodine, compounds that produce inotropy by enhancing calcium release from the SR will be ineffective in producing inotropy.

Cooling of the tissue causes inhibition of ATP-dependent processes, and of sarcolemmal calcium transport mechanisms (Bers *et al*, 1989). Rapid cooling causes an apparent release of calcium from the SR possibly from a backward leak through the calcium uptake channels and not through ryanodine-sensitive channels (Feher and Rebeyka, 1994). During the cooling calcium is not taken back into the SR since it is an

ATP-dependent process, and the membrane exchange process does not function at very cold temperatures. This produces a contracture at the low temperature (RCC) and the amplitude of the contracture is an index of the amount of calcium that was present in the SR immediately before cooling (Bridge, 1986). SR calcium content may be enhanced by a number of mechanisms, including increased sarcolemma calcium entry.

During diastole calcium is taken up into the longitudinal SR and must be transferred to the terminal cisternae to be available for release. A basic stimulus interval of 0.5Hz in canine tissue is not sufficient to allow all the calcium taken up in the longitudinal cisternae of the SR to be transported to the terminal cisternae of the SR. A short rest period inserted into a train of stimuli allows more calcium to be transferred to the terminal cisternae and more calcium will be released during the first stimulus after the rest. Post-rest contractions are therefore potentiated with respect to the contraction before rest. Compounds that increase cytosolic calcium levels during resting state will increase the amount of calcium taken into the SR to produce positive inotropy and potentiate post-rest contractions (e.g.: cardioactive glycosides, Weir and Hess, 1984). Compounds that promote calcium leak from the SR, such as BAY K 8644 (Hryshko *et al*, 1989) will attenuate the post-rest contraction.

TRANSSARCOLEMMA CALCIUM ENTRY.

Drugs that increase calcium entry or decrease calcium removal through the sarcolemma are capable of producing inotropy in the absence of SR function, but will not be capable of increasing contractile strength when the sarcolemma is saponified or

permeabilized. Sarcolemmal calcium entry may occur either through calcium channels, or via sodium-calcium exchange. Positive inotropy may be produced by either enhancing calcium movement through L-type calcium channels, such as with BAY K 8644 (Hryshko *et al*, 1989) or by inhibition of the forward mode or enhancement of reverse-mode of sodium-calcium exchange.

These two transsarcolemmal calcium transport systems can produce positive inotropy by indirect mechanisms as well. Two commonly discussed mechanisms of positive inotropy are cytosolic sodium build-up, such as with ouabain or other cardioactive steroids (Weir and Hess, 1984) and prolongation of the action potential by inhibition of potassium channels (Kennedy *et al*, 1986). Compounds that interfere with ionic currents of the sarcolemma also produce changes in the profile of the action potential. Measurements of the action potential will therefore provide reasonable predictions of the effects of an inotrope on the sarcolemmal ionic processes.

GENERAL HYPOTHESES

Unpublished observations with permeabilized canine trabeculae suggested that calcium sensitivity of myofibrils was not altered by phenamil. Therefore the general hypothesis was that phenamil produces positive inotropy by increasing the amount of calcium available for contraction. It was further hypothesized that phenamil affects transsarcolemmal calcium movement as opposed to increasing SR calcium uptake or release. This hypothesis was tested with a series of experiments designed to separate and

measure the effects of the two pools of calcium on contraction. The following section describes the possible mechanisms for the production of positive inotropy. Once it was determined that the inotropic effect of phenamil was of a sarcolemmal origin, a second series of experiments was performed to determine the mechanism by which calcium may enter the cells. Three hypotheses for the mechanism of transsarcolemmal calcium entry were tested. 1) Phenamil enhances calcium entry through L-type calcium channels. 2) Phenamil does not directly affect the calcium entry pathways, but prolongs the action potential to increase the duration of calcium entry into or decrease the amount of calcium removal from the cells. 3) Phenamil enhances calcium entry through sodium-calcium exchange or through some mechanism that affects sodium-calcium exchange. More specific hypotheses for each series of experiments are mentioned in the results section.

MATERIALS AND METHODS

Mongrel dogs of either sex (8-12 Kg) were anesthetized with sodium pentobarbital (30 mg/kg i.v.). The portal vein was removed via a midline abdominal incision. The heart was removed via a lateral intercostal incision. The tissue was quickly rinsed with and placed into cold (4°C) Krebs solution. Thin free-running canine right ventricular trabeculae less than 1 mm thick were tied at either end using number 5 silk thread, then were dissected from the free wall of the dog heart.

Guinea pigs (200 to 350 mg) or rats (250 to 350 mg) were made unconscious by cervical dislocation and the heart was quickly removed by an incision along the diaphragm and separation of the thorax by two lateral cuts. This allowed complete removal of the heart from the animal and rinsing with cold Krebs solution in 1 to 1.5 minutes after cervical dislocation. Guinea pig or rat right ventricular papillary muscle was tied with number 5 silk thread and dissected free of the heart. Guinea pig hearts that were used to obtain cells for the measurement of ionic membrane currents were removed from the animal and suspended directly onto a Langendorff apparatus without intermediate cooling.

Caution was used to avoid excessively stretching the muscle during tying and dissection. Stretched muscles were found to have a gradually rising baseline tension during measurement of twitch tension.

SMOOTH MUSCLE

TISSUE PREPARATION

Canine portal vein was cut free of connective tissue (tunica serosa) then cut into longitudinal strips 1 mm wide and 10 mm long while submersed in Krebs Henseleit solution (in mM: NaCl 118, KCl 4.72, $MgSO_4$ 1.2, KH_2PO_4 1.4, $CaCl_2$ 2.5, glucose 11 and $NaHCO_3$ 25, pH 7.4). The endothelium was removed mechanically by blotting the surface of the tissue with Kim-wipes. The smooth muscle strips were suspended vertically in a 5 ml organ bath by threads tied to a steel wire loop at the bottom and to a mechanical force transducer (Grass FT03) at the top. The L_o or the length required for maximal active tension development during electrical stimulation was found to be at a resting tension of 1g. The preparation was allowed to equilibrate for one hour in Krebs solution aerated with 95% O_2 and 5% CO_2 at a pH of 7.4 at 37°C with a preload of 1g. Signals of muscle tension were amplified and recorded by a Grass 4-channel chart recorder (Grass Polygraph 5, Model 5C) or 6-channel brush recorder (Gould Inc., Bedford, Mass, USA).

EVALUATION OF SODIUM-POTASSIUM PUMP INHIBITION

The procedure using a portal vein preparation to test for sodium-potassium pump inhibition was similar to that described by Bose and Innes (1973) for smooth muscle. After one hour equilibration, the solution was replaced with potassium-free Krebs Henseleit solution in order to inhibit the sodium-potassium pump and cause sodium-loading of the smooth muscle. The resulting depolarization and reversal of sodium-

calcium exchange led to an increase in tone of the muscle. Restoration of potassium caused immediate relaxation of the preparation due to reactivation of the sodium pump. Test drugs were added after the tension stabilized in potassium-free Krebs Henseleit solution. After one hour in the presence of the drug, potassium (5 mM) was restored to reactivate the pump.

CARDIAC MECHANICAL STUDIES

TISSUE PREPARATION

Isolated muscle preparations were transferred to 5 ml vertical organ baths containing oxygenated (95% O_2, 5% CO_2) Krebs Henseleit solution maintained at 37°C and at pH 7.4. The muscle was tied at one end to a force transducer (Grass FT 03C) and anchored to the bath at the other end. Muscles were stretched to an optimal length for maximal isometric force production during a 45-60 min equilibration period. Tension traces were recorded on a Grass 4-channel chart recorder (Model 5D Polygraph, Grass Instrument Co., Quincy, Mass., USA). Muscles were field stimulated with rectangular pulses through two stainless steel electrodes adjacent to the muscle. The train of stimuli was generated from a computer-controlled stimulus sequencer (Boyechko and Bose, 1982) where a computer-driven TTL signal initiated first a calibration step to 0 mV for 5 msec, then to -50 mV for a further 5 ms. The Haer stimulator was driven by the TTL signal, but the stimulus was delayed until after the calibration steps, and was timed so that the stimulus artifact was partially hidden by a sample-and-hold circuit immediately after

the last calibration step. A calibration step was performed with each stimulus. Canine trabeculae were stimulated with a basic cycle length of 2000 ms (0.5 Hz), 2 ms pulse duration, at an amplitude approximately 100% greater than threshold. Up to four trabecular preparations per dog were used simultaneously. In the majority of experiments, one of the four tissues was used as a time-based control. A dose response relationship with phenamil was obtained using individual non-cumulative concentrations of phenamil (2 μM to 120 μM).

POST-REST CONTRACTIONS

The trabeculae were stimulated continuously at a basic cycle length of 2000 ms. Into this continuous train of stimuli was inserted a short rest period from 5 seconds to 4 minutes in duration. The tissue was allowed to reach steady state twitch tension before another rest period was imposed.

The stimulator was computer driven using software that allowed different trains of stimuli to be sequenced. Each train had a programmable initial delay, number of stimuli in the train, basic cycle length, and stimulus duration. Four signal amplifiers were controlled simultaneously by the software, and served as four independent stimulators. Each stimulator had a voltage control that allowed adjustment of the stimulus strength to 200% above threshold for producing a contraction twitch.

BIPHASIC CONTRACTIONS

Biphasic contractions in canine trabeculae were produced as described by King and Bose (1983). Trabeculae were equilibrated in Krebs Henseleit solution by stimulating at 0.5 Hz for one hour. This was followed by replacement of the solution with a calcium-free solution containing strontium (2.5 mM). A small amount of calcium (about 50 to 200 μM, 5-10% of the normal) was then added to maintain a stable biphasic contraction. The early and late phases of contraction, P1 and P2, had approximately equal tensions before the test drugs (Phenamil, norepinephrine, ouabagenin, or 4-aminopyridine) were added.

RAPID COOLING CONTRACTURES

Canine ventricular trabeculae were suspended in a 2 ml horizontal bath machined from a solid piece of nylon and perifused with a HEPES-buffered solution (in mM: NaCl 128; KCl 4.3; $CaCl_2$ 2.5; $MgCl_2$ 2.0; HEPES 20; Dextrose 10). The muscle was tied on one end to a stainless steel extension from a tension transducer (Grass FT03C), and anchored on the other end to a stainless steel rod attached to a micromanipulator to allow fine adjustment of preload tension. The muscle was stretched to a preload tension of 0.5 g.

Figure 5 is a schematic representation of the apparatus for producing rapid temperature changes. Two jacketed reservoirs maintained 60 ml of solution at 0°C and 30 ml of solution at 38°C. In order to maintain the cold temperature without freezing the water in the water bath, antifreeze was added to the water bath. Two manual switches at

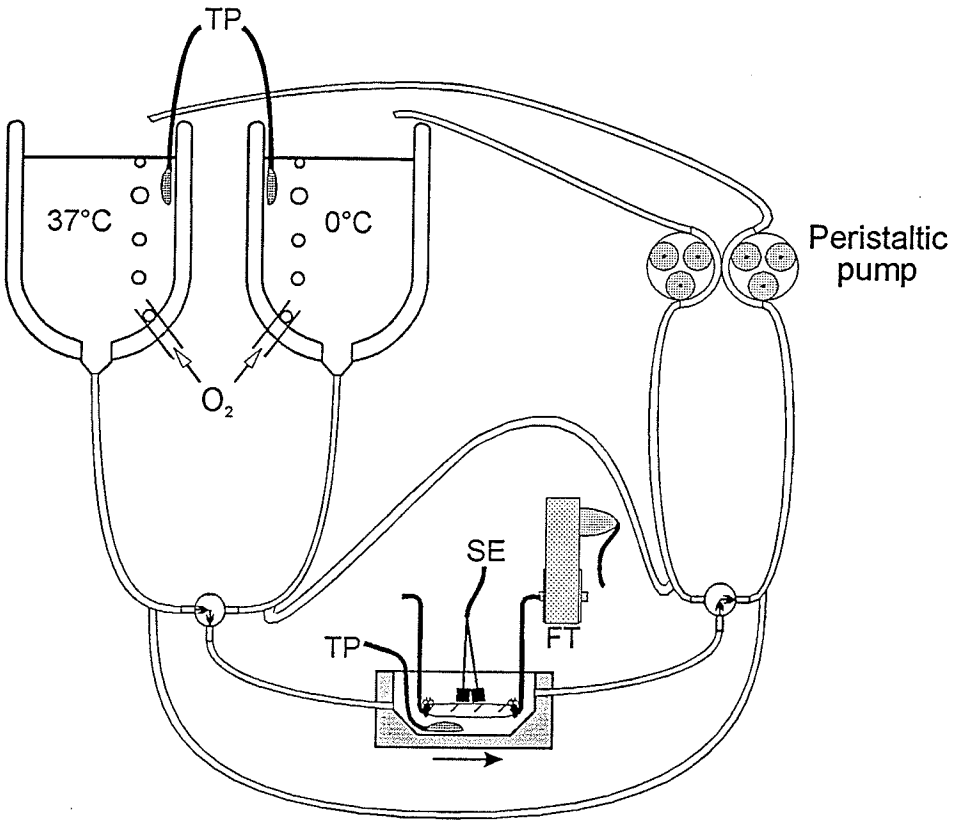

Figure 5

Apparatus for producing rapid cooling contractures. Solutions were maintained at 38°C or at 0°C (total circulating volume of 30 ml or 60ml respectively) in water-bathed chambers. Antifreeze was added to the 0°C water bath to prevent freezing. Temperature loss in tubing was minimized by insulation on the tubing, and by maintaining a high flow rate (300mL per minute). Mixing time was minimized by a small bath volume (2mL) and a short distance from the switch to the bath (5cm). Switching was done manually. Solution not being circulated through the bath was bypassed in order to prevent dead space of solution with uncontrolled temperature or unoxygenated. Air inlets in the bypass system adjusted the circulating volume so as to maintain the same volume in the bathed chamber. This aparatus allowed a 95% change in temperature inside the tissue chamber within one second. The muscle was suspended in the tissue chamber with one end tied to a force transducer (**FT**) and the other to a stainless steel adjustable anchor. The muscle was stimulated by field stimulation with tungsten stimulation electrodes (**SE**). Temperature was measured in each holding chamber, and inside the bath by the use of temperature probes (**TP**).

either side of the tissue chamber selected whether the muscle was perifused with cold Krebs HEPES or with warm Krebs HEPES solution. The solutions were allowed to flow by gravity at approximately 300 to 400 ml/min, which was sufficient to change the temperature of the medium in the tissue chamber from 37°C to 7°C or from 4°C to 35°C within one second of switching. Five seconds of flow resulted in a stable temperature of 4°C or 37°C at the tissue chamber. Temperature was measured at the outflow end of the tissue chamber, and in each of the two reservoirs. At the outflow end, a Cole-Palmer roller pump returned the solution to the reservoirs. Solution not passing through the chambers was passed through a bypass circuit in order to maintain well oxygenated solution and to keep a constant temperature in each circuit. All tubing was insulated with pipe insulation. The flow of solution was adjusted with a clamp so that, at a single pump speed setting, the flow from each of the reservoirs was just sufficient to almost equal but remain slower than the pump speed. A 22-gauge needle was placed into the bypass system to allow air intake into the solution which was not circulating through the chamber. This allowed the level of solution in each of the reservoirs to be constant, and hence the surface area of solution in contact with a heating or cooling surface was kept constant.

The trabeculae were stimulated with 10 ms square pulses at a voltage 50% over threshold, and paced at a basic cycle length of 2000 ms (model SD5 Stimulator, Grass Instruments, Quincy, Mass., U.S.A.). One second before switching to cold solution the stimulator was stopped. The tissue was perifused with cold Krebs HEPES solution for 30 seconds, then switched back to 37°C for one minute without stimulation. After this rest period a second cooling was imposed for a further 30 seconds. This procedure was

repeated once more for a total of three rapid cooling contractures (RCC). At the end of the third contracture the muscle was allowed to rest for 30 seconds before the stimulator was restarted. Only the first two RCC were used for measurements and are referred to as twin RCC. The experimental protocol involved the following in chronological order: a) equilibrate the muscle for an hour, b) do control twin RCC, c) equilibrate in 50 μM phenamil for an hour, d) do twin RCC, e) wash the drug out and equilibrate for an hour, f) do twin RCC, g) equilibrate with 14.3 mM total KCl for 20 minutes, h) do twin RCC, i) wash out the extra KCl and equilibrate for an hour, j) do twin RCC, k) equilibrate in 3 μM ouabagenin until maximum inotropy is reached, and l) do twin RCC. Tension traces were simultaneously recorded on a 4-channel chart recorder (Grass Polygraph 5, Model 5C), and, through a signal reverter (Grass, model R5DC), and sampled digitally (Scientific Solutions Labmaster DMA A-D Converter with Axotape software, Axon Instruments, California, USA). Data was stored on a computer hard disk for later analysis of RCC peaks.

FLUORESCENCE: CYTOSOLIC PH

A calibration method which is dependent on the amount of dye left in the cells has been described for smooth muscle (Yu *et al*, 1991). However, this approach does not work reliably with cardiac muscle and had to be modified. To assess cardiac cellular pH_i, a technique was developed which compensates for dye leakage seen in cardiac tissue during long experimental protocols. This was necessary for evaluating if phenamil produces positive inotropy by increasing cytosolic pH by modulating sodium-hydrogen

exchange. The *in situ* calibration curve of BCECF in cardiac tissue was found to be sensitive to the amount of dye present at the time of measurement. An adjustment was made to the calibration curve based on the amount of dye present inside the cells.

Tissue preparation

Canine right ventricular trabeculae were isometrically suspended in a horizontal bath of a Jasco model TI02 tissue fluorescence measuring assembly with the light beam from a Jasco model CAF100 intracellular ion analyzer (Jasco Inc., Easton, Maryland) focused on its undersurface. One end of the trabeculae was tied to a Grass FT03 force transducer (Grass Instrument Co., Quincy, Mass.), and the other end was anchored to the horizontal bath. Stainless steel stimulation electrodes were placed on either side within 5 mm of the muscle to provide field stimulation at a site away from the light beam. The muscles were stimulated at 0.3 Hz with a voltage 50% above threshold. The 3 x 5 cm horizontal bath had an aeration inlet and recirculation inlet and outlet; it was kept at 37°C with a Peltier effect thermoelectric device. The solutions were recirculated at 25 ml/min to external water-jacketed reservoirs at 37°C. A temperature probe and miniature pH probe (MI404, M440, Microelectrode Inc., Londonderry, NH) were placed in the bath adjacent to the muscle.

Equipment

A schematic representation of the apparatus used is shown in figure 6. Light from the 50 Watt lamp of the Jasco CAF100 fluorimeter passed through a rotating filter assembly

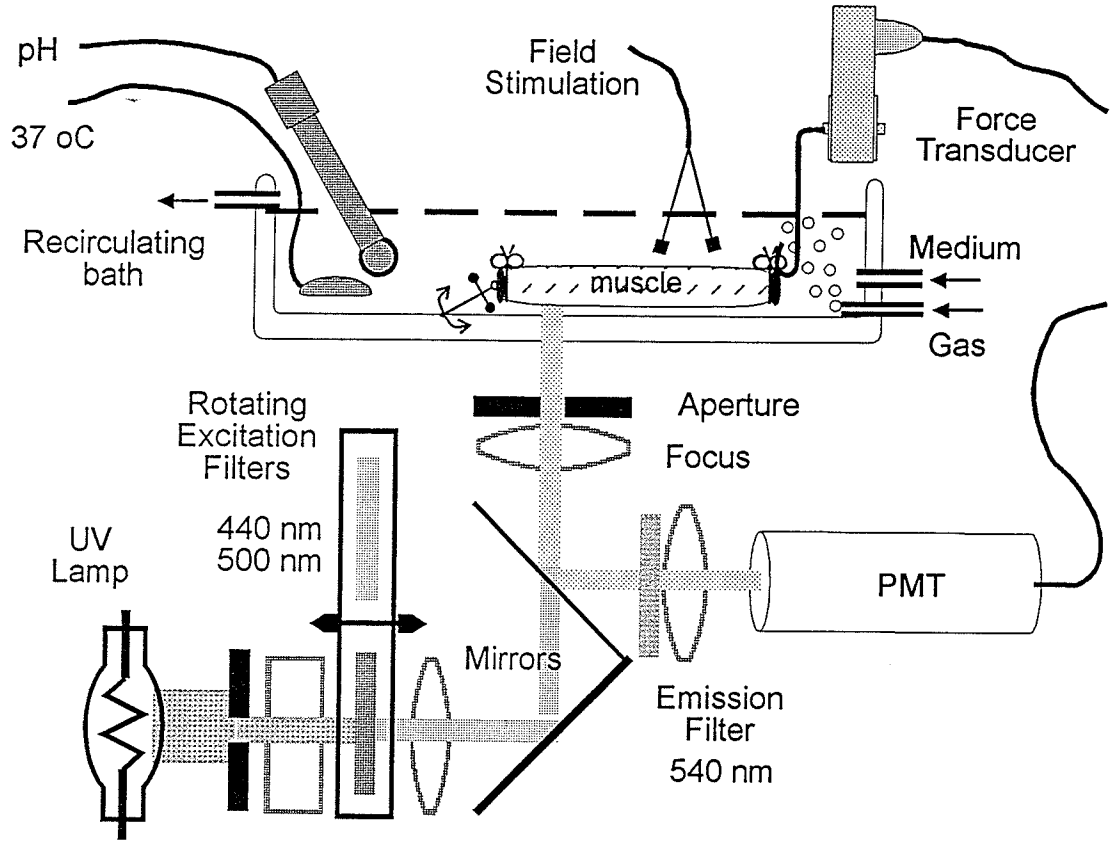

Figure 6

Aparatus for measuring cytosolic pH simultaneously with contractile tension in trabeculae. Ventricular trabeculae were isometrically suspended in the horizontal bath of a Jasco Model TI02 tissue fluorescence measuring assembly with one end tied to a grass FT03 tension transducer and the other anchored to the bath with a thread. Temperature and pH of the medium was measured adjacent to the muscle. Stainless steel electrodes provided field stimulation at a locus away from the light beam. Light of a Jasco CAF-100 intracellular ion analyzer passed through a rotating filter assembly alternately placing a 500 nm or a 440 nm filter into the light path. The excitation light was reflected and focused on the surface of the tissue. Emission light was collected along the same path, but light greater than 500 nm wavelength was reflected and passed through a 540 nm filter onto a photomultiplier tube (PMT) for measurement.

which placed either a 440 nm or 500 nm filter into the light path. The incident light at 440 nm or 500 nm was reflected from a mirror on the Jasco TI02 and focused on the muscle surface through a quartz glass window. Epifluorescence returned along the same path and was reflected from a mirror through a 540 nm filter, and focused on the photomultiplier tube (PMT) of the Jasco CAF100 for measurement. Fluorescence emission at each excitation wavelength (FI_{500}, FI_{440}), fluorescence ratio (FI_{500}/FI_{440}), tension, temperature, and pH were measured simultaneously and recorded on a 6-channel chart recorder (model SE-400, BBC-Metrawatt/Goerz, Broomfield, Colorado).

Dye loading

The tissues were bathed in recirculating Krebs-Henseleit bicarbonate-buffered (Bicarb) solution or HEPES-buffered (HEPES) solution (same composition except that $NaHCO_3$ was replaced with 25 mM HEPES, pH 7.40). The bath had 5 ml volume; total recirculating volume was 20 ml. After equilibration at optimal preload tension (L_O), in either Bicarb or HEPES solution bubbled with either 95% O_2—5% CO_2 or 100% O_2 respectively, at 37°C, the muscles were exposed to a final concentration of 8 μM 2',7'-bis(carboxyethyl)-5,6-carboxyfluorescein acetoxy methyl ester (BCECF-AM). BCECF-AM is capable of adsorbing on the cell membrane, and will randomly distribute between the intracellular and extracellular facets of the membrane. Intracellular esterases cleave cytosolic BCECF-AM and trap BCECF free acid inside the cells. BCECF in buffer solution has a peak emission at 540 nm when excited with 500 nm light (FI_{500}). This fluorescence is pH sensitive, exhibiting higher intensity at higher pH values. Fluorescence

at 540 nm emission with 440 nm excitation (FI_{440}) is not pH sensitive in the buffer and may be used as an indication of dye concentration. BCECF-AM does not contribute to the fluorescence at FI_{500} or FI_{440}, hence liberation of free BCECF acid inside the cells results in an increase in FI_{440}. In one to two hours, the cells in the trabeculae were loaded with BCECF after which the tissues were washed with five changes of fresh solution over 30 minutes to remove any BCECF-AM and BCECF from outside the cells before any experiments were performed. Autofluorescence accounted for 75%±3% of the total signal at 440 nm, and 12%±1% at 500 nm (n=9). Autofluorescence was subtracted from the total fluorescence measurements.

Experimental protocol

BCECF free acid, untreated trabecular tissue, or BCECF-loaded tissue was added to, or mounted in a cuvette containing oxygenated HEPES-buffered medium and their excitation and emission fluorescence spectra were obtained using the Perkin-Elmer Spectrophotometer. The unstimulated muscles were stretched to 0.5 to 0.7 grams preload tension. The progression of loading after the addition of 8 μM final concentration of BCECF-AM was monitored in two tissues by performing multiple scans over a 95 minute period. Spectral scans were also obtained in HEPES-buffer acidified with acetic acid or alkalinized with NaOH medium to different pH values. A similar protocol was performed in the absence of trabeculae: five different concentrations of BCECF free acid in an intracellular electrolyte solution (120 mM KCl, 1 mM $MgCl_2$, 25 mM HEPES, pH 7.00) were exposed to different pH values and fluorescent spectra were scanned.

In separate experiments, different concentrations of BCECF free acid were added to a solution of intracellular electrolytes (contents above) in the Jasco CAF-100. Fluorescence measurements were made (540 nm emission with 440 nm or 500 nm excitation) at different medium pH values (with NaOH/HCl)

During calibrations, the muscles were pH-clamped using 4.5 μM nigericin and 80 mM potassium (Eisner *et al*, 1989; Yu *et al*, 1991). The dye fluorescence was measured at steady state after changing the pH of the bathing solution. Calibrations were performed at various times between 1 and 16 hours after loading with BCECF. Four tissues were subjected to repeated calibrations at various times over a 12 hour period. One tissue was tested 24 hours after loading with BCECF. Calibrations were also performed using 4.5 μM nigericin and different KCl concentrations for each pH calibration. In two trabeculae the medium pH and 4.5 μM nigericin were maintained constant and KCl was added in 40 mM concentration steps.

In verifying that we were measuring cytosolic pH, the medium was acidified by addition of ammonium chloride, (+) lactic acid or acetic acid from 10 mM stock solutions, or by bubbling 100% CO_2 in the medium.

Spectral characteristics of BCECF

The fluorescence spectra (figure 7) were scanned with a Perkin-Elmer Fluorescence Spectrophotometer (model LS-5, Oak Brook, Illinois) using a 5 mm slit width. The

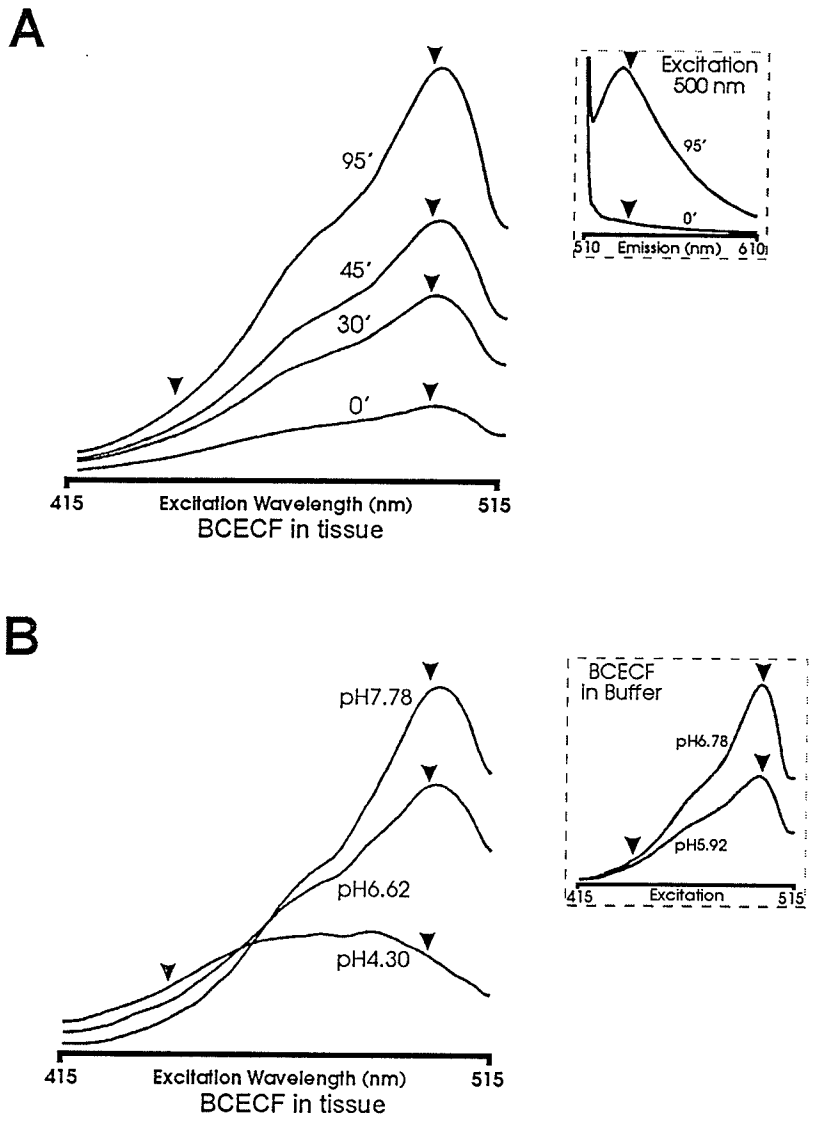

Figure 7

Fluorescence scans of BCECF were done in a Perkin Elmer Spectrofluorimeter. Excitation spectra between 415 nm and 515 nm are shown with emission measured at 540 nm. Scans were done with a 5 mm slit width and light intensity was plotted in arbitrary units as a function of wavelength (λ). Arrows indicate FI440 at 440 nm and FI500 at 500 nm. HEPES buffer solution was maintained at 37°C. **A**. The fluorescence excitation spectrum of a ventricular trabeculum at pH 7.45 before (**0'**) and after the addition of 8 μM BCECF AM for 30 minutes (**30'**), 45 minutes (**45'**), and 95 minutes (**95'**). The excitation peak in the tissue was at 507 nm, and in buffer at 502 nm. *Inset*: The emission scan from 510 nm to 610 nm with excitation at 500 nm. Spectra are shown from tissue alone (**0'**) and with BCECF AM (**95'**) at pH 7.45. Arrows indicate FI500 at 540 nm. The emission peak in the tissue was at 532 nm, and in the buffer at 527 nm. **B**. Fluorescence excitation spectrum of a trabeculum loaded with BCECF at pH 7.78, 6.62, and 4.30. The isosbestic point occurs at 463 nm. *Inset*: 0.58 μM BCECF free acid in a buffer of cytosolic electrolyte concentrations at pH 6.78 and pH 5.92. The isosbestic point occurs at 415 nm.

sample chamber of the Spectrophotometer was adapted to accommodate an aeration tube and tissue suspension hooks inside a 1 cm square cuvette.

The addition of BCECF-AM to the bathing medium results in incorporation of BCECF into the cells of the trabeculae (figure 7A), producing maximal fluorescence emission at 532 nm (figure 7A, inset) with excitation at 507 nm (figure 7B). Maximal emission of fluorescence of BCECF free acid in a high potassium intracellular electrolyte buffer solution occurs at 527 nm when excited at 500 nm (figure 7B, inset), therefore there was a shift in the peaks to 532 nm emission with 500 nm excitation inside the muscle. There was also a shift of the isosbestic point from 440 nm to 463 nm in the excitation spectra (540 nm emission) (figure 7B). Since the isosbestic point is shifted when the dye is loaded intracellularly, calibrations must be done with BCECF in situ. BCECF free acid was added to the high potassium electrolyte buffer solution until the change in FI_{440} was equal to the average change in FI_{440} seen at the completion of tissue loading with BCECF-AM. Cytosolic BCECF was estimated to be 0.58 μM. BCECF-AM in solution or solution alone did not exhibit pH-dependent changes in fluorescence in the range measured. Before dye-loading, tissue exhibited less than 3% of the pH-dependent fluorescence of tissue loaded with BCECF.

Calibration technique

Dissociated $BCECF^-$ exhibits maximal fluorescence ratio (R_{Max}) whereas BCECF-H has minimal fluorescence ratio (R_{Min}). The proton activity can be calculated by equation [1] (James-Kracke, 1992).

$$[H^+] = K_a \times \frac{(R_{Max} - R)}{(R - R_{Min})} \times \frac{F_{440_{BASE}}}{F_{440_{ACID}}} \qquad [1]$$

$F_{440BASE}/F_{440ACID}$ ratio (the ß factor) was calculated at 0.681 for BCECF *in situ* and was not affected by the amount of dye loaded. Since the ß factor was a constant, it was combined with the dissociation constant, K_a, to produce the apparent dissociation constant, K_a'. A Henderson-Hasselbach logarithmic transformation of equation [1] yields equation [2] which is used to fit calibration curves.

$$pH_i = pK_a' - \log\frac{(R_{Max} - R)}{(R - R_{Min})} \qquad [2]$$

Figure 8A shows the pH-dependence of the ratio of fluorescence of various concentrations of BCECF free acid in a high potassium intracellular electrolyte medium. Calibration curves were constructed by plotting the fluorescence ratios against the pH of the bathing medium and fitting the data to equation [2] using a χ^2 method of least squares. PKa' was found to be 6.968±0.027 (n=5). Since FI_{440} may be linearly correlated with dye concentration (r^2=0.98, data not shown), we used FI_{440} to represent dye concentration. Different concentrations of BCECF in solution produce linearly correlated R_{Max} values (figure 8B; intercept = -22.5, slope = 0.202, r^2=0.988). There is comparatively little change in R_{Min} with the different concentrations of BCECF (intercept = 0.701, slope = -0.003, p>0.05).

During the course of experiments with BCECF loaded in the trabeculae, FI_{440} showed a slow, progressive decline of about 30% per hour. This decline was also observed in the

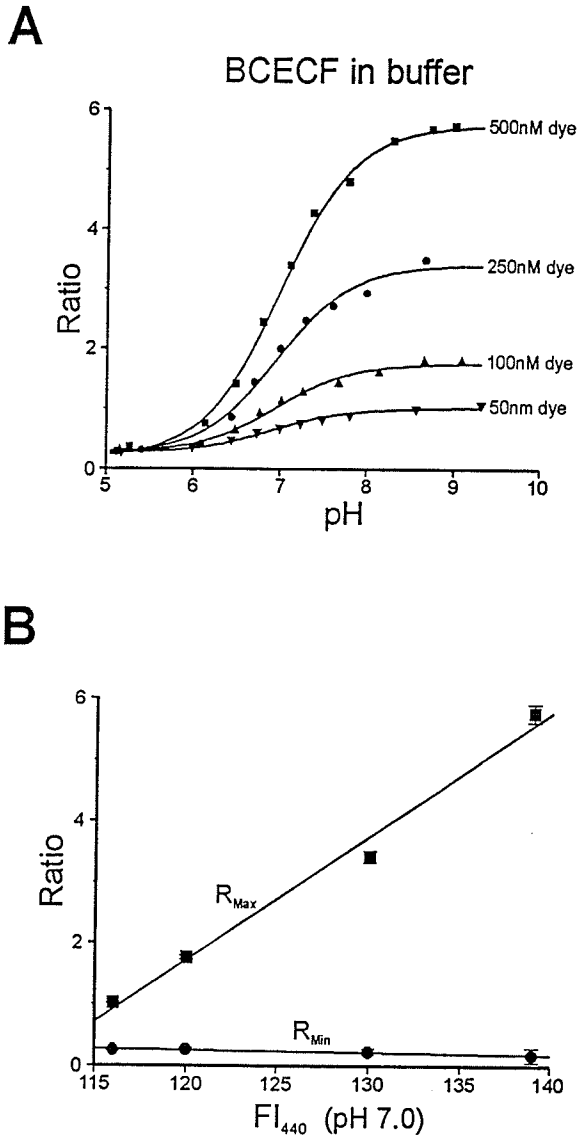

Figure 8

Multiple calibrations were done with different concentrations of BCECF free acid in high potassium intracellular electrolyte solution. **A.** The steady-state fluorescence ratio (Jasco CAF100 fluorimeter) of FI_{500}/FI_{440} is plotted against pH. The lines are described by a best fit to equation [2] using a χ^2 test (see text). Concentration of free acid is indicated to the right of each plot. **B.** The parameters of the best fit lines in A, R_{Max} and R_{Min}, are plotted against FI_{440}, representing the amount of dye, measured at pH 7.0 during the calibration. Lines were fit by linear regression (pKa, r^2= 0.988; ■, R_{Max}, r^2=0.99; ●, R_{Min}, r^2=0.96).

dark after the tissues were left in the recirculating bath for over eight hours. The drop in FI_{440} was more prominent during acidic to alkaline transitions in the bathing solutions. Thus this decrease in FI_{440}, or in BCECF, was considered to be largely due to leakage of the dye, and not due to photobleaching. Since there is a decrease in intracellular BCECF with time, equation [2] needs to be corrected to account for dye leakage.

At the end of each experiment the tissues were pH-clamped with nigericin, an ionophore selective for hydrogen and potassium ions, and 80 mM KCl (Eisner *et al*, 1989; Yu *et al*, 1991). The calibration curves for three different tissues are shown in figure 9A. The parameters from the best-fit curves in figure 9A were plotted against the amount of BCECF loaded in the tissue as indicated by FI_{440} at pH 7.0 (figure 9B) showing a similar correlation to that seen with BCECF free acid. For each experiment the curve had different R_{Max} and R_{min} values. The apparent dissociation constant (pK_a') did not change significantly in different experiments, hence it was taken as a constant. In our experimental conditions, the mean pK_a' from 23 tissues was 7.135±0.027. As was found with BCECF free acid, R_{Max} and R_{Min} of the tissue-loaded dye were both dependent on the amount of dye loading (figure 9B). A linear regression of R_{Max} and of R_{Min} with FI_{440} (plots shown in figure 9B) yields the correction equations [3] and [4].

$$R_{Max} = 1.652 + .0351 \times FI_{440} \qquad (r^2 = 0.989) \qquad [3]$$

$$R_{Min} = 0.3196 + .00859 \times FI_{440} \qquad (r^2 = 0.957) \qquad [4]$$

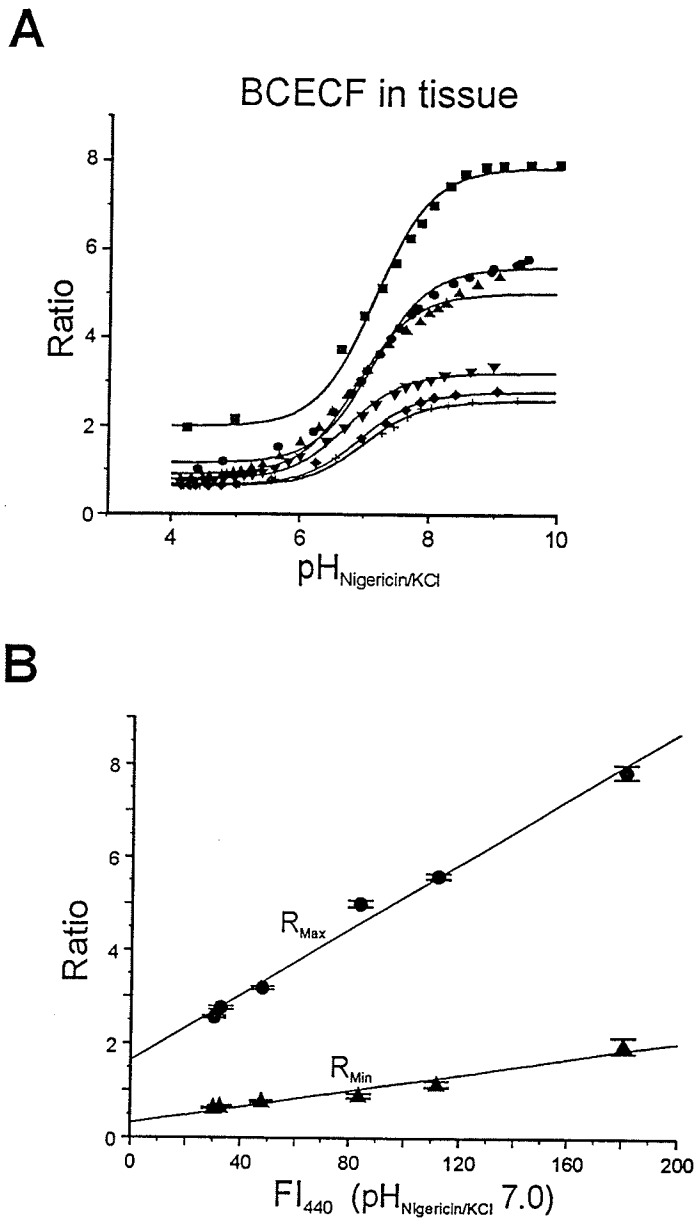

Figure 9

Multiple calibrations were done in BCECF-loaded canine ventricular trabeculae pH-clamped using 4.5 μM nigericin and 80 mM KCl. Six calibrations from 3 preparations are shown: 2 from each tissue. **A**. The steady-state fluorescence ratio (Jasco CAF100 fluorimeter) of FI500/FI440 is plotted against pH. The lines are described by a best fit to equation [2] using a χ^2 test. **B**. The parameters of the best fit lines in A are plotted against the amount of dye loading (FI440) measured at pH 7.0 during the calibration. Lines were fit by linear regression (●, R_{Max}, r^2=0.99; ▲, R_{Min}, r^2=0.96). Measurements were corrected for autofluorescence.

R_{Max}, is more sensitive to changes in BCECF concentration than is R_{Min}, however since the values of both R_{Max} and R_{Min} are important in equation [2], both correction equations were incorporated into the calculation of pH_i. The corrected formula for the calculation of pH_i incorporates equations [3] and [4] into equation [2] to yield equation [5].

$$pH_i = 7.135 - \log\frac{(1.652 + 0.0351 \times FI_{440} - R)}{(R - 0.3196 - 0.00859 \times FI_{440})} \qquad [5]$$

Due to the shift in the isosbestic point, the value of FI_{440} was also pH-dependent. The slopes and intercepts of the correction equations [3] and [4] are hence pH-dependent. Since the magnitude of the changes in FI_{440} with pH is small we assumed this variation to be insignificant. To calculate the amount of error produced by this assumption, we replotted the slope and intercept data in figure 9B using FI_{440} values measured at different medium pH values ranging from 6.5 to 8.5. The slopes and intercepts in equations [3] and [4] were themselves linearly correlated with pH (data not shown). The assumption that FI_{440} is not pH-dependent results in an error of 0.027 per calculated pH unit using equation [5] in the range of pH 6.5 to 8.5. The pH_i predictions using this equation would hence have a variability of 0.055 per unit of pH_i (contributed to by the pH-dependence of FI_{440} and by the variability in pK_a'), *i.e.*; 94.5% confidence. In the absence of any corrections for dye leak (using equation [2]), the calculated pH_i values were off by as much as 4 to 5 pH units if the measurement was made a few hours before the calibration.

Figure 10 shows the effect of changing potassium concentration on the calibration curves of tissue with 4.5 μM nigericin. In the same tissue, three consecutive calibrations were performed with different concentrations of KCl. Although there was a decrease in R_{Max} related to dye leakage, there was no change in the calculated pK_a' with 40 to 120 mM KCl. In a separate experiment on the same preparation but with pH was held constant, KCl concentration was increased from 40 to 140 mM in 20 mM steps (figure 10, inset). Fluorescence of BCECF-loaded tissue was not appreciably affected by different concentrations of KCl between 80 and 120 mM. Similar results were observed in two tissues. The use of a high-potassium solution of intracellular electrolytes, instead of adding KCl to HEPES-buffered solution, did not produce a calibration curve different from that done with the muscle in HEPES-buffered solution with KCl added.

Verification of the technique

The method was verified with intact, non-permeabilized canine ventricular trabeculae. Ischemia is commonly simulated *in vitro* by slowing or stopping perfusion thereby producing hypoxia and acidosis by modifying many parameters at once. Measurements of intracellular pH during ischemia-reperfusion have led to controversy over the mediators of cardiac tissue damage in ischemia-reperfusion experiments (Allen and Orchard, 1987; Bright and Ellis, 1992; Carter and Gavin, 1989; Cobbe and Poole-Wilson, 1980; Lazdunski *et al*, 1985). One of the possible reasons for discrepancies in the literature is the use of different buffering systems in the experimental protocols. We measured the effect of acidification on pH_i and tension recovery in the presence and absence of

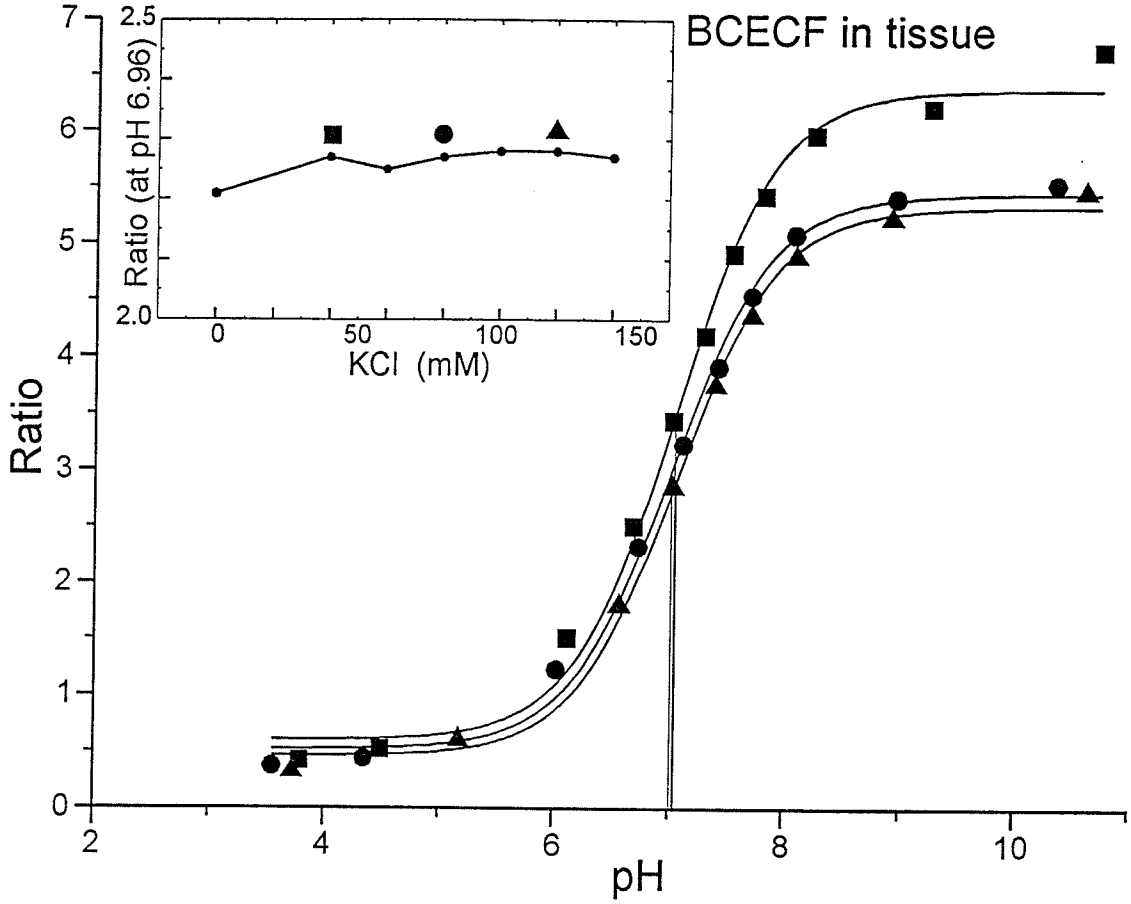

Figure 10
Multiple calibrations were done in BCECF-loaded canine ventricular trabeculae pH-clamped using 4.5 μM nigericin. Three calibrations from the same tissue are shown. The steady-state fluorescence ratio (Jasco CAF100 fluorimeter) of FI500/FI440 is plotted against pH. Different concentrations of KCl were used in each curve (■, 40 mM; ●, 80 mM; ▲, 120 mM). The lines are described by a best fit to equation [2] using a χ^2 test. Lines dropped to the pH axis indicate pKa of each curve. RMax, and RMin show dye leak-related changes. Inset shows the dependence of the steady-state fluorescence ratio on KCl concentrations (pH was kept constant at 6.96) stepped up to 140 mM.

bicarbonate in the buffer medium. The results show that in either buffer medium, prolonged intracellular acidification (45 minutes) with lactic acid or hypercapnia did not produce significant irreversible damage to the ventricular trabeculae, as judged by developed isometric contractile tension or intracellular pH.

To verify that we were in fact measuring cytosolic pH, NH_4Cl experiments were carried out. In six experiments using five different dogs, ammonium chloride changed the intracellular pH without affecting the extracellular pH (figure 11, pH_o, second trace from top). Upon addition of 10 mM NH_4Cl there was an immediate alkalization of the cytosol, followed by positive inotropy (figure 11, second trace from bottom, and bottom trace, respectively). After washout of NH_4Cl there was an immediate acidification of the cytosol, followed by the eventual return of pH_i and twitch tension to pre-exposure level. Twitch tension returned to pre-treatment level quickly whereas the return of pH_i was slower and outside the time-frame of figure 11. In bicarbonate-buffered solutions, it was difficult to change solutions without a small change in pH of the bathing solution, however, results were similar to those seen with HEPES-buffered solutions.

The dependence of pH_i on pH_o was found by changing pH_o either with CO_2 or acetic acid (figure 12). Figure 12 contains a typical trace from 5 experiments showing the effects of the addition of acetic acid (arrows) to the bathing medium. The pH_i, as indicated by the ratio (middle traces), follows pH_o (top traces), and the contractile strength follows pH_i (bottom traces). In Bicarbonate-buffered solutions, with each addition of acetic acid there was a rapid transient drop in pH_o followed by a return to

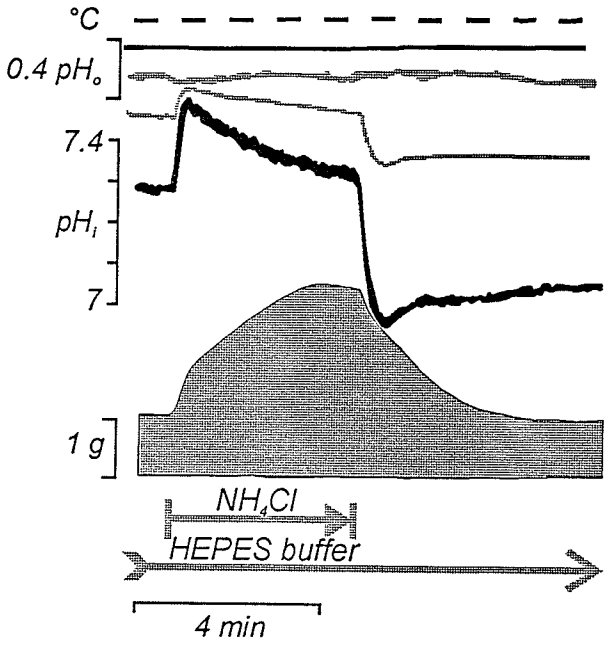

Figure 11
Sample tracings show the effects of a short pulse of NH_4Cl (10 mM) on the measured parameters of the function of canine ventricular trabeculae in HEPES-buffered medium. Lines from top to bottom represent temperature (Temp), pH of the bathing solution (pHo), FI_{440}, FI_{500}, cytosolic pH (pH*i*), and tension. Calibration bars from top to bottom describe pH*o*, pH*i*, and tension. Similar results were found in 6 experiments with 5 tissues from different animals.

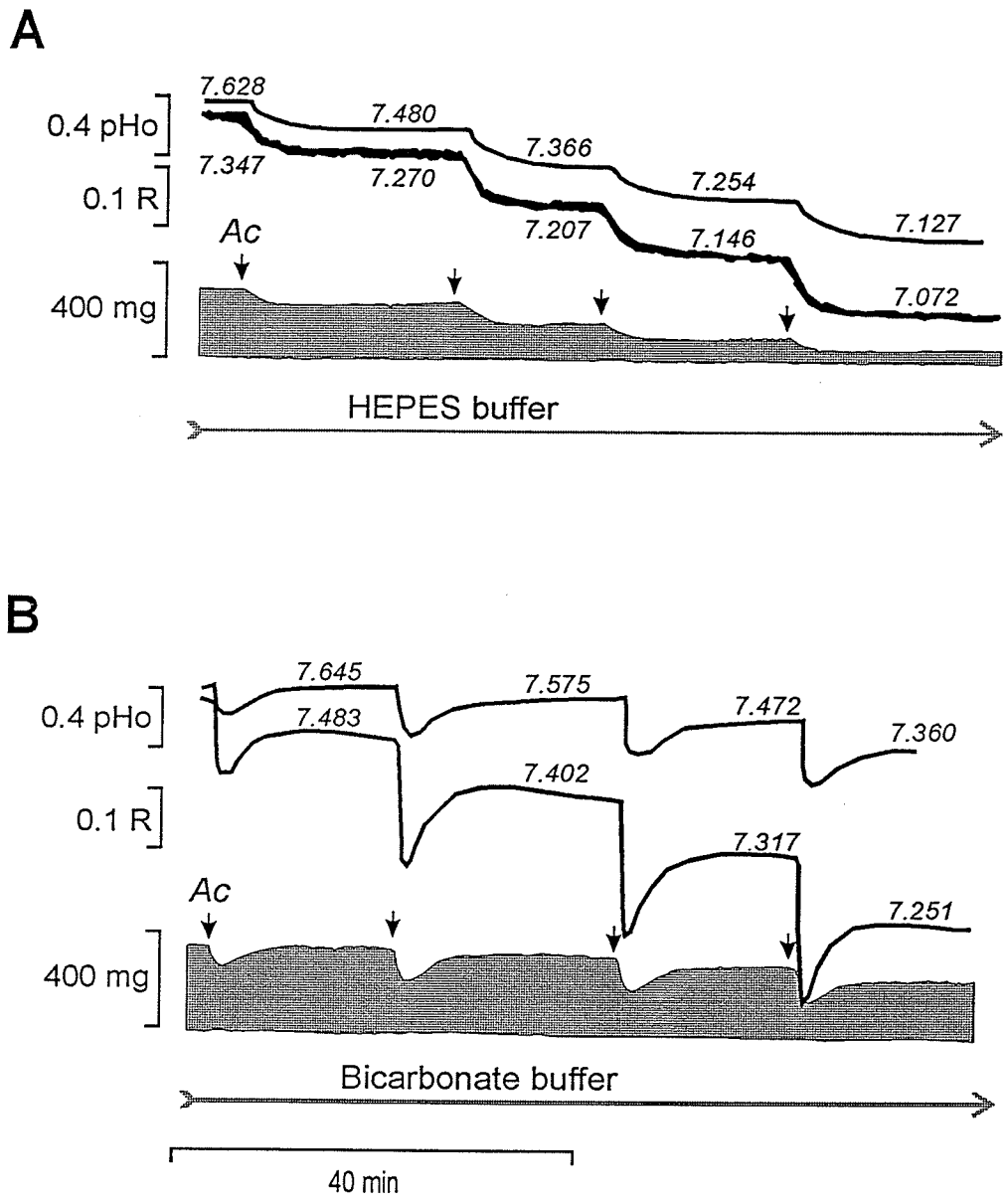

Figure 12
Sample tracings show the effects of a progressively increasing concentration of acetic acid on the pHi and tension from one canine ventricular trabeculum bathed in A. HEPES-buffered medium and B. bicarbonate-buffered medium. Acetic acid was added to the bathing solution in small steps (↓, Ac) to acidify the medium. From top to bottom, the tracings and calibration bars represent pH of the bathing solution (pH*o*), ratio of fluorescence, and tension. Steady-state values of pH*o* and pH*i* are shown over the trace for each step.

steady state showing a relatively small acidification of the medium (figure 12B). With the same tissue in HEPES-buffered solution each addition of acid had a less pronounced effect on pH_o and pH_i (figure 12A). This reflects the small instantaneous, but large steady-state buffering capacity of bicarbonate buffered solutions. Although pH_i appears to decrease more in bicarbonate-containing buffer, with each transient acidification a further drop in FI_{440} was observed, suggesting a leak of the dye. The dye leak is also indicated by the relative difference between the ratio trace and the tension trace since cytosolic acidification would be reflected in the twitch tension.

Fluorescent dyes such as BCECF are used to measure pH_i in cardiac trabeculae simultaneously with tension. BCECF leaks out of the cells of the tissue, making long experimental protocols difficult to perform. Our findings with this calibration technique show that tissues in buffer acidified with CO_2 are able to buffer pH_i more easily than those in buffer acidified with organic acids. Previous studies have shown a slow time-dependent decrease in FI_{440} (Aalkjær and Cragoe, 1988; Putnam and Grubbs, 1990; Yu *et al*, 1991), but few have investigated the reasons for this phenomenon. We also observed a similar slow decrease in fluorescence with time, which was accelerated with acid to base transitions. We describe a method for correcting the calibrations to account for this dye leakage. This technique estimates pH_i more closely during long experimental protocols using cardiac trabeculae. We investigated the recovery of pH_i simultaneously with tension after 45 minutes of acidification with a high concentration of CO_2 and with the addition of lactic acid in bicarbonate- and HEPES-buffered media. We could not observe tissue

damage caused by the acidification and realkalinization as judged by the recovery of generated tension and of pH_i, which was complete.

The calibration of BCECF *in situ* was previously found not to be different from that of BCECF in buffer (Rink *et al*, 1982). We observed a shift in the excitation and emission peaks, and in the isosbestic point, a phenomenon which has been observed by others (Thomas *et al*, 1979). Unpredictable cytosolic ionic strengths and interaction of BCECF with intracellular proteins may change the *in situ* fluorescence without reducing the pH sensitivity of the dye (Reers *et al*, 1989; Yu *et al*, 1991, work from our lab; for a discussion of the effect of ionic strengths on microelectrodes see Illingworth, 1981), hence calibrations need to be performed with BCECF *in situ*. In our preparations there was leakage of the dye from the cells over time, which caused a slow reduction in the ratio. A calibration of BCECF done in a tissue at the end of a long experiment is therefore invalid for calculating pH_i from a part of the experiment done long before the calibration. The leakage of the dye from the cells was dependent on the treatment performed. Transitions from acid to base result in faster dye leakage than transitions from base to acid or steady pH maintenance. This suggests the presence of an acid transporter on the membrane. Although such a transporter has not been described in cardiac tissue, the use of probenecid has been advocated for the prevention of dye leak from cardiac tissue (Mohabir *et al*, 1991) as well as from other cell types (Gerard *et al*, 1990). FI_{440} decreases with time even in the absence of any incident light, hence the phenomenon is not due to photobleaching of the dye, or if any photobleaching does occur, then the products do not fluoresce at 540 nm when excited at 440 nm or 500 nm. This is concluded from the fact that the formula

parameters from calibrations done at different times in the same muscle strip (time-dependent decrease in cytosolic dye concentration) match the parameters from calibrations done with different initial cytosolic dye concentrations. This is also evidence that compartmentalization of the dye does not arise slowly during experiments. It is possible that during the presence of an acidic intracellular environment the protonated form of BCECF is lipophilic enough to cross the membrane and hence leak out (Thomas *et al*, 1979). This being the case one would expect a high degree of compartmentalization of the drug into intracellular organelles. Compartmentalization of BCECF has been shown not to occur (Borzak *et al*, 1990). We did not attempt to further characterize the leakage phenomenon. Compartmentalization of the dye would result in a slower response of the dye to changes in cytosolic pH since H^+ would have to equilibrate with the compartments as well before reliable readings could be used. If the calibration curve was done in the presence of the compartmentalized dye then it would still hold true for the steady-state measurements done during the experiment if one makes the assumptions that the compartments do not change their pH_i dependence and that the dye does not accumulate slowly into the compartments during the experiments.

Some studies of intracellular pH describe relative pH change rather than absolute pH. With microelectrodes this may be due to electrode drift over time. Studies with BCECF derive pH_i from the calibrations performed at the end of the experiment. During an experiment there is leakage of the dye out of the cells as evidenced by a decrease in the FI_{440} reading. It has been assumed that the only change in time during an experiment with BCECF is a downward shift of the calibration curve (Aalkjær and Cragoe, 1988; Putnam

and Grubbs, 1990), implying that relative changes intracellular pH should be reliable regardless of the amount of leakage of the dye. However, since R_{Max} changes more than R_{Min}, the slope of the linear portion also changes, decreasing with dye leakage. If one is to use the calibrations at the end of an experiment where the amount of dye loaded is low, and extrapolate those values to the beginning of the experiment where the amount of dye loaded is high, the extrapolated results are not only offset from the real absolute pH_i, but measured changes are exaggerated. As a result of the leakage of the dye, in order to obtain more reliable results one must limit the experiment to a short duration, and only relative changes can be described unless the calibration is done immediately after the experimental protocol. This is limiting to the kind of experiments that could be performed using BCECF. Only a few studies have incorporated measurements corrected for the dye leakage in smooth muscle (Yu *et al*, 1991) or renal tubule cells (Noël *et al*, 1989). In our preparation, uncorrected calibration curves consistently gave us an overestimation of both absolute pH_i values and of relative pH_i changes (data not shown).

The calculated pH_i values are most reliable in the range of pH 6 to 8 since beyond these values the ratio approaches the asymptotes at R_{Min} and R_{Max}. A linear correction for the data in this range may also be used (Yu *et al*, 1991) but at the expense of greater variability in the results (data not shown). There is no way around this difficulty since FI_{440} must be fixed in order to calculate pH*i* and in order to assume the F ratio of equation (2) to be constant (James-Kracke, 1992). Contribution to the pH_i calculation by the pH-dependence of FI_{440} is minimal (0.055 units per pH unit) and was left out of the equation by necessity. If anything, the shift in the isosbestic point actually serves to make the ratio

more sensitive to pH changes since FI_{440} will change in the opposite direction from FI_{500}, producing a larger change in the ratio per change in pH unit. The ß factor in equation [1] was found to be constant, therefore the apparent pK_a' did not change with pH. In order to minimize any error in calculated pH_i, the FI_{440} values at pH 7.0 were used to find the correction factors. Since R_{Max} is the parameter most sensitive to variation in FI_{440}, The calculations of pH*i* will be slightly underestimated for pH*i* values greater than pH 7.0 and slightly overestimated for pH*i* values less than pH 7.0 (up to 0.027 per pH unit).

Our medium-to-tissue volume ratio was 4000:1 and the muscle surface was continuously superfused by rapid flow; hence the contribution of extracellular dye to fluorescence was negligible. The ammonium chloride pulse has been used to induce transient cytosolic pH changes without affecting extracellular pH. In solution NH_4Cl is in equilibrium with NH_3 which freely diffuses through the cell membranes. Inside the cells NH_3 and NH_4^+ establish an equilibrium, thereby taking up H^+ and resulting in alkalization of the cytosol. The removal of the ammonium chloride produces the same series of events in the reverse direction, resulting in acidification of the cytosol. Experiments with the ammonium chloride pulse demonstrated that pH_i was being measured independently of pH_O. The overall buffering power of the cell includes transmembrane pH control mechanisms and the specific buffering capacity of the cell cytosol. The measurement of the specific buffering capacity requires the use of pharmacological blockers of the membrane events which actively buffer pH. Amiloride and its analogs are commonly used to block the sodium-hydrogen exchanger. Amiloride also changes cytosolic calcium concentrations in that it produces relaxation of smooth

muscle and inotropy in cardiac muscle. Calcium shares many of its cytosolic binding sites with hydrogen (Fabiato and Fabiato, 1978) hence a change in cytosolic calcium may change the intrinsic buffering capacity of the cells.

Acidification of the external buffer results in cytosolic acidification without greatly affecting the driving force for the sodium-hydrogen exchanger. pH_i directly affects the force of contraction by interaction of H^+ with binding sites for Ca^{2+} on troponin C (Fabiato and Fabiato, 1978; Orchard and Kentish, 1990) and by more indirect effects such as on calcium release sites (Rousseau and Pinkos, 1990), potassium channels (Harvey and Ten Eick, 1989b), calcium channels (Irisawa and Sato, 1986), and other mechanisms (Kaila *et al*, 1987; Orchard and Kentish, 1990). The relationship between pH_i and cell or muscle contraction has been described in detail elsewhere (MacLeod and Harding, 1991; Vaughan-Jones *et al*, 1987). The buffering capacity of the cells is affected by not only membrane events such as the sodium-hydrogen exchanger, anion exchangers, and the sodium-dependent anion exchangers, but also intracellular enzymes and metabolism. We found that the dependence of pH_i on pH_o was not contingent on the presence of bicarbonate in the medium. One of the cytosolic enzymes which specifically control pH is carbonic anhydrase. The presence of carbonic anhydrase may explain the improved cellular buffering when the medium is acidified with CO_2. The observation that tension is less dependent on pH_i when bicarbonate is present in the medium implies some additional role of bicarbonate on tension development which is independent of the changes in pH_i.

In summary, the calibration curves for the fluorescence of BCECF must be adjusted to compensate for dye leakage from the cells throughout each experiment; hence the pH-dependence of the dye fluorescence is dependent on the concentration of the dye. *In vitro* calibration of BCECF fluorescence to pH does not correlate to *in situ* calibrations due to intracellular interactions and a shift in the isosbestic point. These changes are linear such that measurement of FI_{440} provides the data required to correct the calibrations to correct the pH_i calculations from the fluorescence ratio of FI_{500}: FI_{440} with emission at 540 nm.

CARDIAC ELECTROPHYSIOLOGY

HIGH RESISTANCE MICROELECTRODE STUDIES

Tissue preparation

Canine trabeculae were suspended horizontally with one end pinned to a silicone rubber base and the other attached to a tension transducer (FT 03C). Guinea pig right ventricular papillary muscle was horizontally suspended in a manner similar to the canine trabeculae. A flow-through bath kept the tissues perifused with Krebs Henseleit solution (pH 7.4, 37°C, and bubbled with 95% O_2, 5% CO_2). Guinea pig tissues were field stimulated at a basic cycle length of 1000 ms, with pulses 1 ms in duration, at a voltage 20% above threshold. Canine tissues were stimulated similarly but at a basic cycle length of 2000 ms.

Measurement of Action Potentials

Glass capillary tubes (1.2 mm O.D., 0.75 mm I.D.) with a microfilament were heated and pulled using a model P-77 Brown-Flaming micropipette puller (Sutter Instruments Co., San Francisco, California, USA) to yield microelectrodes with tip resistances of 8-20 megaohms. These were filled with 3 M KCl solution and connected to the preamplifier via a $AgCl_2$ electrode. The reference consisted of a Ag-$AgCl_2$ wire suspended in the bathing solution. Surface cells from the tissue were impaled with the microelectrodes to measure action potentials. The membrane potential was measured using a model 1600 Neuroprobe amplifier (Transdyne General Corp., Ann Arbor, Michigan, USA) with the headstage mounted on a mechanical micromanipulator (Brinkmann Instruments, Rexdale, Ontario, Canada). Both transmembrane potential and tension were recorded digitally using a data acquisition program (Scientific Solutions A-D converter with Axotape software, Axon Instruments, California, USA). With each action potential a calibration signal was recorded consisting of 0 mV for 5 ms, followed by -50 mV for 5 ms then back to resting potential for a further 5 ms. A computer driven TTL signal triggered both the calibrator which initiated immediately, and the floating ground stimulator (Frederick Haer & Co., Brunswick, ME, USA, model Pulsar 6i) which was delayed 20 milliseconds to allow time for the calibration step. The stimulation of each action potential was delayed until after the calibration steps and timed so as to almost completely suppress the initial stimulus artifact.

LOW RESISTANCE MICROELECTRODES: IONIC CURRENTS

Guinea-pig cell isolation:

The technique used to isolate guinea-pig ventricular myocytes was modified from that described by Hume and Uehara (1985). Guinea-pigs weighing 250-350 grams were killed by cervical dislocation and their hearts quickly removed and quickly canulated through the aorta and perfused in Langendorff mode with warm (33°C) Krebs solution (in mM: 120 NaCl; 25 $NaHCO_3$; 4.2 KCl; 1.2 KH_2PO_4; 1.2 $MgSO_4$; 1.8 $CaCl_2$; 11 Glucose, bubbled with 95% O_2-5% CO_2, pH 7.4). The connective tissue and pericardium were mechanically removed while perfusing the coronary arteries in an anterograde direction by gravity (65 cm column) at 33°C for 10 to 15 minutes at a flow rate of 0.8 ml/min. After rinsing the vasculature free of blood, the perfusate was then switched to a nominally calcium-free perfusing solution for 5 minutes, after which the drippings of solution from the heart were collected and reperfused. To the calcium-free reperfusing medium, crude collagenase (type Ia, Worthington or Bohringer Manheim) was added at a concentration of 60 U/ml (0.2-0.3 mg/ml) and digestion was allowed to proceed at a flow rate of 0.5 ml/min for 45 minutes during which time the perfusate was recycled. The right ventricle was then cut from the heart and placed into enzyme-free and calcium-free perfusing solution and cut into small pieces approximately 3 mm in size. These pieces were subjected to a second digestion, this time incubated in 1.8 mM calcium-containing solution with 40 U/ml of the same collagenase. For each experiment, a few pieces were removed at 5 minute intervals to a maximum of 40 minutes digestion to find the optimal exposure to the second digestion. Upon removal from the digesting medium, the pieces

were rinsed and stored at 33°C in fresh enzyme-free 1.8 mM calcium-containing solution until needed. All solutions were bubbled with 95% O_2, 5% CO_2. Cells were liberated from the pieces by trituration. Fifteen minutes of the second digestion was found to be optimal.

Measurement of ionic currents

The "standard" bathing solution for whole-cell clamp experiments was of the following composition (mM): 140 NaCl; 5.4 KCl; 0.5 $MgCl_2$; 5 HEPES-NaOH (pH 7.40±0.01); 2.5 $CaCl_2$; 5.5 Glucose. Cesium external solution contained 10 mM CsCl instead of KCl, at pH 7.40±0.01 (balanced with NaOH).

The standard pipette solution was as follows (mM): 110 K-Gluconate; 30 KCl; 0.5 $MgCl_2$; 5 HEPES-KOH (pH 7.20±0.01); 10 NaCl; 0.1 ethylene glycol tetraacetic acid (EGTA); 1 Mg-ATP. Cesium-containing pipette solution was as follows (mM): 105 CsOH, 105 Aspartic Acid, 20 CsCl, 20 TEA-Cl, 0.5 $MgCl_2$, 5 HEPES-CsOH (pH 7.20±0.01), 10 NaCl, 0.1 EGTA, 5 Mg-ATP.

External solution was perfused in the stage-mounted chamber (approximately 3 cm x 1 cm) by gravity, at a flow rate of 2-3 ml/min. The perfusate was evacuated by a suction line and discarded. The fluid volume was kept at approximately 1 ml so as to enable changing the bathing solution within one minute. All experiments were carried out at room temperature (22°C). The junction potential between the intra-pipette solution and the bathing solution was determined by placing a pipette tip into a bath with intra-pipette

solution and offsetting the tip potential measurements to zero, then switching the bath to external solution and measuring the junction potential produced.

Calcium tolerant cardiac ventricular myocytes (figure 13) were clamped using the standard whole-cell configuration of the patch clamp technique (Hamill *et al*, 1981). Large diameter micropipettes were pulled using a two-stage micropipette puller (Narishige Scientific Instruments, Tokyo, Japan; model PP-83) and polished using a microforge (Narishige Scientific Instruments; model FP-83). With tip diameters of about 1.0 μm, the pipette resistances were in the range of 2 to 5 MΩ when filled with the internal solutions described above. A Marzhouser Micromanipulator (MS 314, Fine Science Tools Inc., #25711-10, #25501-00) was used to approach the cell with the tip of the microelectrode. With the tip near the cell, the output of the measured potential was offset to reflect the junction potential between the pipette solution and the bathing medium. Gentle suction was applied to the micropipette to form a gigaohm seal between the glass tip and the cell membrane such that no current was required to produce a 20 mV change in the tip potential (measured using a Hitatchi VC6025 oscilloscope). Once a seal was formed, the cell was raised off the bottom of the chamber in order to improve access of the bathing medium and to prevent vibration from tearing the membrane and producing leaks in the seal. After compensating for tip capacitance and clamping the tip potential to -40 mV, stronger suction was applied for a short time in order to break the membrane attached to the tip. This produced whole-cell access without causing the cell to contract and destabilize the seal. Series resistance compensation was done for all experiments using a 10 to 60 ms decay constant. Voltage clamp protocols were computer driven using

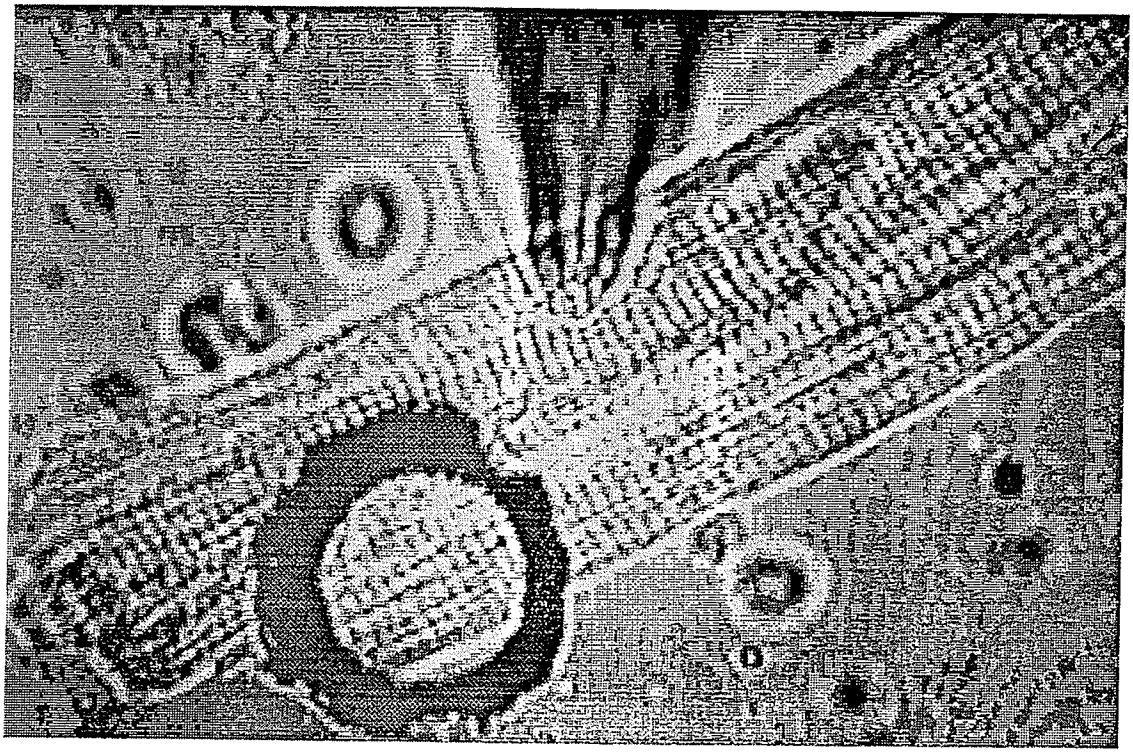

Figure 13
Isolated cardiac myocyte. Guinea pig cardiac ventricular myocytes were isolated by using a two-step digestion method (see text). Cells used for whole-cell voltage clamp experiments were calcium tolerant in 2.5mM calcium-containing solution. Only cells displaying clear striations and a sharp uniform membrane under 400× magnification were selected for experiments. Cells were triturated from the tissue when needed. Shown is a representative cell. Included in the field is the tip of a 4 megaohm pipette attached to the cell, and a circle where a red filter has been drilled (as a requirement for other experiments).

PClamp software (version 5.5.1) and an Axopatch 1D amplifier or Axopatch 200 integrating patch amplifier (Axon Instruments, Foster City, CA). In current clamp experiments, action potentials were recorded in standard internal and external solutions. Action potentials were elicited by short (1.5-2 ms) depolarizing current pulses applied intracellularly via the patch micropipette once every 10 seconds. The amplitude and duration of the pulses were adjusted for each cell to elicit a voltage change sufficient to surpass the excitation threshold and elicit an action potential, thereby minimizing the stimulus artifact. Drug was added after the characteristics of the action potential had reached steady-state. In voltage clamp experiments, currents were recorded in standard internal and external solutions for I_{K1} measurements, standard external and sodium-free internal solutions for I_K measurements, and cesium internal and external solutions for L-type calcium currents (I_{CaL}) measurements. All data were acquired using a PC-486 computer interfaced with a 12-bit analog-to-digital acquisition board (TL-125 with a Scientific Solutions Labmaster DMA A-D Converter, Axon Instruments Inc.), and temporarily stored on the computer hard disk for later analysis (using PClamp version 5.5.1) and display (Hewlett Packard LaserJet).

Chemicals

Except for CsOH (Aldrich Chemical Company, Milwaukee, Wisconsin, USA), chemicals used to make physiological bathing solutions were purchased from Canlab (Winnipeg, Man.) and Sigma (St. Louis, Missouri, USA) Chemical Companies. Solutions used for voltage clamp experiments were prepared fresh every week. Phenamil,

3',4'-dichlorobenzamil (DCB) and 5-(4-chlorobenzyl)-2',4'-dimethylbenzamil (CBDMB) were purchased from E.J. Cragoe, Jr (P.O. Box 631548, Nacogdoches, Tx 75963-1548). Preparation of these derivatives is described elsewhere (E.J. Cragoe, Jr. *et al*, 1967). tetrodotoxin, Ouabagenin, and ouabain were purchased from Sigma Chemical Co. (St. Louis, MO). Stock solutions were prepared for the following chemicals in dimethylsulfoxide: amiloride hydrochloride (100 mM), 5-(4-chlorobenzyl)-2',4'-dimethylbenzamil (CBDMB, 100 mM), phenamil (100 mM or 200 mM), 5-(N-methyl-N-guanidinocarbonyl methyl)-amiloride (MGCMA, 100 mM). Pentobarbital was prepared in 70% ethanol. The remaining compounds were prepared in deionized, distilled water.

Between experiments all solutions were kept frozen at -20 C in the dark due to the light sensitivity of some of the compounds. Aqueous dilutions of phenamil were not frozen. Tissues were tested with DMSO controls to verify that the measured effects were due to the drug and not to the vehicle. The drugs were added directly to the bathing medium of the preparations during the experiments. In voltage clamp experiments the drugs were added to a reservoir for external solution to achieve the final desired concentration before each experiment.

STATISTICAL ANALYSIS

Data are expressed as means $\pm$ SE, n=number of animals or cells from different animals in a sample. When two groups were compared, the differences were tested for

significance using a two-tailed Student **t**-test. A multiple analysis of variance (ANOVA) test for repeated measures was used for comparisons of control to several doses of a drug or in the determination of a drug effect during a continuously and unidirectionally changing event where measurement is taken before, during, then after the drug. Several groups of data using different drugs or different treatments were tested for significant differences using a two-tailed simple ANOVA. Where tests were being compared to a control done on the same tissue, blocked ANOVA or paired **t**-tests were used. In measurements of action potential with high resistance microelectrodes, the absolute values of peak and resting membrane potential were tested with unpaired **t**-tests due to electrode drift over time. Individual differences were determined by Duncan's new multiple range test, or by Tuckey's test. Unless otherwise stated, differences were considered significant when a 95% level of confidence could be achieved ($p<0.05$). Slopes of regression lines were compared using a **t**-test. No more than one tissue per animal was used in each data set so that all data in a comparison was from different animals. When the curve is not described by a formula, it was fit by a Spline method. Curves described by an equation were fit to their equation by a least squares or χ^2 method. In figures, significant differences are indicated by * ($p<0.05$), ** ($p<0.01$), and *** ($p<0.001$).

RESULTS

MECHANICAL STUDIES

ISOMETRIC TENSION

Both amiloride and phenamil were found to produce positive inotropy. Addition of phenamil to canine trabeculae caused a slow increase in twitch tension over a prolonged period of time (30 to 40 minutes). Phenamil concentration of 60 μM produced significant and reproducible inotropy which was stable after 40 min (figure 14) phenamil exposure. Within 15 min, 60 μM phenamil increased twitch tension from 147±31 mg to 526±126 mg (expressed as mean±S.E; 119 mg SE of difference, $p<0.01$). Figure 15 shows the tension-concentration relationship of phenamil. At concentrations below 30 μM, phenamil caused no significant change in the isometric twitch tension within 15 minutes, higher concentrations resulted in a significant positive inotropy. Concentrations greater than 120 μM produced automaticity in the tissue, followed by unresponsiveness to electric stimuli before stable inotropy could be achieved. These toxic effects were observed without any increase in baseline tension during decline of twitch tension. The resulting irregular twitch tensions precluded meaningful measurement of isometric tension. Inotropy with phenamil was also observed in the presence of tetrodotoxin at concentrations (5 μM,

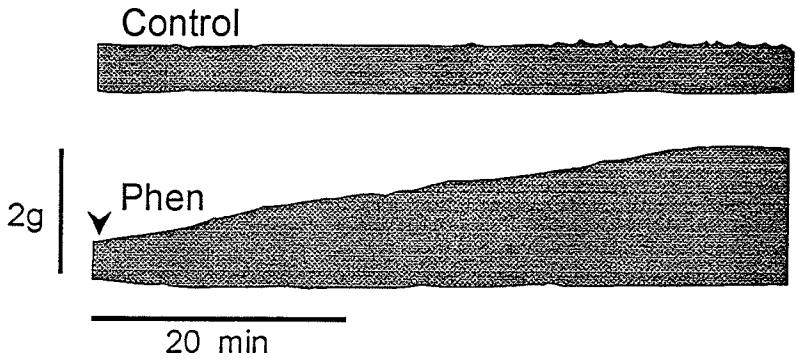

Figure 14
Effect of phenamil on electrically driven canine right ventricular trabeculae. Tension development without any drugs (**Control**) and with 60 μM phenamil (**Phen**). Phenamil was added when the muscle twitch tension was at steady state. The point at which the drugs were added is indicated by the pointers.

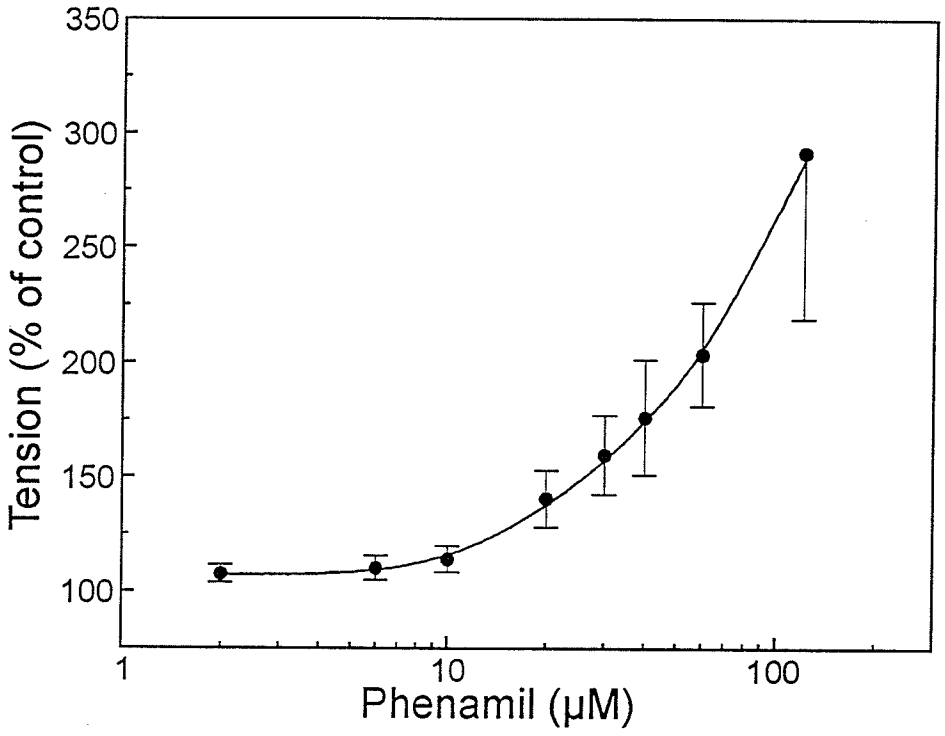

Figure 15

Non-cumulative dose-response plot of phenamil. The force of isometric contraction in electrically driven canine right ventricular trabeculae (paced at a basic cycle length of 2000 ms) is expressed as relative twitch tension, with 100% being the active tension before the addition of phenamil. Tissue toxicity induced by phenamil prevented evaluation of concentrations greater than 120 μM. (n=5 to 23 animals; 50% maximal inotropy with 59.0 μM phenamil, by extrapolation from a least squares best-fit curve.)

data not shown) which reduced steady state contractions and produced an increase in threshold stimulus voltage.

It has been hypothesized that amiloride compounds produce positive inotropy by inhibiting sodium-calcium exchange. In order to test this hypothesis, we tested the effects of CBDMB on the contractile tension of canine cardiac tissue (figure 16). Twitch contractions in the presence of CBDMB (5-(4-chlorobenzyl)-2',4'-dimethylbenzamil) did not differ from those in control conditions in the same amount of time. This finding was similar in three tissues.

In order to analyze the effects of phenamil on the twitch duration, the twitch tensions of the trabeculae in the absence of phenamil were normalized to the level of those seen in the presence of phenamil (60 μM). Figure 17A (left) shows two overlapping traces of the twitch response, showing that phenamil elicits significant positive inotropy. Normalized twitches (figure 17A, right) emphasize that phenamil caused a slight lengthening of the twitch duration. Norepinephrine (1 μM) produced a similar amount of inotropy in the muscle (figure 17B, left), but shortened the twitch duration (figure 17B, right). The effect of phenamil on twitch duration was significantly different from that of norepinephrine. Phenamil increased the twitch duration by 7.2±3.7 % whereas norepinephrine decreased it by 7.3±4.6 % after 10 min. (Control twitch durations were 256.6±11.1 ms for Phenamil, and 328.0±20.0 ms for NE.)

In spite of the effects of phenamil being different from those of norepinephrine, figure 18 shows that the effects of phenamil can be reduced by nadolol (1 μM), a beta

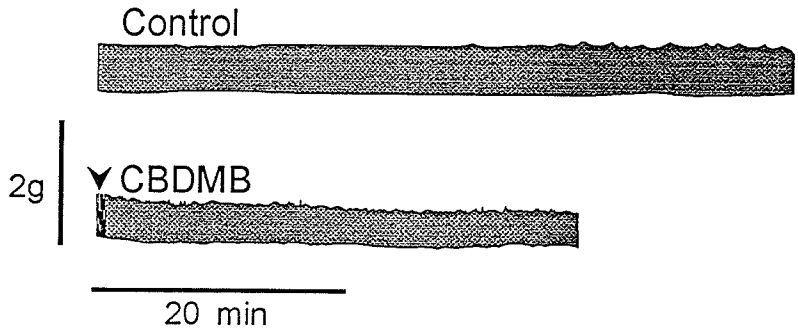

Figure 16
Effect of CBDMB on electrically driven canine right ventricular trabeculae. Tension development without any drugs (**Control**) and with 50 μM CBDMB. CBDMB was added when the muscle twitch tension was at steady state. The point at which the drug was added is indicated by the pointers.

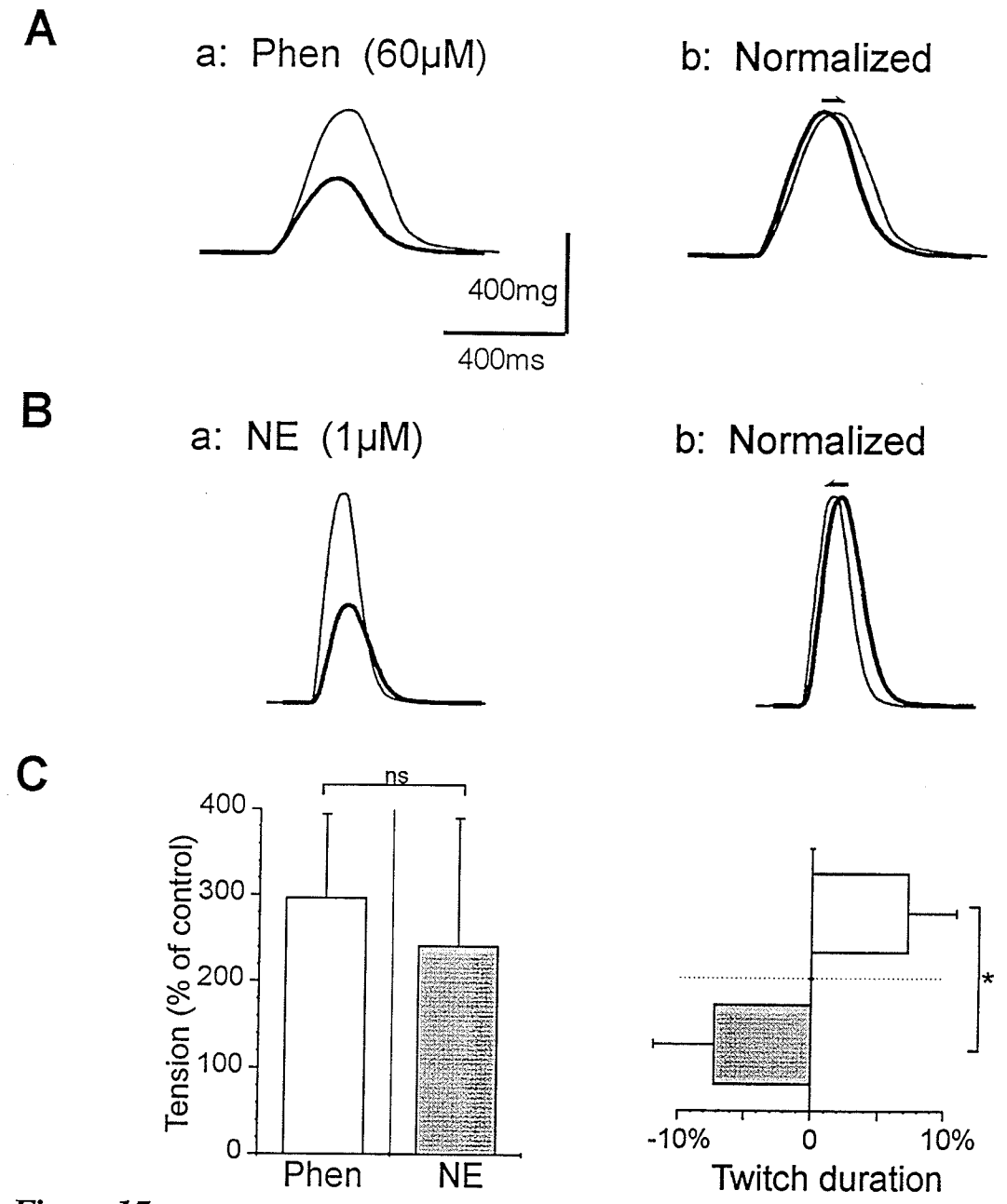

Figure 17

Comparison of the twitch durations of electrically driven canine right ventricular trabeculae in the presence of phenamil or norepinephrine. Traces are aligned by the time of stimulation. **A.** The twitch profile in the presence of 60 μM phenamil (a; left) is overlapped with its control (thicker line) showing positive inotropy. On the right (b) the control twitch has been normalized to the level of the treated twitch to emphasize the prolongation of the twitch duration. **B.** The same was done for muscles exposed to 1.0 μM norepinephrine emphasizing the shortening of the twitch duration. Arrows above normalized twitch traces indicate the direction of change induced by the drug. C. Inotropic effects of both drugs are plotted as tension as a percent of control (left). The effects of the two drugs on the twitch durations are plotted as a percent of change from control (right). (☐ 60 μM phenamil, n=9; ▩ 1 μM norepinephrine, n=3; *, $p<0.05$. : phenamil lengthened the twitch duration by 7±11% and norepinephrine shortened the twitch durations by 7±8%. (n=9 for phenamil, n=3 for norepinephrine.)

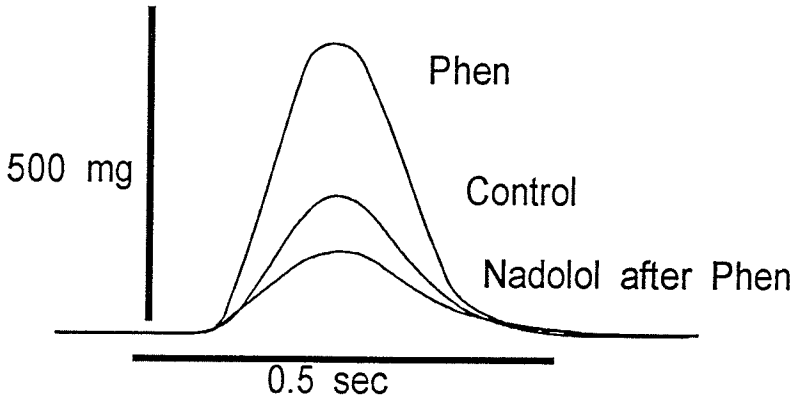

Figure 18
Isometric contraction recordings in canine right ventricular trabecula in control, with 50μM phenamil (**Phen**), and with 1μM nadolol added on top. (n=5)

adrenoceptor blocker. This blockade was seen whether nadolol was added before phenamil, or after phenamil. Other beta blockers (e.g.: sotolol, propranolol) also had a similar effect, although more variable. Thus the effect of the beta blockers is not mediated via the blocking of the action of released norepinephrine.

BIPHASIC CONTRACTIONS

Biphasic contractions were produced and the effect of phenamil studied to test the hypothesis that it affected transsarcolemmal movement of calcium. In these experiments calcium was first replaced by strontium to result in a prolongation of the action potential. This was accompanied by a contraction which had a longer latency of duration. This contraction lacks a sarcoplasmic reticulum-mediated component since strontium is not stored in the sarcoplasmic reticulum in any appreciable amount. Addition of about 10% of the normal amount of calcium resulted in the appearance of an earlier component of contraction (P1) whose peak was clearly separated from the delayed peak (P2) of the strontium mediated contraction. P1 is affected by agents acting on the sarcoplasmic reticulum while P2 is affected by agents acting on transsarcolemmal calcium influx (King and Bose, 1983). In tissues made to contract biphasically (figure 19), 60 μM phenamil caused an increase in P2 of the contraction. This differed from the effects of 1 μM norepinephrine which caused a preferential increase in P1. 0.5 μM ouabagenin caused an increase in P2. Similarly, 4AP increased P2. The effect of phenamil on biphasic contraction was similar to that of ouabagenin and 4AP.

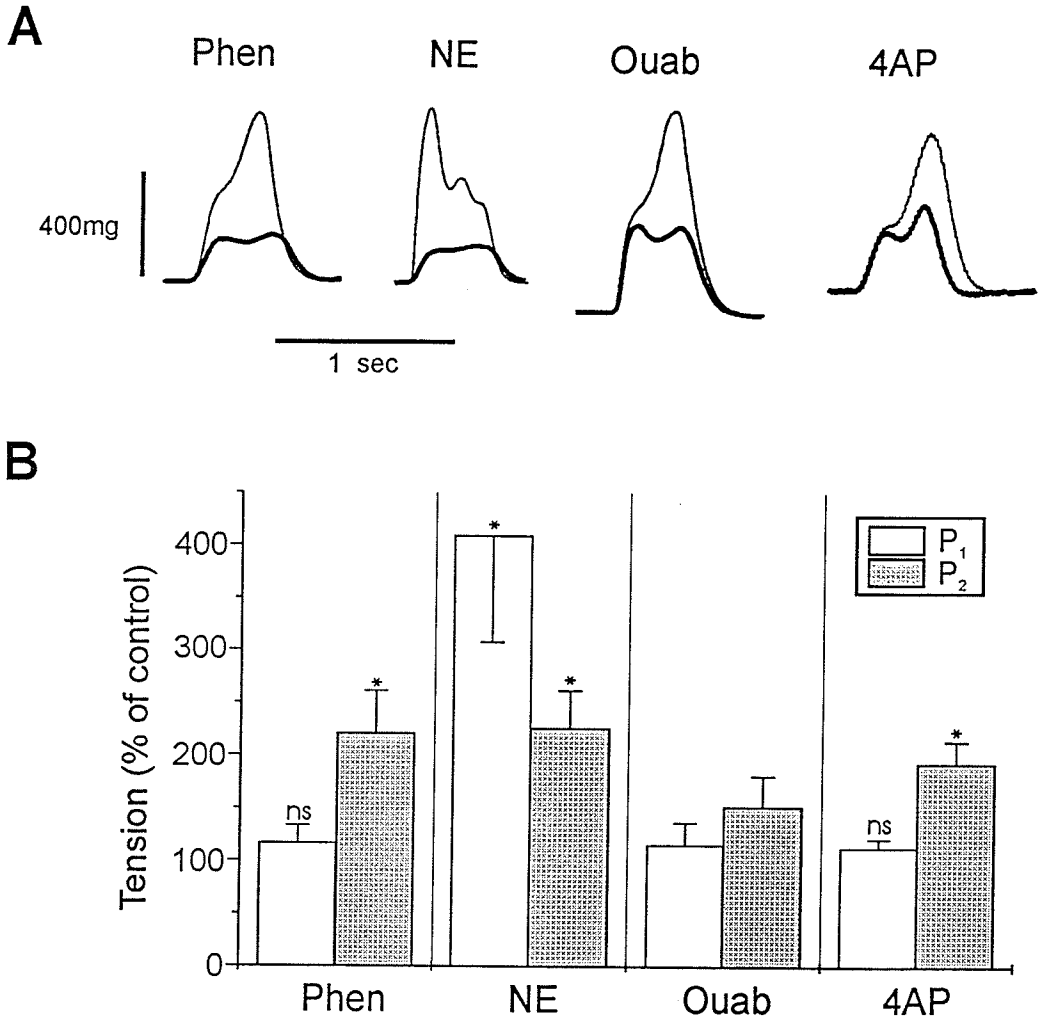

Figure 19
Effect of phenamil, ouabagenin, norepinephrine, or 4AP on biphasic contractions elicited by replacing 90-95% of the external Ca^{2+} with Sr^{2+}. **A.** Control twitches are overlapped with twitches in the presence of phenamil (**Phen**, 60 μM), norepinephrine (**NE**, 1.0 μM), ouabagenin (**Ouab**, 0.5 μM) or **4AP** (5 mM) showing the positive inotropy elicited by these agents. **B.** The average percent change in each phase of the contraction (□ P1, and ■ P2) by each of the agents is shown. (n=5; Data for ouabagenin are from King, 1982. n=3 for 4AP, 3 mM 4AP also potentiated P2.)

One feature that differentiated the effects of phenamil from those of ouabagenin is that ouabagenin toxicity caused a rise in diastolic tension, whereas phenamil toxicity did not produce a rise in diastolic tension. At very high concentrations of phenamil toxicity was manifested as extra beats or in more severe cases as automaticity.

SARCOPLASMIC RETICULUM

Figure 20 shows the twitch responses in the presence of ryanodine, an agent shown to deplete the stores of calcium from the SR (Hilgemann, 1982). When 100 nM ryanodine was added, the twitch tension decreased to 23% of control tension. The resulting contraction was predominantly dependent on transsarcolemmal calcium movement. When 60 μM phenamil was added in the presence of ryanodine, it prolonged the twitch duration and caused the appearance of a second phase of contraction; phenamil continued to induce positive inotropy after 40 min in the presence of ryanodine (figure 20A). In spite of phenamil's similarity to 4AP in its effects in biphasic contractions, 4AP did not elicit a second phase of contraction in the presence of ryanodine (figure 20B). After-contractions induced with phenamil at toxic concentrations could not be abolished with ryanodine (0.4 μM) hence toxic concentrations probably did not result in cytosolic calcium overload.

Cyclopiazonic acid (CPA) has been used to deplete calcium stores by inhibiting ATP-dependent calcium uptake into the sarcoplasmic reticulum (Baudet *et al*, 1993). CPA (100 μM) reduced twitch tension to 12% of control tension (figure 21). Addition of phenamil (100 μM) after CPA resulted in a relatively rapid increase in tension (figure 21A)

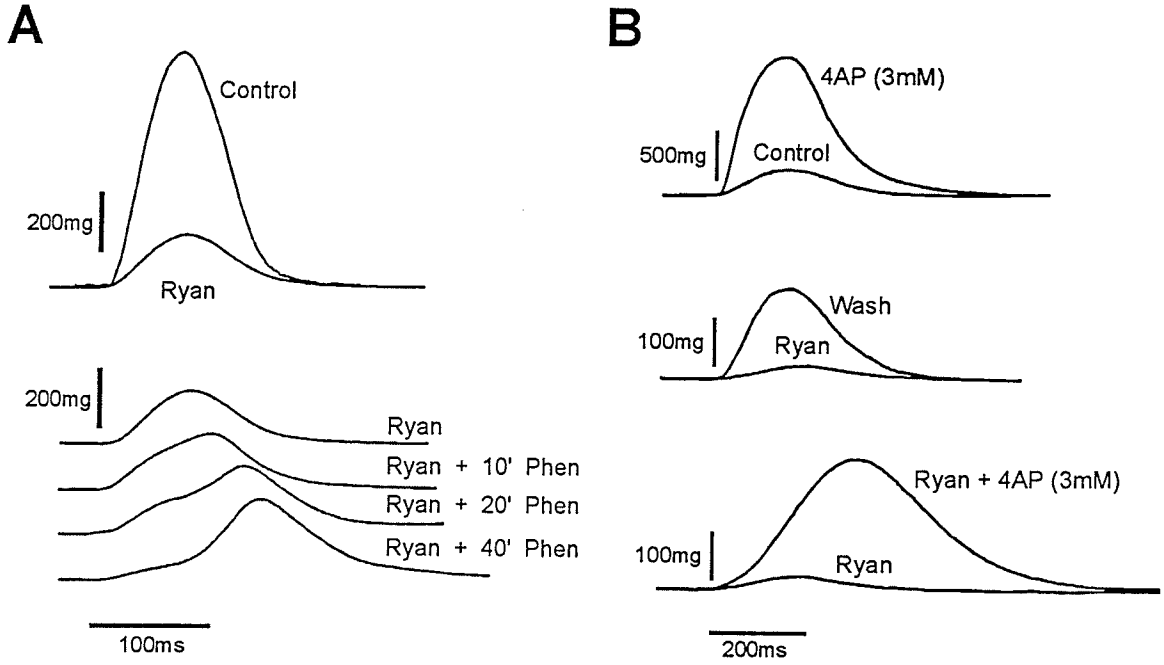

Figure 20

Prolongation of the twitch duration by phenamil in the presence of 100 nM ryanodine (**ryan**). Traces are aligned by the time of stimulation. **A**. A twitch in the presence of ryanodine is overlapped with a control twitch from the same muscle (top). In the presence of ryanodine, phenamil (**phen**, 60 μM) increased the twitch tension and prolonged the twitch duration in this muscle (bottom). Under these conditions, phenamil elicited a second phase of contraction. Similar results were seen in 4 tissues. **B**. Twitches in the presence of **4AP** (3 mM; top) or of ryanodine (middle) are overlapped with their control twitches. In the presence of ryanodine, 4AP produced positive inotropy and prolongation of the twitch but did not elicit a second phase of contraction (bottom). Similar results were seen in 6 tissues.

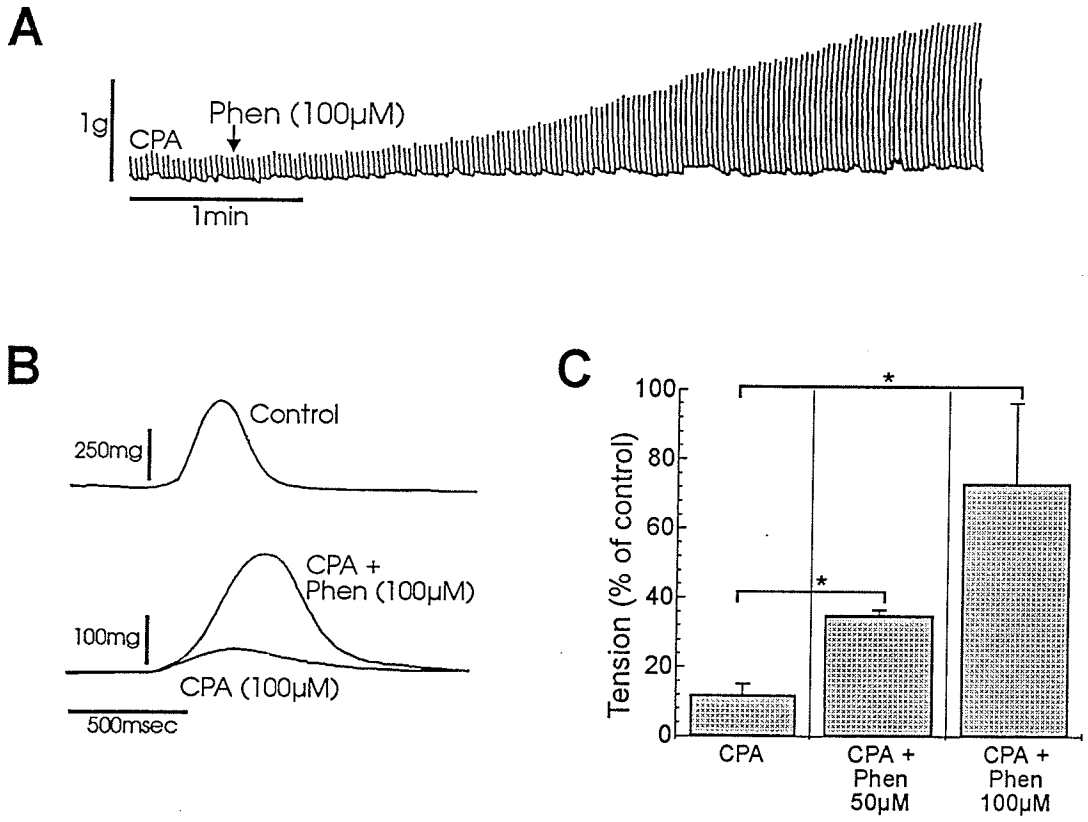

Figure 21

Positive inotropy by phenamil in the presence of cyclopiazonic acid (**CPA**). **A.** Phenamil (**Phen**, 100 μM) was added after equilibrating the tissue in solution containing CPA (100 μM). **B.** Sample twitches were recorded before addition of any drugs (control), in the presence of CPA (100 μM), and with both CPA and phenamil (100μM). Traces are aligned by the time of stimulation, emphasizing effects on twitch duration. **C.** Inotropy produced by phenamil in the presence of CPA is plotted as a percent of control tension (*, $p>0.05$; $n=4$).

and prolongation of the twitch duration (figure 21B). In the presence of CPA, 50 μM phenamil produced over 200% positive inotropy (figure 21C).

Thus the inotropic effect of phenamil is not dependent on intracellular calcium release from the SR.

POST-REST CONTRACTIONS

Calcium in the muscle cell is rapidly taken up into the longitudinal element of the sarcoplasmic reticulum (SR) between contractions. It is then translocated to the terminal cisternae in preparation for release during the next action potential. This translocation step is slow so that if the interval between beats is increased, then more calcium will be available for release from the SR causing a transient potentiation of the subsequent contractions. Rest periods of 10, 30, 60 and 120 sec within a regular train of electrical stimuli (basic cycle length of 2000 ms) were applied and potentiation of the first twitch after the rest period was compared after 40 minutes of phenamil (60 μM) ouabagenin (1 μM) or 4AP (3 mM) (figure 22). At these concentrations, the three inotropes all produced 200% to 500% positive inotropy. Both 60 μM phenamil and 3 mM 4AP reduced the PRC potentiation more than 1 μM ouabagenin (n=6 to 14).

CYTOSOLIC pH

Cytosolic pH measurements were made to test the hypothesis that phenamil may activate protein kinase C, which would activate the sodium-hydrogen exchanger and alkalinize the cytosol resulting in positive inotropy.

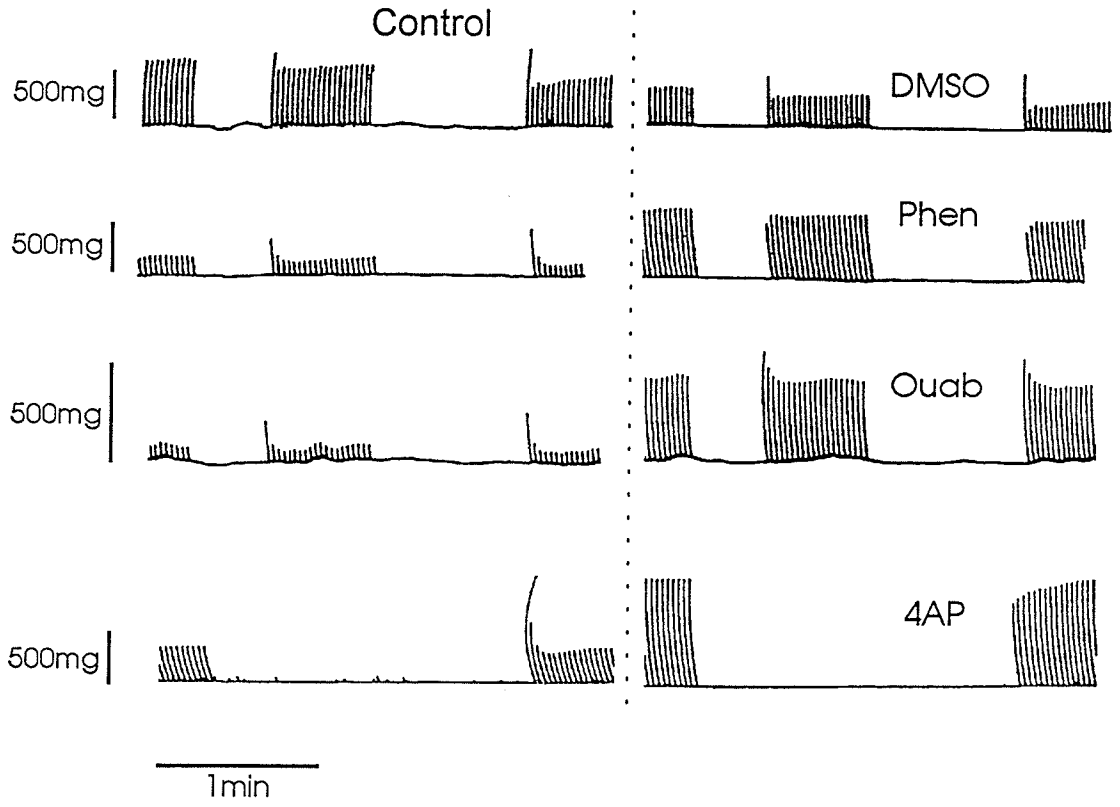

Figure 22

Post rest potentiation of canine ventricular trabeculae in control and in the presence of phenamil (**Phen**, 60 μM), ouabagenin (**Ouab**, 1 μM) or **4AP** (3 mM). The muscle was stimulated at a basic cycle length of 2000 ms. In control (traces left of the dotted line), the first beat after a rest period has a higher twitch tension than the last steady state beat. Top to bottom: the effects of the vehicle, DMSO alone, phenamil (60 μM), ouabagenin (1 μM) and 4AP (3 mM) are shown on tracings on the right, matched with their own controls on the left. Tracings of both control and test compound are shown for a rest period of 30 and 60 sec. For 4AP only a 2 min rest period is shown. Tracings are typical representatives from experiments in 6 animals.

In our system phenamil (50 μM) produced positive inotropy (223±17% of control, n=5) without alkalinizing cytosolic pH (figure 23A) or, in 3 of those 5 tissues, with a slight drop in the apparent cytosolic pH. Cytosolic pH in the bicarbonate-containing buffer was found to be 7.24±0.05. Other compounds can produce inotropy simply by alkalinizing the cytosol. Ammonium chloride produced positive inotropy (283±10% of control) without changes in extracellular pH, which was maintained at pH 7.44±0.02 (figure 23B). Increase in cytosolic pH with NH_4Cl was 0.15±0.05 pH units at steady state tension.

SODIUM-POTASSIUM PUMP

Some of the effects of phenamil were similar to those of inhibitors of the sodium pump. We tested the hypothesis that phenamil may inhibit the sodium pump. Smooth muscle was used for supporting evidence that phenamil does not inhibit the sodium pump. The sodium-potassium ATP-ase in smooth muscle is inhibited by similar concentrations of the same drugs that inhibit this pump in cardiac tissue (Skou and Esmann, 1992).

In the absence of extracellular potassium the sodium pump is blocked, resulting in an accumulation of sodium in the cells, which brings calcium into the cells via the sodium-calcium exchanger (Bose and Innes, 1973). The inability of phenamil to block the sodium-potassium pump is shown in figure 24. Removal of potassium from the extracellular medium augmented the tension in all three portal vein strips. In the control preparation, the increase in tension was reversed when potassium was restored to the solution (figure 24, top trace). Ouabagenin (1 μM) caused a further increase in tension of the smooth

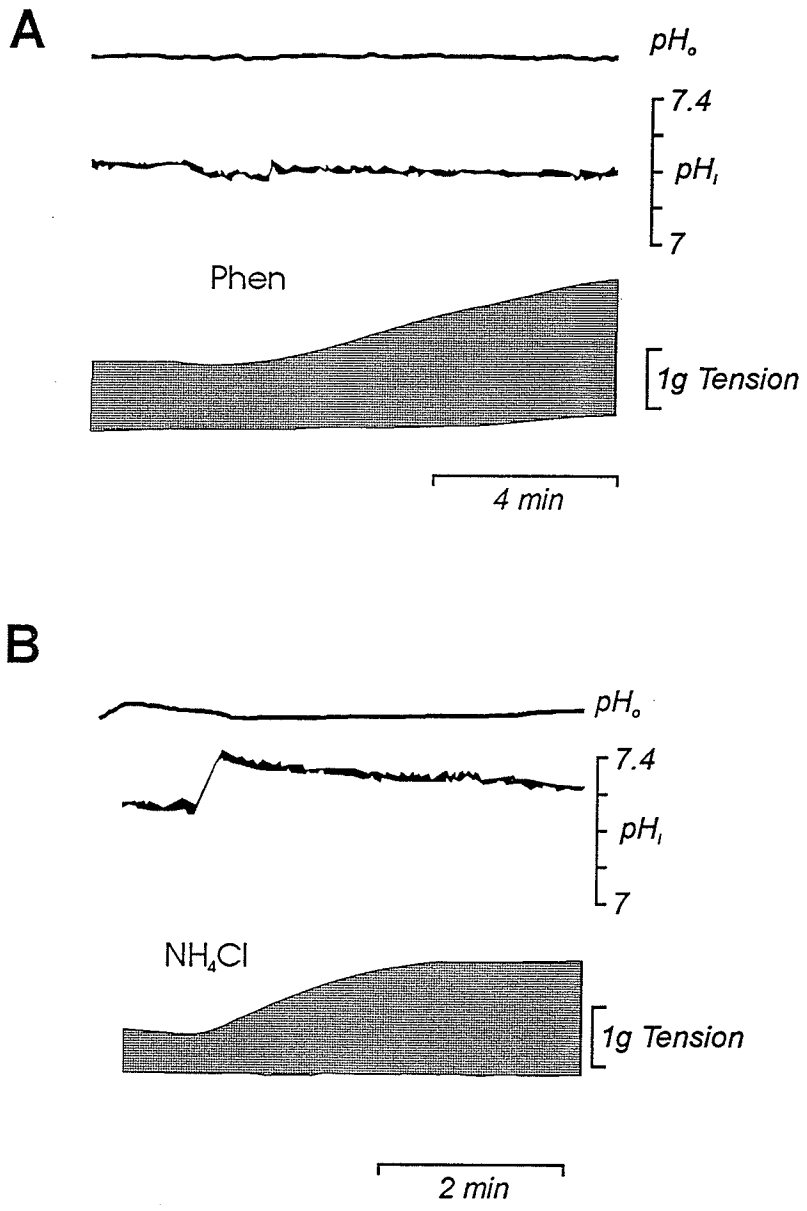

Figure 23
A. Sample tracings show the effect of phenamil (**Phen**, 50μM) on cytosolic and extracellular pH during the time-course of positive inotropy. Similar observations were made in 5 tissues. **B**. Sample tracings show the effects of a short pulse of NH_4Cl (10 mM) on the measured parameters of the function of canine ventricular trabeculae in bicarbonate-buffered medium. Similar results were obtained in 6 tissues.

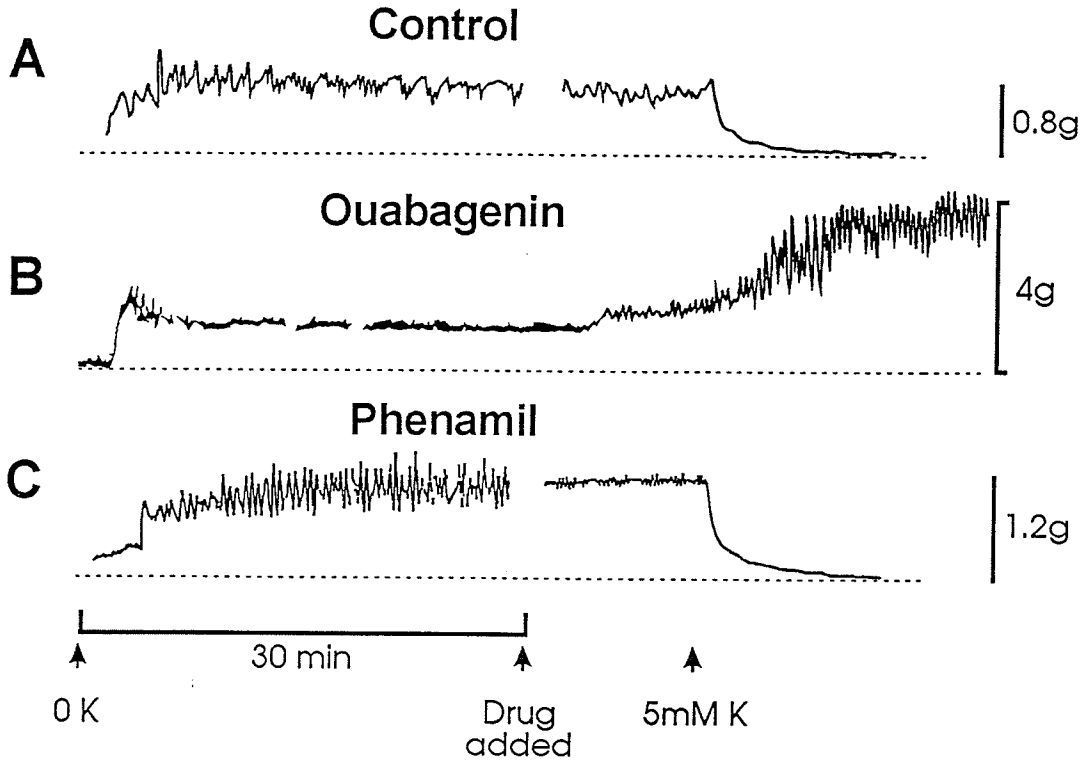

Figure 24
Effect of restoration of normal potassium medium on canine portal vein contracted in a potassium-free medium in control, and in the presence of 1 μM ouabagenin or 60 μM phenamil. Dotted lines below each tracing represents the resting tension of the muscle after equilibration in normal K^+ containing solution, immediately before replacement with potassium-free medium. Similar results were observed in 4 tissues. Baseline tension with a preload of 1g is indicated for each trace as a dotted line under the trace. Tension calibration bars extend from baseline tension to maximum tension attained during the contracture.

muscle after restoration of potassium into the bathing medium (figure 24, center trace), while phenamil did not impair the K^+-induced relaxation of the muscle (figure 24, bottom trace).

SODIUM-CALCIUM EXCHANGE

In order to test the hypothesis that phenamil could directly inhibit the sodium-calcium exchanger to produce inotropy, we employed the rapid cooling contracture technique.

Rapid cooling of the tissue results in calcium release from the SR (Bridge, 1986). Due to the cold temperature, the calcium pump does not remove calcium from the cytosol, resulting in a contracture. This is an effective method for quantitating changes in SR calcium content. During reheating, calcium is removed from the cytoplasm into the SR or out of the cell. Before the tissue reheats completely, the most active method for calcium removal is the sodium-calcium exchange. The calcium pump becomes fully activated later, after the temperature comes closer to 37°C, but only after calcium levels are lower in the cells. When the muscle is then left unstimulated and a second rapid cooling contracture (RCC) is produced, the height of the second RCC, with relation to the first, reflects the amount of calcium that moved through the sarcolemma during reheating, and hence reflects the amount of calcium removed predominantly by sodium-calcium exchange. The relative heights of twin RCC's are therefore an index of the activity of sodium-calcium exchange (Bridge, 1986). These experiments make the assumption that the compound being tested does not make the SR leaky, nor does it modulate the calcium pump.

Figure 25 shows the results of twin RCC experiments with phenamil (50 μM) and with ouabagenin (3 μM). Figure 25A reveals that phenamil produced positive inotropy without greatly changing SR calcium content. In 5 experiments phenamil did not significantly change the relative levels of the twin RCC as compared to either control, or to washout of the drug (figure 25B). Ouabagenin significantly decreased the reduction of the second RCC hence it reduces the activity of the forward mode of the sodium-calcium exchanger. This sodium pump inhibitor produced positive inotropy and greatly reduced the amount of calcium that was removed after the first RCC as compared to control (figure 25C).

The driving force for the sodium-calcium exchanger is the difference between the membrane potential and the reversal potential for the exchanger. Depolarization of the membrane potential can reduce the ionic flux through the exchanger and mimic an inhibition of the exchanger. According to the Nernst equation, the membrane is depolarized by approximately 30 mV in the presence of 14.3 mM KCl (4.3 mM in solution, and 10 mM added). This depolarization of the membrane potential reduced the activity of the sodium-calcium exchanger (figure 25D).

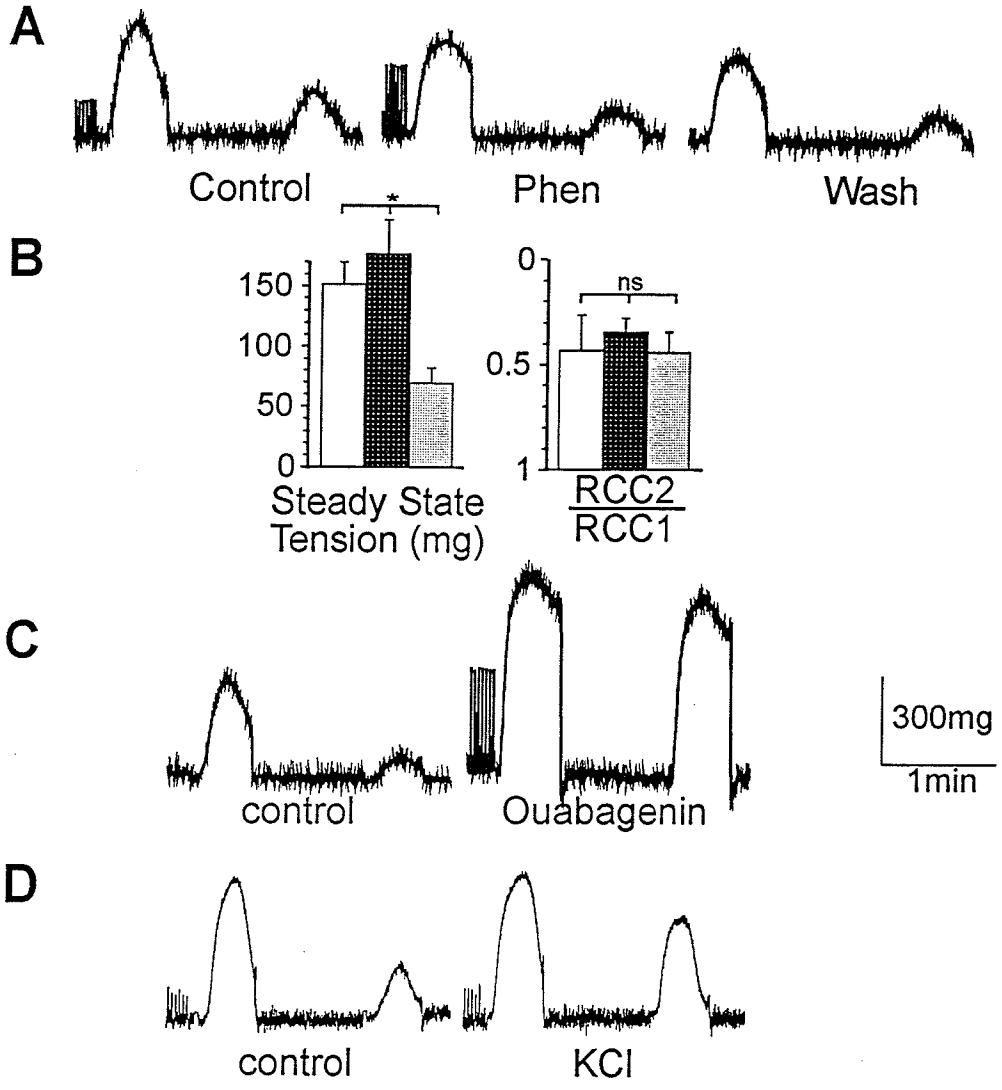

Figure 25

Rapid cooling contractures. **A**. Rapid cooling contractures before (**control**), with phenamil (**Phen**, 50μM), and after the washout of the drug (**Wash**). Electrical stimulation of the tissue was stopped within 2 seconds of the first cooling contracture and was not restarted until much beyond the end of the traces shown. Similar results were obtained in 5 of 6 experiments. **B**. Bar graphs showing the effects of phenamil on steady state contraction in control (white bars), with phenamil (50μM; dark bars), and after washout of the drug (light bars). Due to the gradual decline in tension over time, a two way ANOVA was performed to determine statistical significance between control, with drug, and after washout. Effect of phenamil on the twin RCC's (right) is graphed as the ratio of the second contracture to the first contracture in the couplet. **C**. Rapid cooling contractures before (control) and in the presence of ouabagenin (3μM). Similar results were seen in 4 experiments. D. Rapid cooling contractures before and in the presence of a depolarizing KCl solution (14.6mM). Similar results were obtained in 3 of 5 experiments.

ELECTROPHYSIOLOGY EXPERIMENTS

ACTION POTENTIAL: WHOLE TISSUE

Since it was determined that phenamil produces positive inotropy through some transsarcolemmal event, I needed to assess whether phenamil affects membrane channels to alter the action potential profile.

Phenamil prolonged the action potential in canine trabecular tissue (figure 26). This prolongation followed the time-course of positive inotropy and was dose-dependent (figure 26A). APD_{90} was prolonged with 40 μM, and APD_{50} with 60 μM phenamil ($p<0.05$, figure 26B); hence phenamil had a more prominent effect during phase 3 of the action potential. With 60 μM phenamil, the resting membrane potential became partially depolarized (figure 26B). The peak of the action potential was not significantly affected. Phenamil (60 μM) prolonged APD_{50} from 172±5 msec to 212±11 msec; prolonged APD_{90} from 207±6 msec to 262±12 msec; and depolarized RMP from -83±3 mV to -76±2 mV. With higher concentrations of phenamil (>80 μM), the muscles became insensitive to stimulation and sometimes became automatic (figure 27). The twitch tension and the action potential traces are shown in the absence and presence of 80 μM phenamil from a tissue that eventually became automatic and then insensitive to stimulation. Phenamil caused both positive inotropy and a lengthening of the twitch duration (figure 27B, and C) as compared to control (figure 27A). Prolongation of the action potential was seen, but as the muscle became less excitable, the latency before phase 0 increased progressively up to 100 ms while the resting membrane potential depolarized by up to 20 mV (figure 27D).

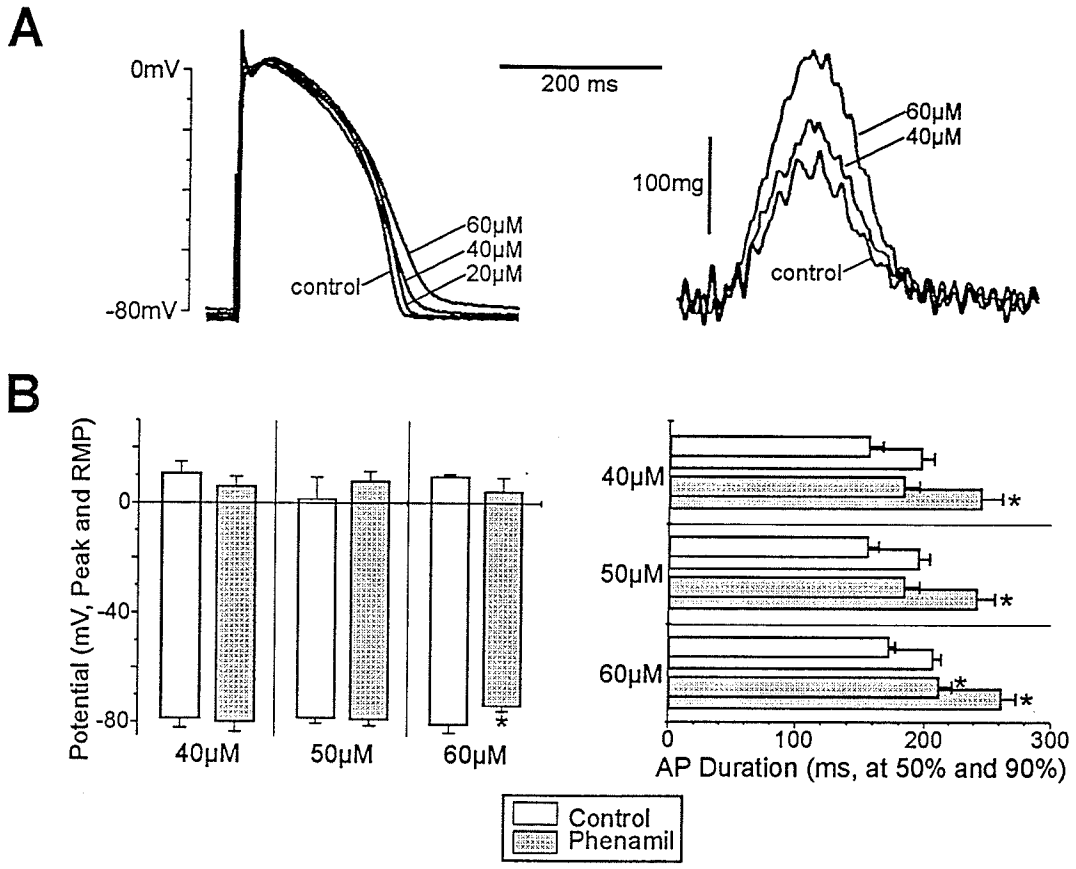

Figure 26

Effect of phenamil on the action potentials of canine ventricular trabeculae. **A**. Prolongation of the action potential by different concentrations of phenamil (20μM; 40μM; and 60μM) is shown on the left. In the same tissue, potentiation of the twitch tension by phenamil (40μM and 60μM) is shown on the right. **B**. Bar graphs show the effects of three concentrations of phenamil (40, 50, and 60 μM) on peak and RMP (left), and on the action potential duration (right). Data from control traces are shown in open bars. Duration bars (right) for APD_{50} are overlapped on those for APD_{90} of the same traces. Forty and 50 μM phenamil produced significant prolongation of APD_{90}; 60 μM phenamil significantly prolonged both APD_{50} and APD_{90}. ($P<0.05$, n=5 for 40 and 60 μM, n=7 for 50 μM phenamil.)

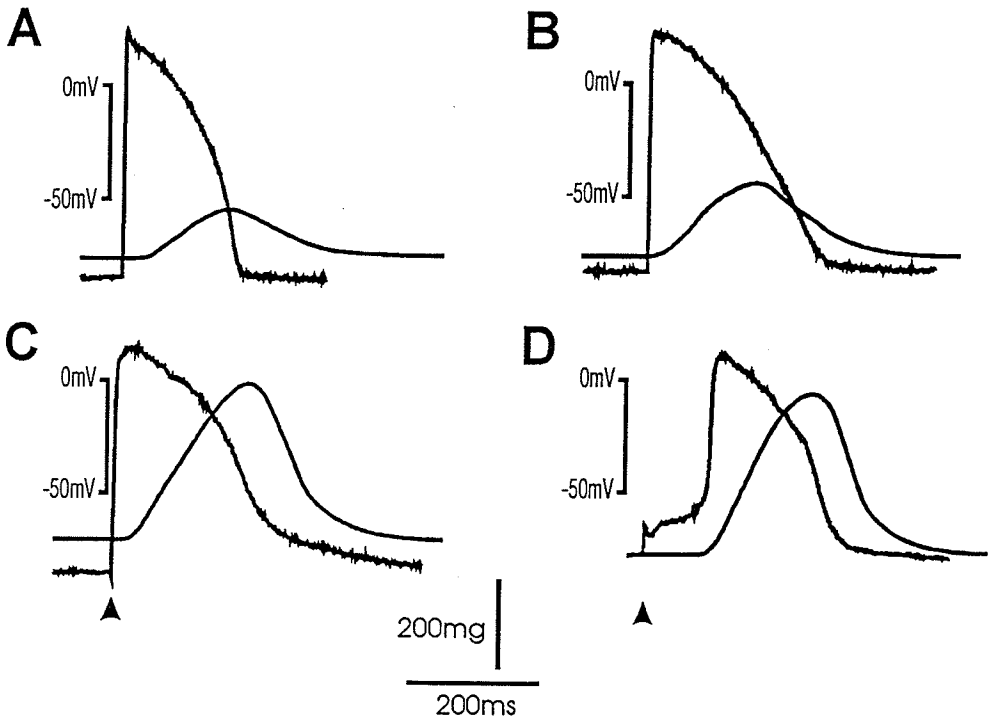

Figure 27
Action potential and twitch tension of a canine ventricular trabecula in control and with phenamil (80 μM). Calibration bars to the left of each set of traces are for the action potential traces. **A**: control; **B**: 5 min after phenamil addition; **C**: 10 min after phenamil addition; **D**: toxic effect of phenamil, taken immediately before the canine trabecula became unresponsive to stimulation. The four traces are lined up by time of stimulus indicated by arrows. The stimulus artifacts were suppressed except in D where the small upward deflection of trans-membrane potential at the start of the action potential trace is caused by the stimulus.

The upstroke velocity was slowed when the resting membrane potential became slightly depolarized. If stimulation was stopped for a short period, the lag time decreased for the first stimulus, but reappeared with each successive stimulus. In about 5 min the muscle became insensitive to stimulation. This could be temporarily corrected by increasing the strength of the stimulus.

Phenamil has been shown to prolong the action potential of guinea-pig ventricular myocytes (Guia *et al*, 1992) at room temperature. Prolongation of the action potential duration in guinea pig papillary muscle was also observed at 37°C (figure 28). The prolongation of the action potential was proportional to the dose of phenamil (figure 28B) and was reversed upon washing out the drug. Within 15 min the action potentials increased in duration from 164±6 ms to 207±14 ms in the presence of 60 μM phenamil (12 ms SE of difference; $p<0.01$; figure 28C). Maximum prolongation of the action potential duration took place during the next 20 min. In this species, concentrations greater than 80 μM led to toxicity (automaticity and inexcitability to external electrical stimuli).

Guinea pig ventricular myocytes do not exhibit a noticeable phase 1 of the action potential, which has been shown to be attributable to I_{to} and blocked by 4AP (Giles and Imaizumi, 1988). The action potential profile of rat ventricular myocytes is largely controlled by I_{to} (Josephson *et al*, 1984). The effects of phenamil were hence compared to those of 4AP in rat ventricular papillary muscle (figure 29). In rat ventricular tissue, phenamil (100 μM shown, similar results were observed with 50 μM) produced reversible

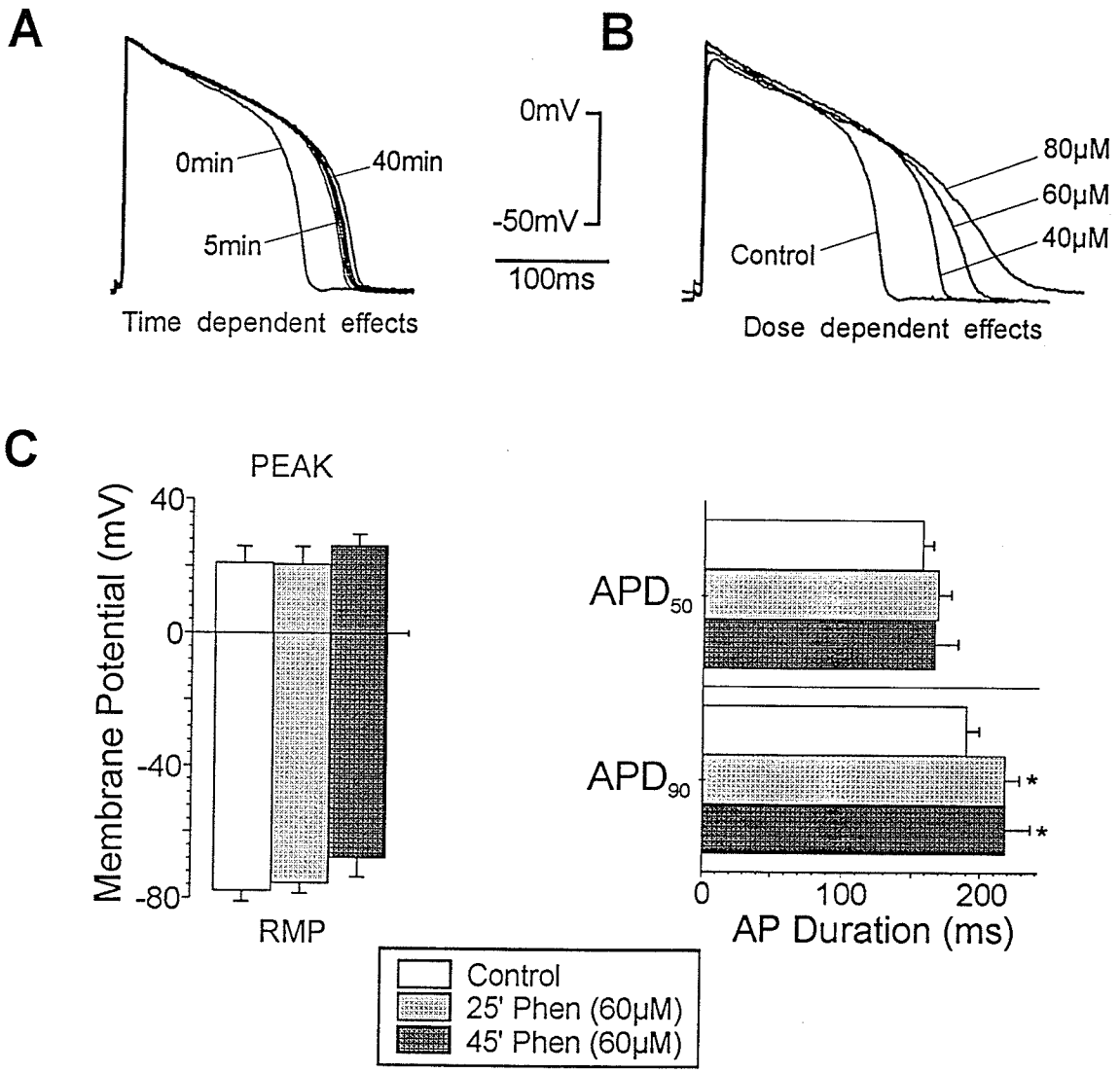

Figure 28
Effect of phenamil on the action potentials of guinea-pig left ventricular papillary muscle. **A**. Time-dependent effect of 40 μM phenamil on the action potential. **B**. Effect of cumulative doses of phenamil on the action potential. The increase in action potential duration was significant within 10 min (APD_{90} changed from 164 ms to 207 ms; $p<<0.01$, using 60 μM Phen). **C**. Electrophysiological effects in control (open bars) after 25 minutes (middle bars), or after 45 minutes (shaded bars) in the presence of phenamil (60 μM) on the action potential. Left: Effect of phenamil on the resting membrane potential (RMP) and the peak of the action potential (Peak). Right: Time to 50% repolarization (APD_{50}) and to 90% repolarization (APD_{90}). Major lengthening of the action potential occurred after 50% repolarization. (n=7)

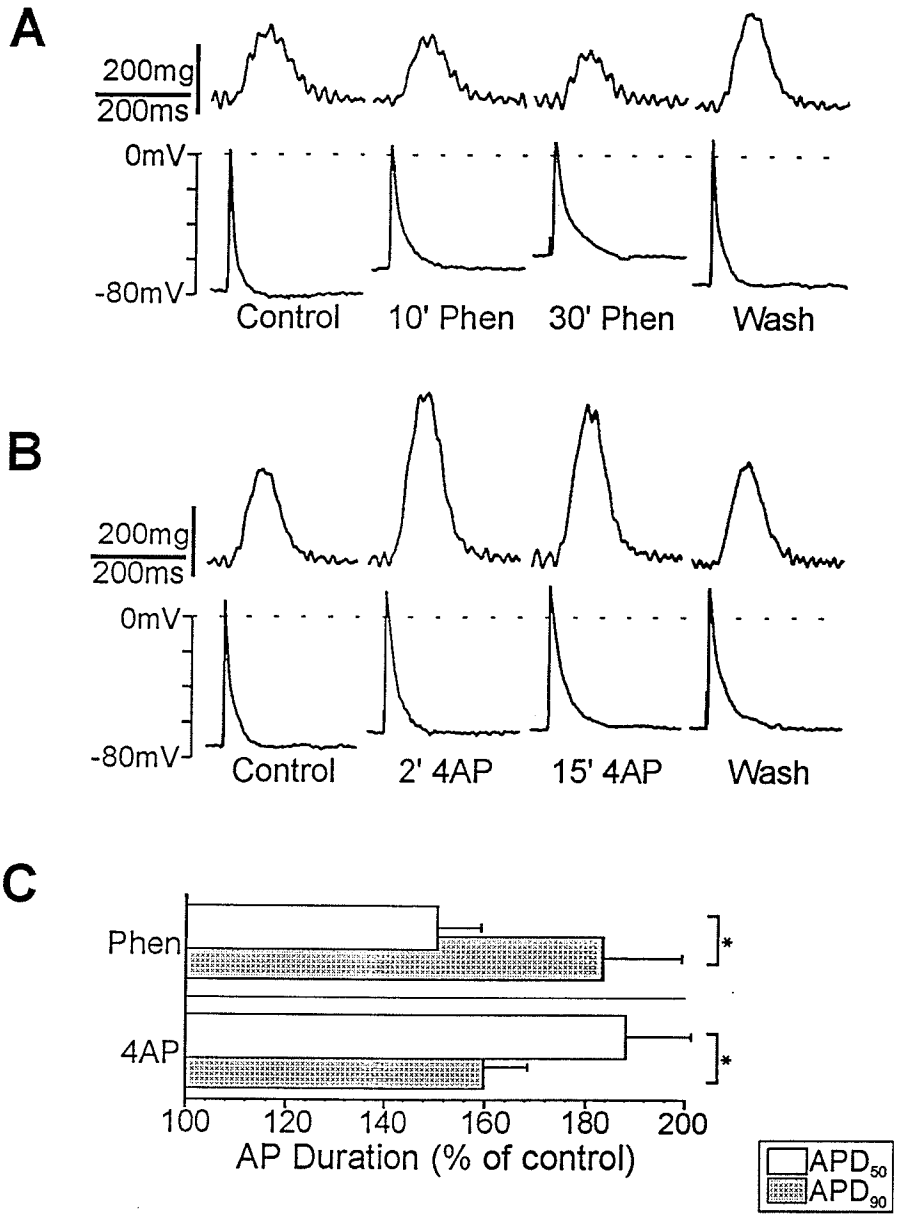

Figure 29

Effect of phenamil or 4AP on the action potentials of rat ventricular papillary muscle. **A.** Measurements of twitch tension (above) and membrane potential (below) in control, with 50μM phenamil for 10 minutes (**10' Phen**) or 30 minutes (**30' Phen**), and after washout of the drug (Wash). **B.** A similar experiment using 1 mM 4AP with measurements after 2 minutes (**2' 4AP**) or 15 minutes (**15' 4AP**). Similar results were seen in tissues from 3 animals. **C.** A Bar graph shows the effect of phenamil (50 μM) or 4AP (3mM) on the action potential duration. Data is expressed as a percent of control duration. APD_{50} is shown with open bars, and is overlapped on APD_{90}. (n=3)

negative inotropy and depolarization of the resting membrane potential (figure 29A). There was a transient period of positive inotropy upon washout. In contrast, 4AP (3 mM) resulted in positive inotropy (figure 29B). The decrease in resting membrane potential with 4AP was not consistent (n=3), and not reversible on washout hence it was likely due to electrode drift. Figure 29C demonstrates that phenamil and 4AP had different effects on the rat action potential duration. Phenamil prolonged predominantly APD_{90} (dark bar) whereas 4AP prolonged predominantly APD_{50}.

ACTION POTENTIAL: SINGLE-CELL

Whole-cell voltage clamp studies were done on freshly dispersed guinea pig ventricular myocytes.

Myocytes were studied under current clamp conditions using the standard potassium-containing internal and external solutions. Cells exhibited an average resting membrane potential (RMP) of -82±1 mV, a peak overshoot of +47±2 mV, action potential durations of 369±58 ms at 90% repolarization (APD_{90}), and 296±53 ms at 50% repolarization (APD_{50}; n=20; figure 30). Phenamil (10 μM) progressively increased the action potential duration. The lengthening of the action potential was accompanied by a delayed decline in RMP after 10-15 min. A higher concentration of phenamil (60 μM) caused a more prominent and faster change in the APD_{90} and RMP (figure 30B). These effects were almost completely reversible upon washout of phenamil (figure 30A and B). Phenamil (60 μM) was also tested in other myocytes with variable results, including delayed afterdepolarizations, intermittent series of spontaneous action potentials, or

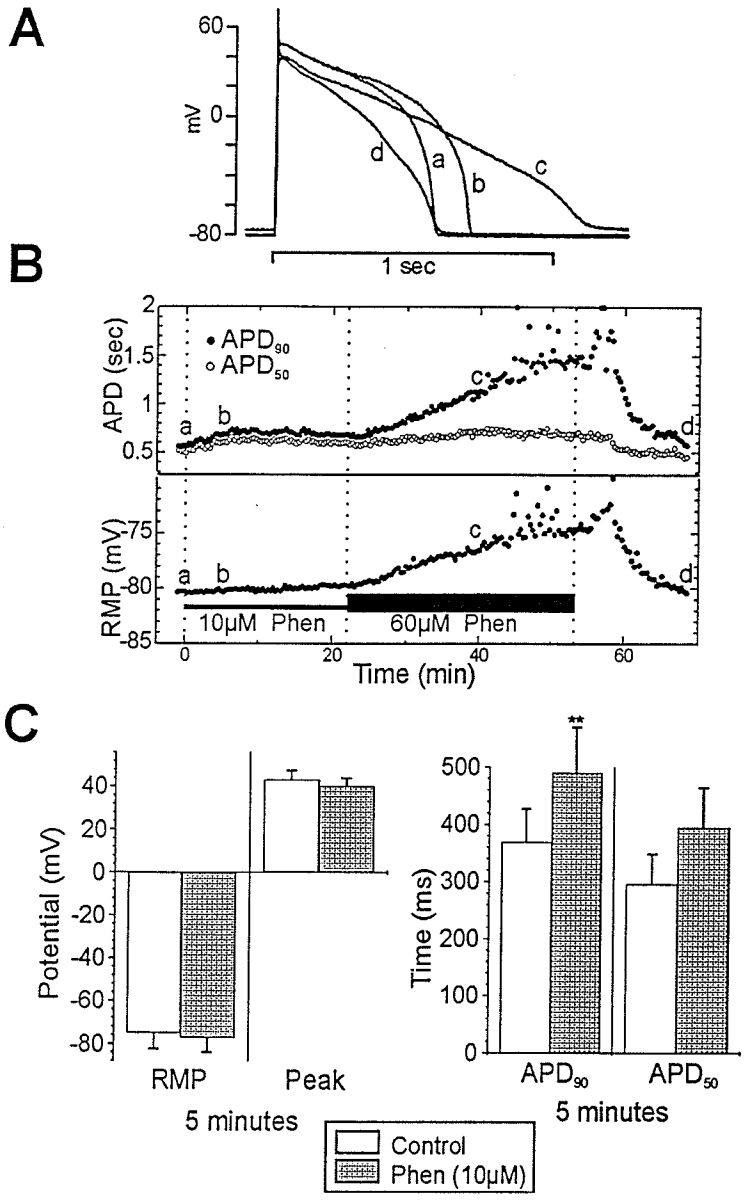

Figure 30

The effects of phenamil on the action potential of guinea-pig ventricular myocytes. **A.** Action potentials from one cell before (**a**), after 5 minutes with 10 μM phenamil (**b**), with 60 μM phenamil (**c**), and after its removal (**d**). Letters correspond to the time-curve in panel B. **B.** Time-course of effects of phenamil (10 and 60 μM) on the resting membrane potential (RMP) and action potential duration (APD) at 90% repolarization (closed circles) and at 50% repolarization (open circles). Letters on the curve correspond to traces in panel A. Phenamil (10μM) was added at time=0 and the concentration was increased to 60μM at time=22 min. **C.** Left panel. The voltages of the resting membrane potential (RMP) and the overshoot of the action potential (Peak) in control (open bars) were not different from those recorded at 5 minutes in the presence of 10 μM phenamil (closed bars). Right panel. In the presence of 10 μM phenamil, time to 90% repolarization (APD_{90}) was significantly different from control (**, p=0.009, n=10). Time to 50% repolarization (APD_{50}) was different from control, but with less confidence (p=0.07, n=10). Action potentials were elicited with a short positive pulse of current applied in the clamp pipette in current-clamp mode.

oscillatory potentials where a triggered AP remained in phase 2 (stabilized near -35 mV) for several tens of seconds then suddenly repolarized. Even when continuously exposed to lower concentrations of phenamil (10 μM), the cells eventually depolarized, then became inexcitable and failed to recover even after long periods of washout (>60 minutes).

Soon after the addition of phenamil (10 μM, 5 minutes), RMP and peak overshoot of the action potential were unchanged whereas APD_{90} was increased (p=0.009, n=10). The phenamil-induced changes in APD_{50} after 5 minutes were not significant at the 95% confidence level but were at 93% confidence level (p= 0.07;n=10; figure 30C),.

WHOLE-CELL VOLTAGE CLAMP EXPERIMENTS

L-TYPE CALCIUM CURRENT, I_{CaL}

Calcium currents were recorded in cesium- and TEA-loaded myocytes superfused with potassium-free, cesium external solution containing 10 mM TEA to inhibit potassium channels. The cells were held at -80 mV to reduce the run-down of I_{CaL}. A 200 msec preconditioning step to -40 mV was imposed before the test potential in order to inactivate sodium channels. From this level, test potentials from -30 to +60 mV were applied in 10 mV increments for 250 msec and the peak calcium current was plotted to construct the I-V relationship of I_{CaL} (figure 31C).

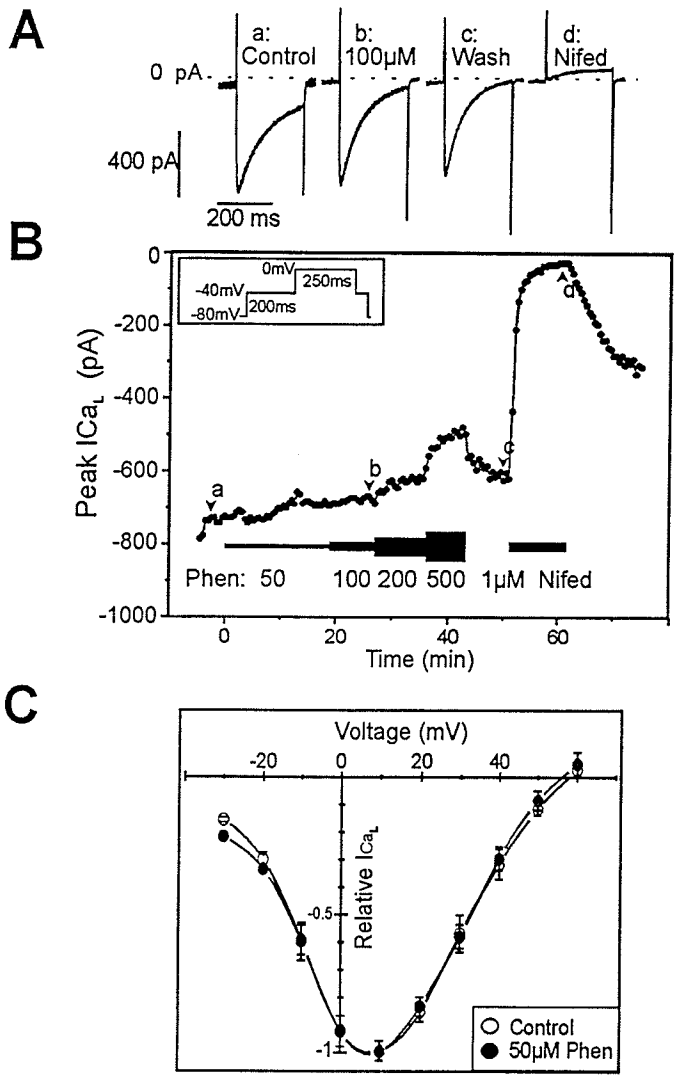

Figure 31

Effect of phenamil on L-type calcium current. Internal and external potassium was replaced by cesium and TEA^+. **A.** Sample traces obtained in one myocyte in response to 250 msec steps to 0 mV in the absence (**a: Control**), in the presence (**b: 100 μM**) and following washout of phenamil (**c: Wash**), and after the addition of 1 μM nifedipine (**d: Nifed**). Each step to 0 mV was preceded by a 200 msec pre-step to -40 mV to inactivate sodium channels (HP=-80 mV; protocol shown in the inset of panel B). Letters correspond to those labelled on the time-course plot illustrated in panel B. **B.** Step pulses to 0 mV were applied every 30 sec. The maximum amplitude of the current was measured during the application of (**Phen**, 50, 100, 200, and 500 μM, solid bars of varying thickness, first exposure started at time=0) and following the removal of phenamil. After the removal of phenamil, nifedipine was added (1 μM **Nifed**, second solid bar). Letters on the curve correspond to traces in panel A. **C.** Relative I-V relationships of peak inward current obtained during step protocols ranging from -30 to +60 mV applied in 10 mV increments (again each test pulse was preceded by a pre-step to -40 mV from HP=-80 mV). Peak inward current measurements (means ± SE) were normalized against maximum current (+10 mV) and plotted as a function of step potential. Phenamil did not affect the shape of the I-V relationship of ICaL (**O**, Control; **●**, 50 μM Phenamil; n=6).

Figure 31A shows sample tracings, taken at times indicated by corresponding labels in panel B, evoked by 250 msec test potentials to 0 mV applied at 30 sec intervals (panel B, inset), under control conditions (a), in the presence of 100 μM phenamil (b), after removal of phenamil from the bathing solution (c), and during the application of 1 μM nifedipine (d). Panel B shows the time course of changes of peak inward current during the application of various concentrations of phenamil (50, 100, 200, or 500 μM). At concentrations of 50 or 100 μM, phenamil had no observable effect on I_{CaL}. A small dose-dependent inhibition of I_{CaL} was evident with 200 or 500 μM phenamil (6% and 25% inhibition respectively). Nifedipine (1 μM) inhibited I_{CaL} by more than 90%. Similar results were obtained in 7 other cells.

Data from 6 cells were averaged to construct the I-V curves in figure 31C. Due to the time-dependent run-down of I_{CaL} (Belles *et al*, 1988), all data points were normalized against the largest current (+10 mV). The reduction in current after the addition of phenamil is not significantly different from the reduction in current after the washout of phenamil. Phenamil (50 μM) did not appreciably change the voltage dependence of I_{CaL}.

DELAYED RECTIFIER POTASSIUM CURRENT, I_K

Delayed outwardly rectifying potassium current was recorded using five-second step protocols from -30 to +60 mV in 10 mV increments (HP=-80 mV, 200 msec pre-step to -40 mV, 30 sec interval between pulses). The membrane was then repolarized to -40 mV for 5 seconds to record deactivating tail current. Pilot experiments using 5 mM intra-pipette EGTA concentration or calcium-free external medium to inhibit calcium-

dependent ionic currents (sodium/calcium exchange; non-selective cation channels, Ehara *et al*, 1988) resulted in rapid and extensive run-down of I_K which compromised the analysis of the effects of phenamil on this potassium current, an observation consistent with the previously reported calcium-dependence of I_{Ks} (Tohse, 1990). Experiments were carried out using a sodium-free pipette solution containing a low EGTA concentration (0.1 mM). Nifedipine (1 μM) was included in the perfusate to inhibit calcium current. These conditions minimized the contribution of the sodium-calcium exchange currents and transient inward currents which are often observed following long step depolarizations to positive potentials. The delayed rectifier currents may be subdivided into slowly activating (I_{Ks}) and rapidly activating (I_{Kr}) components. At potentials positive to +30, the contribution of I_{Kr} is small (Sanguinetti and Jurkiewicz, 1990). In contrast, the deactivating tail current measured upon repolarization to -40 mV is the sum of both components (Sanguinetti and Jurkiewicz, 1990).

Figures 32A and B illustrate the results of a typical experiment in which we examined the effects of phenamil on I_K. (measured at the end of a step potential to +60 mV as the maximum time-dependent current) and on $I_{Ks} + I_{Kr}$ (measured as the steady-state activation current as seen by the tail current during a -40 mV step). Figure 32A shows sample current traces, corresponding to the labeled measurements depicted in panel B, obtained at different times before, during (panel B, heavy bar) and following application of 50 μM phenamil. Figure 32B is a plot of the time course of changes in I_K amplitude (filled circles) measured during five-second steps to +60 mV and the magnitude of tail current (filled squares) recorded after repolarization to -40 mV; this protocol was

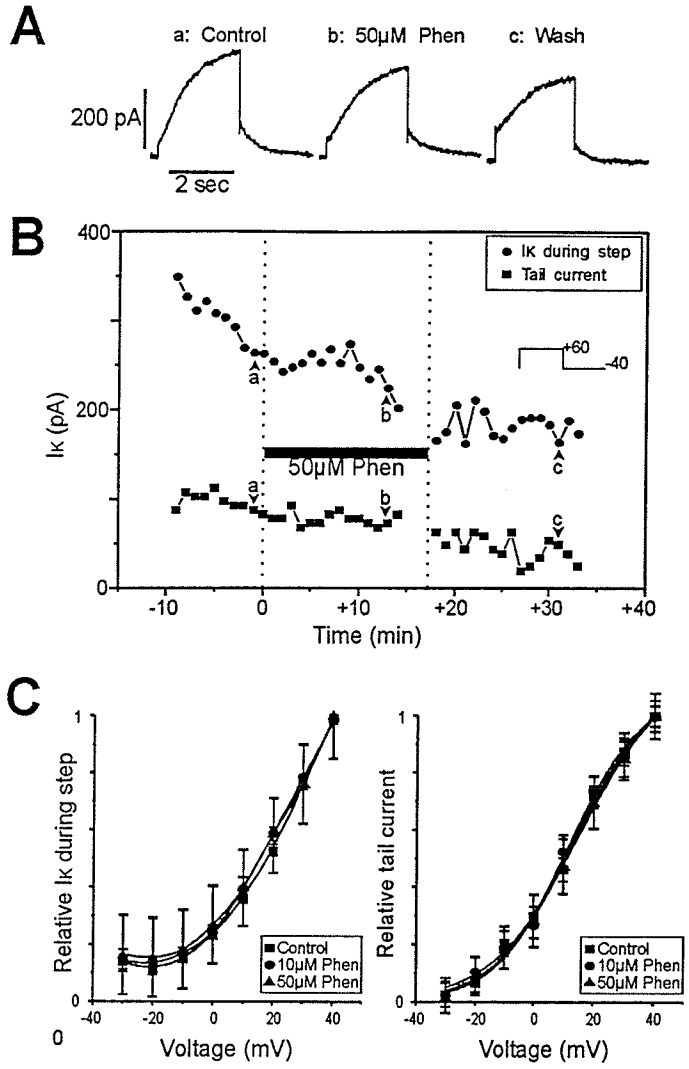

Figure 32

The effects of phenamil on outwardly rectifying potassium current, I_K. **A**. Five-second voltage steps to +60 mV were used to elicit I_K; membrane was repolarized to -40 mV for 5 seconds to record deactivating outward tail current (HP=-80 mV, protocol inset in panel B). Measurements were done using standard internal and external solutions in the presence of 1 μM nifedipine in the bathing medium, and in the absence of internal sodium. Sample traces from one cell were taken at three different times: (**a**) at the beginning of the experiment, (**b**) in the presence of phenamil (10 μM), and (**c**) after washout of the drug. **B**. The time-dependent current (I_{end}-$I_{beginning}$) during steps to +60 mV (**IK during step**, ●) and the tail current amplitude at -40 mV (**Tail current**, ■) are plotted as a function of time during which phenamil (**50 μM Phen**) was added (at time=0) and then washed out of the extracellular medium. Letters on the curve correspond to traces in panel A. **C**. The outwardly rectifying potassium current was normalized relative to the current measured at +40 mV (I-V protocol). The I-V curves in the presence of phenamil (10 or 50 μM) were not different from control. **Left**: The I-V curves of the relative current recorded during voltage steps (relative I_K during step; n=6) were fit to a second degree polynomial function. **Right**: Steady state activation curves of I_K based on relative tail current amplitude measurements (means ± SE, n=4) were fit to a Boltzmann function. (Control: V½=14mV, K=13mV, χ^2=0.37; 10μM Phenamil: V½=12mV, K=12mV, χ^2=0.29; 50μM Phenamil: V½=16mV, K=15mV, χ^2=0.12).

imposed on the cell every 60 seconds. The amplitude of the time-dependent current measured at the end of the pulse (figure 32B, circles) and the tail current seen upon repolarization to -40 mV (squares) gradually declined with time due to run-down of these channels at room temperature (Hume, 1989). The time course of changes in the magnitude of I_K at +60 mV and tail current at -40 mV can be attributed to current run-down rather than to an inhibitory effect of phenamil since these changes were not appreciably altered during the application of phenamil or following washout. Similar results were obtained in 5 other myocytes.

Figure 32C shows plots of voltage-dependence of normalized mean±SE currents during steps (panel a; normalized against the current recorded at +60 mV; n=6) and tail currents (panel b; n=6) recorded under control condition, and in the presence of 10 or 50 μM phenamil (P). Phenamil produced little effect on the voltage-dependence of the time-dependent potassium current recorded during steps. In 4 out of 6 experiments phenamil (50 μM) had no noticeable effect on the voltage-dependence of tail currents evoked after repolarization to -40 mV. Due to run-down, tail currents in the remaining two cells were too small to draw any meaningful conclusions about the effects of phenamil.

INWARDLY RECTIFYING POTASSIUM CURRENT, I_{K1}

Based on our current clamp data (Guia *et al*, 1995), one possible explanation for the prolongation of the action potential is that phenamil may inhibit inwardly rectifying potassium channels (I_{K1}) which are known to play an important role in determining RMP

and phase 3 repolarization in cardiac myocytes (Shimoni *et al*, 1992). We have tested this hypothesis by examining the effects of phenamil on I_{K1} using slow voltage ramps or step protocols. From a holding potential (HP) of -80 mV, positive-slope voltage ramps from -140 to +60 mV over 8 seconds were applied to the cell repeatedly every 30-60 seconds. Such protocols elicited quasi-steady-state membrane currents which have been previously shown to be carried mainly by I_{K1} at potentials negative to -40 mV (Shimoni *et al*, 1992; Harvey and Ten Eick, 1989a). All ramp protocol data were obtained using standard internal and external solutions. Since ramp protocols yield quasi-steady-state membrane currents and not steady-state currents, the effects of phenamil were also tested on I_{K1} evoked during voltage steps.

Inwardly rectifying potassium currents (I_{K1}) are time-independent (Sakmann and Trube, 1984). In a quasi-steady-state curve, the majority of the current seen below -40 mV is carried by the I_{K1}. As shown in figure 33A, phenamil potently blocked I_{K1}. In this cell, application of 10 μM phenamil produced over 90% inhibition of I_{K1} at -60 mV (inset, Phen) and 80% at -120 mV. These effects were partially reversible upon removal of phenamil from the extracellular medium (Wash). The phenamil-sensitive current (figure 33B) obtained by digital subtraction revealed a current-voltage relationship typical of that expected for I_{K1} (Harvey and Ten Eick, 1989a; Shimoni *et al*, 1992). The small phenamil-sensitive inward current at +40 mV most likely reflected run-down of the delayed rectifier potassium current (predominantly I_{Ks}; Sanguinetti and Jurkiewicz, 1990) as seen during long step depolarizations (see figure 32). Indeed, the inward current

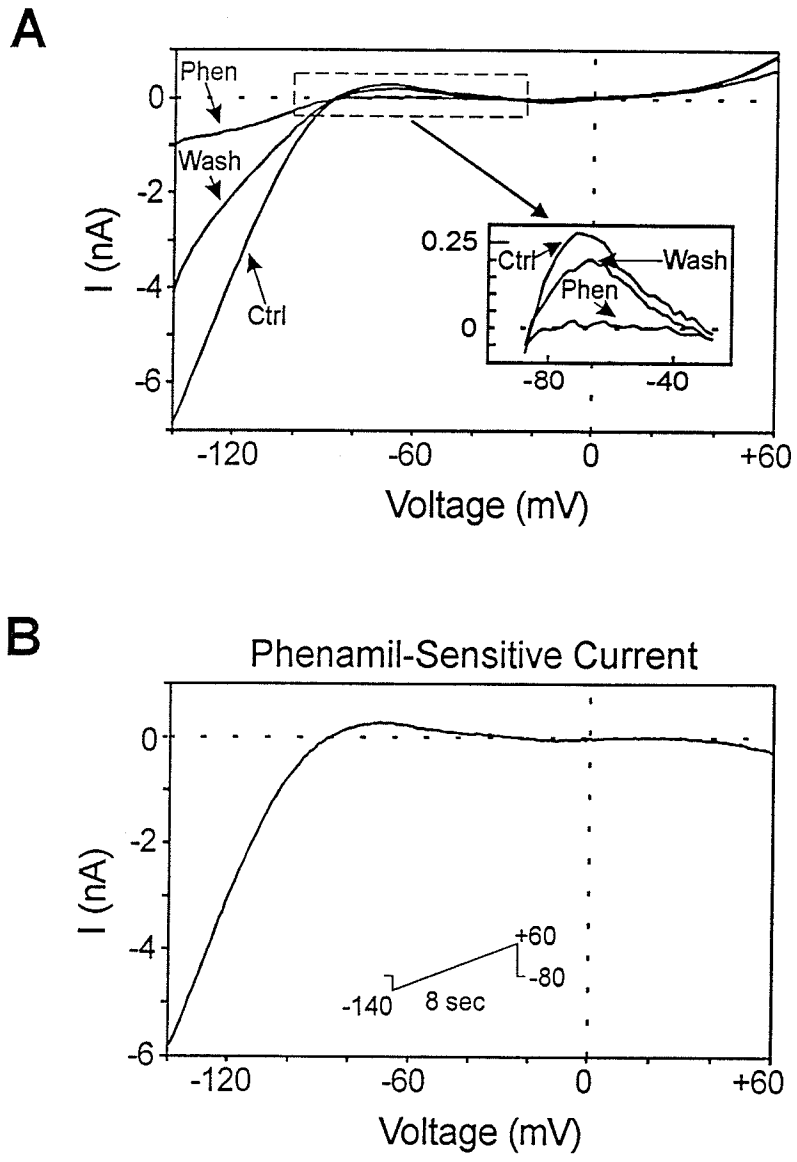

Figure 33

The effect of phenamil on quasi-steady-state membrane current recorded in one cell. **A.** Eight-second voltage clamp ramp protocols from -140 mV to +60 mV (HP=-80 mV, protocol inset in panel B) were applied every 20 seconds. Membrane currents are plotted against ramp voltage. In this cell, phenamil (**Phen**; 10μM; 20 min) caused 80% to 90% inhibition of the inwardly rectifying potassium channels as compared to the trace taken before the addition of phenamil (**Ctrl**). The current partially recovered after removal of phenamil (**Wash**; 25 min). Inset shows a magnification of the "hump" region of the I-V curve. **B.** The phenamil-sensitive current was derived by subtracting the control curve of the trace in panel A from the curve obtained in the presence of phenamil. Reversal potential of the phenamil-sensitive current was at -87 mV.

apparent in the presence of phenamil remained after washout of phenamil (data not shown) whereas the current below -40 mV partially recovered.

The time-dependent effects of phenamil on I_{K1} are shown in figure 34. Sample traces from one experiment (A) show the time course of inhibition of I_{K1} by phenamil (50 μM) using a voltage ramp protocol similar to that used in figure 33. Net current at three different voltages (-135, -100, and -65 mV) during the ramp protocol was measured and plotted as a function of time (figure 34B and C). Addition of phenamil (50 μM) resulted in a slow decrease in current at each of the potentials (~95% at -65 mV). Similar results were obtained from 4 other cells.

Figure 35 reports data of experiments in which the effect of phenamil was tested on I_{K1} elicited during step protocols (from -120 to +30 mV in 10 mV increments, 100 ms steps, HP=-80 mV) instead of ramp protocols. In these experiments, the bathing medium contained 1 μM nifedipine to inhibit calcium currents. Each step was preceded by a pre-step to -40 mV for 200 msec to inactivate sodium current. The current was measured at the end of the test pulse. Figure 35A shows sample traces for I-V relationships in the absence (Control) and presence of 50 μM phenamil (Phen). I_{K1} I-V relationships obtained in control (n=23) and in the presence of 50 μM phenamil (n=12) are illustrated in figure 35B. The phenamil-induced inhibition of I_{K1} elicited during voltage steps was qualitatively similar to that observed during voltage ramps (figures 33 and 34). The inset in panel B shows the voltage dependence of the inhibition of I_{K1} by 50 μM phenamil (n=12). The block by phenamil was weakly voltage-dependent with a slight tendency of

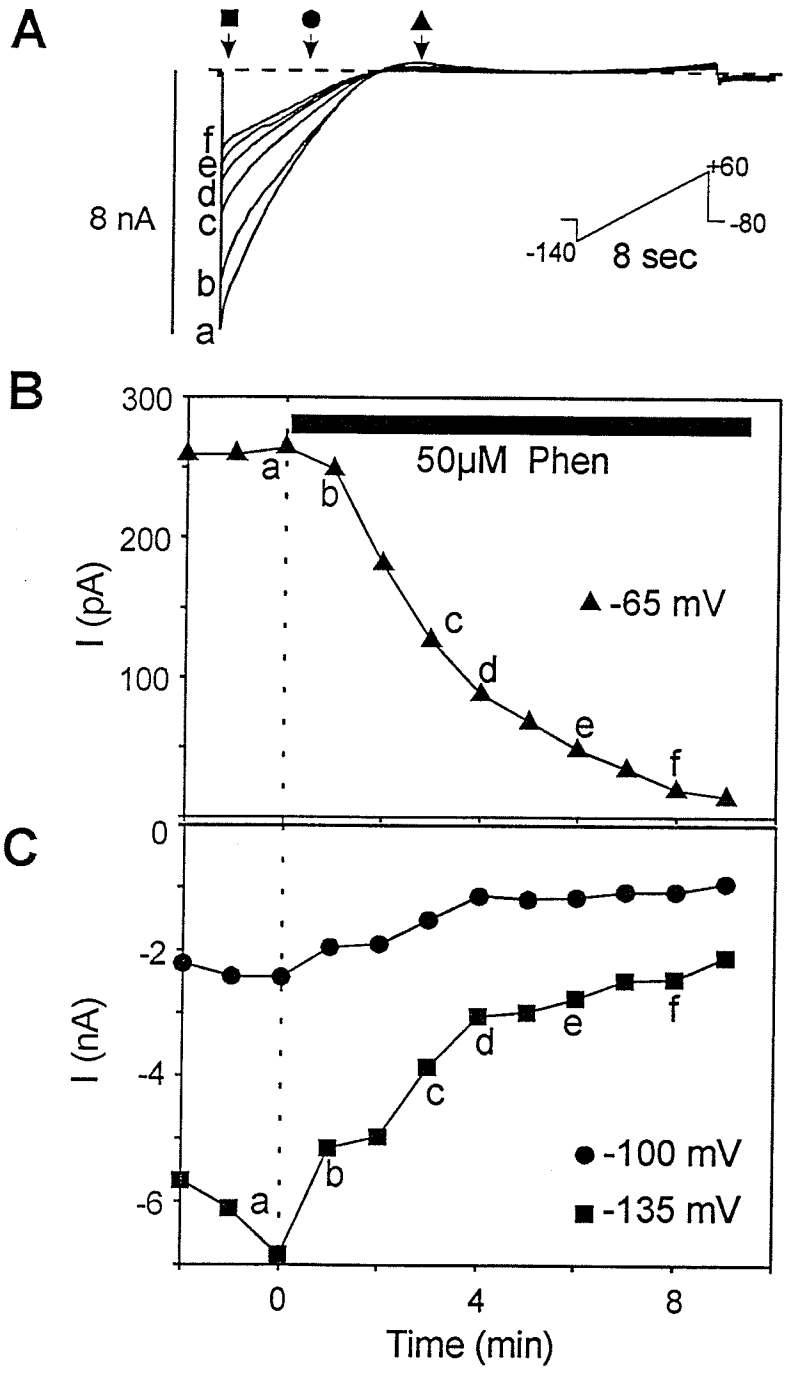

Figure 34

The time-dependent effects of phenamil (50 μM) on quasi-steady-state current. **A.** Ramp protocols (*inset*) were applied once every minute. Letters (**a-f**) represent different times after the addition of phenamil (50 μM) where (**a**) is the trace immediately before the addition of phenamil. Arrows indicate -135 mV (■), -100 mV (●) and -65 mV (▲) and correlate with the voltage at which the current (I) measurements were done in panels B and C. **B, C.** The time-course of the effect of phenamil (50 μM, added at time=0) on currents in the "hump" region (-65 mV, ▲) of the I-V plots of the quasi-steady-state currents, and at two potentials below the reversal potential for potassium (-100 mV, ●; -135 mV, ■). Phenamil (50 μM) was added at time=0.

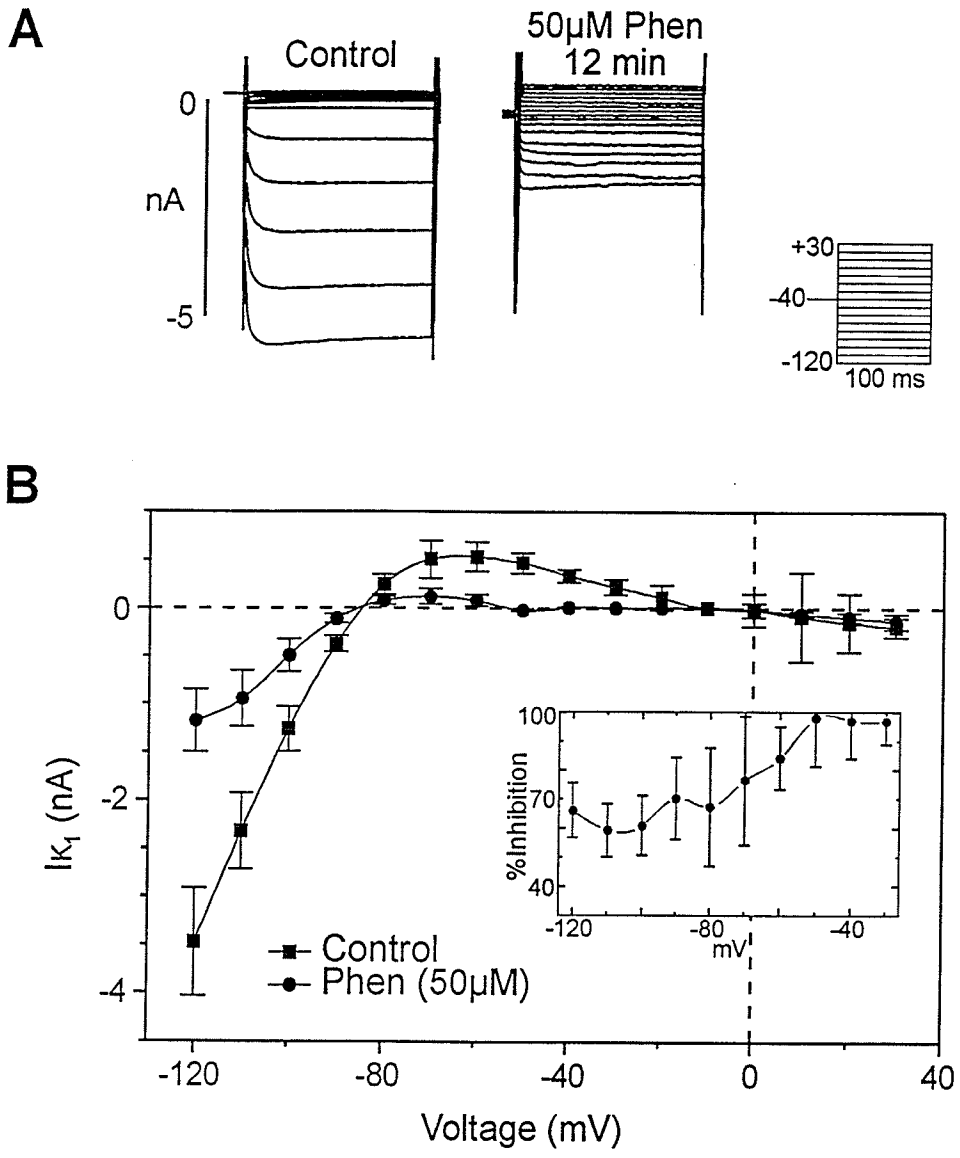

Figure 35
Effect of phenamil (50 μM) on inwardly rectifying potassium current, I_{K1} elicited by 100 ms step protocols on ventricular myocytes. **A**. Sample traces used to construct I-V relationships in the absence (Control) and after 12 minutes exposure to phenamil (Phen, 50 μM). The step protocol is shown to the right. **B**. I-V relationships of membrane current measured at the end of the pulse showing a phenamil-induced inhibition of I_{K1}. Linear leak subtraction was performed on the data. Reversal potential of the inhibited current was at -84 mV and matched theoretical reversal potential for potassium. (■ Control, n=23; ● 50 μM Phenamil, n=12.) *Inset* shows percent of current inhibited by phenamil (50μM) at each voltage (n=12).

the compound to be less potent at voltages more negative than -60 mV. However, a multiple ANOVA revealed no significant differences between the inhibitory effects of phenamil at voltages in the range of -120 to -60 mV. These results demonstrate that phenamil is a relatively potent inhibitor of I_{K1} in the heart. Higher concentrations of phenamil (up to 200 μM; data not shown) produced faster inhibition of I_{K1} with a complete block observed at 200 μM at voltages positive to -110 mV (n=2).

DISCUSSION

SOURCE OF INOTROPY

ISOMETRIC TENSION

Canine cardiac tissue was used to investigate the mechanism of inotropy by phenamil. In right ventricular trabeculae, phenamil produced positive inotropy (EC_{50}=59 μM). Higher concentrations were needed for amiloride and other analogs (Brown *et al*, 1991) to produce the same degree of inotropy. At concentrations that produce positive inotropy, phenamil is known to affect only epithelial-type sodium channels (reviewed in Kleyman and Cragoe, 1988), a channel which has not been described in cardiac tissue. Phenamil has a pKa (7.8) higher than intracellular pH, and is among the more hydrophobic derivatives of amiloride (Kleyman and Cragoe, 1988). The inotropic effect of phenamil was slow in reaching steady state at lower concentrations (40 minutes). This may suggest a requirement for cytosolic or membranous accumulation of phenamil indicating a possible site of action. Compounds that become polar in their protonated forms, and that have a pKa close to the physiological range are known to accumulate in the cytosol due to lower intracellular pH. The inhibition of I_{K1} was shown to be less effective when the membrane became more polarized (Guia *et al*, 1993)

Amiloride blocks alpha-2 adrenoceptors (Shi *et al*, 1990), causing release of norepinephrine (Stjarne *et al*, 1990) which can interact with the cardiac beta adrenoceptors. Since the inotropy by phenamil can be blocked by a beta adrenoceptor antagonist, an inhibitory role of phenamil on alpha-2 receptors of the neurons cannot be ruled out. Dichlorobenzamil is chemically similar to phenamil and also produces positive inotropy in the 5-30 μM range. It was shown to block phosphodiesterase (Floreani *et al*, 1987). Both these events are known to increase cytosolic levels of cAMP which results in positive inotropy. A possible sympathomimetic effect of phenamil was investigated. The effects of phenamil are significantly different from those of norepinephrine in that there is a prolongation of the twitch duration by phenamil. Therefore it is likely that the intracellular concentration of cyclic AMP and the calcium ATP-ase are not affected by phenamil. Many beta blockers have other direct effects aside from beta blockade, such as potassium channel blockade by sotalol (Sanguinetti and Jurkiewicz, 1990). It is not surprising therefore that the effects of phenamil may be blunted by the addition of beta blockers.

RELATIVE IMPORTANCE OF SR VS. SL

To deduce whether positive inotropy was due to SR calcium release or accumulation, biphasic contractions described here and elsewhere (King and Bose, 1983) were used. As described previously, P1 and P2 phases of contraction produced by replacing 90 to 95% of the external calcium with strontium, denote the contribution of SR and sarcolemma calcium movements respectively. Under these conditions, strontium prolongs the action potential by reducing I_K (Tohse, 1990) and by reducing the calcium

dependent inactivation of the calcium channels. Furthermore it is not taken up by the SR to any significant amount. This delayed component of contraction (P2) is caused by a direct effect of strontium on the contractile apparatus (Kerrick *et al*, 1980). The small amount of calcium present in the medium causes an early component of contraction mediated by the SR. Under these conditions, compounds, such as norepinephrine, which enhance calcium storage in and release from the SR (Bers, 1991) will potentiate P1. Ouabagenin is known to increase cytoplasmic calcium levels by transmembrane movement through sodium-calcium exchange (Lazdunski *et al*, 1985). 4AP produces positive inotropy by inhibiting I_{to} and increasing the height of phases 1 and 2 of the action potential (Ruiz-Petrich and Leblanc, 1989), promoting calcium entry. Compounds, such as ouabagenin that decreases transsarcolemmal removal of calcium, or 4AP which prolongs the action potential, also enhance the transsarcolemmal movement of strontium. These compounds potentiate P2, which is sensitive to the action potential duration. Phenamil had effects similar to those of 4-AP and ouabagenin hence it affected transsarcolemmal calcium movement.

POST-REST CONTRACTIONS

Post-rest potentiation of the contraction is a useful indicator of the amount of calcium in the SR and available for release (Bers *et al*, 1985). Between contractions the calcium in the cells is taken up into the longitudinal element of the SR very quickly. It then passes to the terminal cisternae to be made available for release during the next action potential. Since the transfer from the longitudinal element to the terminal cisternae is

time-dependent, a longer rest period between beats allows more calcium to accumulate in the terminal cisternae and become available for release, eliciting a potentiated PRC. Calcium continuously leaks from the SR and is subsequently removed from the cells by sodium-calcium exchange or by calcium ATP-ase between beats, hence longer rest periods reduce the amount of calcium available to produce contraction (Bose *et al*, 1988). Positive inotropes that produce inotropy by increasing the amount of stored calcium will potentiate the PRC. Phenamil did not potentiate the PRC with respect to the steady-state contractions. Although this could be taken as evidence that phenamil makes the SR more leaky to calcium, the PRC is larger than in control; it is possible that the steady state contraction in the presence of phenamil produced saturation of the calcium binding sites on the myofilaments so that a period of rest will not potentiate the PRC, but instead show only the effect of leak of calcium from the SR. If in fact phenamil was predominantly producing a calcium leak from the SR, then it would have produced negative inotropy, and P1 of biphasic contractions would be attenuated. These observations suggested that the inotropic effect of phenamil is predominantly on the sarcolemmal movement of calcium rather than on the SR storage or release of calcium. Ouabagenin increased calcium levels in the cytoplasm of resting muscle and therefore was able to augment the amount of calcium which was sequestered into the SR. This increase in calcium storage in the SR made more calcium available for release and potentiated the PRC. 4AP causes more calcium to enter the cells through the sarcolemma during the prolonged action potential. It therefore has little potentiating effect on PRC. Thus the effects of phenamil on rest potentiation resemble those of 4AP in canine cardiac muscle.

SARCOPLASMIC RETICULUM

Strontium does not inactivate calcium channels. It can be argued that in biphasic contraction experiments phenamil's effect may have been altered by the presence of strontium. Further elucidation of the SR function in phenamil's action was done by two methods. Ryanodine has been shown to empty intracellular calcium-release stores (Hilgemann, 1982; Bers *et al*, 1987). In the presence of ryanodine any calcium that is taken up into the SR is released upon reaching the terminal cisternae. Ryanodine interferes with calcium-loading of the SR by increasing leak (Hilgemann, 1982). The contraction is reduced with a leaky SR and becomes more sensitive to the transsarcolemmal calcium movement. This preparation was similar to the one causing biphasic contractions where the amount of calcium-loading of the SR was reduced in the presence of strontium (King and Bose, 1983). In the presence of ryanodine the twitch duration was very dependent on transsarcolemmal calcium movement (reviewed in Bers, 1991). CPA does not interfere with calcium-release, but produces similar effects by inhibiting calcium uptake into the SR (Baudet *et al*, 1993). Under these conditions phenamil was still capable of producing positive inotropy. Phenamil also prolonged the twitch in the presence of either ryanodine or CPA, indicating that phenamil affects a transsarcolemmal event rather than the SR. The prolongation of the twitch duration results from prolongation of the action potential. Phenamil generated a second phase of contraction in normal calcium-containing medium in the presence of ryanodine with the same time course as that seen for the inotropy. This second phase of contraction was probably due to the prolongation of the action potential by phenamil.

SODIUM DEPENDENT EXCHANGERS AND TRANSPORTERS

Sodium-calcium exchange

The concentrations at which phenamil prolongs the action potential duration are too low for the effect to be due to the direct inhibition of the sodium-calcium exchange (K_I=200 μM, Kleyman and Cragoe, 1988). In fact, the relative potencies of the different analogs and amiloride at prolonging the action potential (Bielefeld *et al*, 1986; Kennedy *et al*, 1986; Satoh and Hashimoto, 1986; Pierce *et al*, 1993) do not correlate with their potencies for inhibiting the sodium-calcium exchanger (Pierce *et al*, 1993; Kleyman and Cragoe, 1988). Dichlorobenzamil is 8 times more potent than phenamil in blocking sodium-calcium exchange (K_i=30 μM; Bielefeld *et al*, 1986, K_i=17 μM; Siegl *et al*, 1984). This, coupled with inhibition of phosphodiesterase, should make it a better inotropic agent (Floreani *et al*, 1987). In spite of these properties, it produces the same amount of positive inotropy as phenamil. This may be attributed to other properties of DCB, such as inhibition of I_{CaL} (Bielefeld *et al*, 1986). In our preparations CBDMB, a specific sodium-calcium exchange inhibitor (Kleyman and Cragoe, 1988) did not inhibit I_{CaL} (unpublished observations). Sodium-calcium exchange, in forward mode, produces an inward current. Direct inhibition of this exchange process would shorten the action potential. Furthermore, CBDMB, an amiloride derivative with specificity for inhibiting the sodium-calcium exchanger, did not produce positive inotropy in canine trabeculae in normal physiological solutions, nor did it affect guinea pig membrane currents measured with a ramp protocol with normal internal and external solutions, nor calcium currents in potassium-free internal and external solutions (unpublished results). In fact, in some

tissues in order to block the sodium-calcium exchanger amiloride analogs must be added to the voltage clamp pipette solution and applied to the internal surface (cardiac myocytes, D. Hilgemann, personal communication). However in other tissues these compounds are effective blockers of the sodium-calcium exchanger when provided externally (lymphocytes, Kraut *et al*, 1992). This makes it unlikely that phenamil produces positive inotropy by blocking the sodium-calcium exchanger.

The sodium-calcium exchange activity is dependent on the intracellular ion concentrations (with a reversal potential between RMP and 0 mV) and on the membrane potential. An increase in intracellular sodium concentration could result in decreased activity of the forward-mode sodium-calcium exchange, and possibly increased activity of reverse-mode sodium-calcium exchange, both of which would produce positive inotropy. Since phenamil did not produce an increase in the baseline tension even at toxic doses, it is unlikely that phenamil inhibits calcium extrusion by either the sodium calcium exchanger or via calcium ATP-ase. The exchanger has been shown to be responsible for a prolongation of the action potential at the end of phase 3 of the action potential of rat ventricles (Schouten and Ter Keurs, 1985). In this light, one would expect that if intracellular sodium was elevated or sodium-calcium exchange was inhibited by phenamil, then the current elicited by the forward-mode sodium-calcium exchange during phase 3 would decrease, and, if anything, this would shorten the action potential duration. In contrast, I have shown a prolongation of the rat ventricular action potential duration by phenamil. It was necessary to rule out the effects of phenamil on sodium-calcium

exchange. Twin rapid cooling contractures were performed to determine the effect of phenamil on sodium-calcium exchange.

The rapid cooling contracture (RCC) is proportional to the amount of calcium present in the SR before the initiation of the cooling contracture (Hryshko and Bers, 1990). Upon reheating the tissue, calcium sequestering mechanisms are once again turned on. The maximally activated sodium-calcium exchange removes enough calcium so that if the tissue is not stimulated between RCC's, a subsequent contracture will be attenuated due to the loss of calcium (Bers, 1991). During the period that the tissue remains unstimulated there is a leak of calcium from the SR. This calcium is removed from the cytosol by calcium ATP-ase (both on the sarcoplasmic reticulum and on the sarcolemma) and by sodium-calcium exchange. One minute rest period was inserted between contractures in order to insure that calcium had sufficient time to reach the terminal cisternae and was available for release during the second contracture. Ouabagenin increases cytosolic sodium and reduces the forward-mode activity of sodium-calcium exchange. With this compound, the attenuation of the second cooling contracture was less and with 3 μM ouabagenin there is no attenuation of the second contracture. Phenamil did not increase the second cooling contracture, therefore it did not decrease the activity of the exchanger. If anything, the second contracture was smaller, although the changes in RCC by phenamil were not statistically significant.

Sodium-potassium ATP-ase

Since some of the effects of phenamil resembled those of ouabagenin, it was important to test whether phenamil blocked the sodium-potassium ATP-ase. Inhibition of this pump results in increased cytosolic sodium concentration. The elevated cytosolic sodium exchanges for calcium to increase diastolic calcium levels, resulting in positive inotropy. Inhibition of the sodium-potassium ATP-ase of the portal vein preparation by extracellular potassium depletion caused intracellular sodium accumulation leading to an elevated cytosolic calcium concentration possibly by sodium-calcium exchange resulting in a gradual rise in tension (Bose and Innes, 1973). When potassium was reintroduced into the solution, sodium-potassium ATP-ase was reactivated and an immediate hyperpolarization occurred because in the sodium overloaded condition the sodium-potassium pump is electrogenic. This promotes the closing of calcium channels and removal of sodium from the cells, and allows the sodium-calcium exchanger to extrude more calcium out of the cell. In the presence of ouabagenin, the replenishment of potassium further depolarized the cells by reducing the transmembrane potassium gradient. Consequently, the increased activity of calcium channels caused spikes of contractile activity. Phenamil did not alter the complete and immediate relaxation of the smooth muscle upon restoring potassium into the solution, proving that it did not inhibit the sodium-potassium ATP-ase. There is evidence that the Na pump is not inhibited by phenamil, in kidney (Barbry *et al*, 1990) and ileal smooth muscle (Sellin *et al*, 1989).

Interestingly, phenamil inhibited the spontaneous activity of the portal vein smooth muscle contracted by potassium depletion. Spontaneous contractions were also blocked

by calcium channel blockers. The concentration of phenamil used in this study did not inhibit the calcium channels of cardiac tissue (Guia *et al*, 1993), and a positive rather than a negative inotropy was observed. Although both tissues express L-type calcium channels (Hille, 1992), their subunit composition is different (Hullin *et al*, 1992).

Phenamil does not elevate intracellular sodium levels by inhibiting the smooth muscle sodium pump as shown in this study. Phenamil prolongs the action potential whereas inhibition of the sodium pump has been shown to shorten the action potential duration in canine ventricular tissue (Vassalle *et al*, 1962; Chilson and Davis, 1985). Furthermore, phenamil has been shown to inhibit sodium channels of epithelial tissue and sodium influx into smooth muscle tissue (Yu *et al*, 1993), hence we do not expect that elevated sodium levels are responsible for the positive inotropy induced by phenamil. Indeed post-rest potentiation by phenamil did not resemble the profile of the post-rest potentiation by ouabagenin. The sarcolemmal calcium pump was not activated by phenamil since that would produce negative inotropy. Indeed, activation of the sarcolemma calcium pump would likely increase the rate of relaxation and shorten the twitch whereas phenamil prolongs the twitch.

Although amiloride produces positive inotropy in cardiac tissue at concentrations in the same range at which it inhibits the sodium-hydrogen exchanger (Kleyman and Cragoe, 1988), in fluorescence measurements using BCECF, phenamil did not acidify or alkalinize the cytosol in the same concentrations that produce positive inotropy. In other tissues also, phenamil does not inhibit this exchange process (Ki>500 μM; Kleyman and

Cragoe, 1988). Inhibition of the proton exchanger would result in negative inotropy due to competition of H^+ for Ca^{2+} binding sites on troponin C (Fabiato and Fabiato, 1978), and by inhibition of calcium channels (Irisawa and Sato, 1986). Alkalization via sodium-hydrogen exchange can be produced by activation of protein kinase C (Rosoff, 1988; Besterman *et al*, 1985). It is therefore likely that phenamil did not have a significant effect on cardiac protein kinase C since there was no phenamil-induced alkalization of the cytosol associated with inotropy. Thus a cytosolic pH-induced inhibition of I_{K1} potassium channels (Moody and Hagiwara, 1982; Harvey and Ten Eick, 1989b) is also ruled out. The sodium-hydrogen exchanger in cardiac myocytes has been shown to be activated in bicarbonate-free medium only at intracellular pH of 6.7 to 7.1. The cytosolic pH in cardiac cells was found to be in the range of 7.24 (this study) to 7.16 (Wallert and Frohlich, 1989).

ACTION POTENTIALS

Inhibition of the cardiac sodium channels would result in negative inotropy since this would decrease reverse mode sodium-calcium exchange during phase 1 of the action potential and increased forward mode exchange during phases 3 and 4. Phenamil in the 10-60 μM concentration range did not produce negative inotropy, thus inhibition of fast tetrodotoxin-sensitive sodium channels is not an expected action of phenamil.

It is possible that sodium channels were blocked by higher concentrations of phenamil. However, these concentrations were usually toxic to the muscle, causing

conduction block and unresponsiveness to stimulation. Conduction block resulted in extra beats. Since this only happens for a short time before the muscle becomes totally unresponsive to stimulation, it was difficult to measure these events. A rise in threshold voltage needed to produce a twitch, and a slowing of phase 0 of the action potential seen in some of the experiments showed that phenamil was capable of blocking fast sodium channels when used in toxic concentrations. The slowing of phase 0 may have been due to a partial depolarization of the resting membrane potential. However this does not explain the positive inotropy. Prolongation of the action potential was seen with relatively low concentrations compared to those which produced a slowing of phase 0 of the action potential.

Phenamil produced positive inotropy in canine tissue in the same time-frame and concentration range in which it prolongs the action potential in canine, guinea-pig and rat tissue, and in guinea-pig cardiac myocytes. The phenamil-induced effect on the action potential was not surprising since amiloride and many of its analogs have been shown to prolong the action potential (Satoh and Hashimoto, 1986; Bielefeld *et al*, 1986; Pierce *et al*, 1993) without effects on phase 0 of the action potential (Duff *et al*, 1988). Alpha-adrenoceptors, ß-adrenoceptors, ACh-, histamine H1-, or H2-receptors are also not affected by amiloride (Kennedy *et al*, 1986; Yamashita *et al*, 1981). It is likely that the positive inotropy may be predominantly due to phenamil's ability to lengthen the action potential. The action potential data obtained from canine trabeculae, guinea-pig or rat papillary muscle showed similar prolongation by phenamil (10 to 60 µM) at 37°C. The time to 50% repolarization was less affected by phenamil. It is likely that this was a

consequence of the prolonged time to 90% repolarization and the effect on the transient outward potassium channels of the canine trabeculae is minimal. The major effect on the action potential duration by phenamil was on phase 3. The prolongation of the action potential adequately explains the prolongation of the twitch duration and the development of a second phase of contraction in the presence of ryanodine.

Increases in inward calcium current could directly increase cytosolic calcium concentrations and produce positive inotropy. The three outward currents that have been shown to control the action potential profile all prolong the action potential when inhibited: the transient outward current, I_{to}; the outwardly rectifying potassium current, I_K; and the inwardly rectifying potassium current, I_{K1}. L-type calcium current, I_{CaL}, outwardly rectifying potassium currents, and inwardly rectifying potassium currents were tested on guinea pig isolated ventricular myocytes. Guinea-pig ventricular myocytes do not exhibit a significant I_{to} current as is evidenced by the lack of a phase 1 repolarization. Canine ventricular tissue possesses an I_{to} component of the action potential. Phenamil was found to produce positive inotropy in rat ventricular tissue (Brown *et al*, 1991), where I_{to} plays an important role in the repolarization phase of the action potential (Josephson *et al*, 1984; Wettwer *et al*, 1993). This channel is blocked by 4AP (Giles and Imaizumi, 1988). Phenamil resembles 4AP in its effects on biphasic contractions and action potential in canine tissue, but not in rat tissue. In the rat ventricular wall, phenamil prolongs phase 3 of the action potential, prolonging predominantly APD_{90}, whereas 4AP prolongs the action potential early in phase 1, thus increasing APD_{50} more than APD_{90}.

Phenamil prolongs the action potential of guinea-pig ventricular myocytes and guinea-pig ventricular tissue. Measurements in ventricular tissue were at 37°C while those in myocytes were at room temperature. Since there was a similar degree of prolongation of the action potential, it may be assumed that the prolongation is not due to modulation of a temperature-sensitive event, such as any of the ATP-dependent processes. In canine tissue, positive inotropy occurs concurrently with the prolongation of the action potential.

IONIC CURRENTS

I_{Ca}

Negative inotropy observed with amiloride and its analogs has been explained on the basis of their inhibitory effects on calcium channels (Garcia *et al*, 1990; Bielefeld *et al*, 1986). Garcia *et al* (1990) attributed the inhibitory effect on the calcium channels to the lipophilicity of the analogs. Although phenamil is lipophilic among the amiloride derivatives (Cragoe *et al*, 1967), it did not inhibit calcium channels in our study at concentrations (<200 μM) which inhibited I_{K1} and prolonged the action potential. It did, nevertheless, require time to produce its effects, possibly due to an accumulation effect in the cell membrane or to some steric hindrance of the drug's approach to the binding site. Satoh and Hashimoto (1986) also reported that amiloride had no effect on the slow inward calcium current at 87 μM but produced 25% inhibition at 400 μM. At these high concentrations, amiloride also has many other membrane effects (Kleyman and Cragoe, 1988).

I_K

Analysis of the effects of phenamil on the delayed outwardly rectifying potassium channels and L-type calcium channels was complicated by the fact that these currents exhibit significant run-down after gaining whole-cell access. Holding the membrane at -80 mV, and the use of pre-steps to -40 mV to inactivate sodium current, minimized but did not prevent run-down of these currents. Recording of I_K was also significantly improved by dialyzing the myocytes with a sodium-free pipette solution which suppressed contaminating sodium-calcium exchange and transient inward currents during the application of long depolarizing steps to evoke I_K. Despite these limitations, our data suggest that phenamil had little, if any, effect on total I_K as evidenced from monitoring the time-course of changes in I_K during the application and washout of 10 or 50 μM phenamil.

Time-dependent run-down of this current when using dialyzing pipettes is well-reported with experiments done at room temperature (Hume, 1989). It also explains the inward deflection that did not wash out which was seen in the +60 mV region of the difference current of the voltage ramp protocol. Run-down of I_K at room temperature was decreased by the exclusion of sodium from the internal solution and to a lesser extent by the addition of nifedipine (1 μM) to the bathing solution, but not by exclusion of calcium from the bathing medium, or by an increased EGTA concentration in the internal solution. The inclusion of nifedipine in the external solution, and removal of sodium from the internal solution served to inhibit the contribution of sodium-calcium exchangers to the current measurements. This further served to stabilize the intracellular calcium

concentration whereas removal of cytosolic calcium results in a negative shift in the voltage-dependence of I_K (Matsuda, 1983; Matsuura *et al*, 1987) thereby reducing I_K in the absence of calcium and possibly enhancing it in increased calcium concentrations.

Sanguinetti and Jurkiewicz (1990) described the voltage dependence for the two components of I_K in guinea pig myocytes, I_{Kr} and I_{Ks}. Pharmacological separation of I_{Kr} and I_{Ks} using sotalol or its derivative E-4031 revealed a minor contribution of I_{Kr} at potentials positive to +30 mV (during steps); in contrast, both I_{Kr} and I_{Ks} were shown to overlap at potentials negative to that value (Sanguinetti and Jurkiewicz, 1990; Chinn, 1993). Thus in our experiments total I_K recorded during steps in the range of +40 to +60 mV would predominantly reflect I_{Ks}, whereas the deactivating tail current at -40 mV would be determined by the sum of the two current components. Chinn (1993) provided the kinetic evidence for these two currents. In this study, the maximum I_K current during the voltage step, the time-dependent potassium current, is comprised mostly of I_{Ks} since I_{Kr} is inhibited by voltages positive to +40 mV. The peak of the tail current (the steady-state activation current) contains both I_{Kr} and I_{Ks} since both are activated by voltages positive to -40 mV. Although we did not attempt to pharmacologically or kinetically separate I_K into its fast (I_{Kr}) and slow (I_{Ks}) components, since the application of phenamil did not alter the time course of changes of I_K during positive voltage steps or the tail current at -40 mV, we conclude that the phenamil-induced prolongation of the action potential is not the result of block of either components of I_K.

Although phenamil did not affect I_K, other analogs of amiloride have been shown to inhibit this potassium channel. Satoh and Hashimoto (1986) and Bielefeld *et al* (1986) showed that amiloride and 3',4'-dichlorobenzamil (DCB) inhibit I_K in canine SA node and frog atrial myocytes respectively. Similar results were obtained with high concentrations (0.5 to 1 mM) of amiloride in guinea-pig myocytes (Pierce *et al*, 1993). Pierce *et al* (1993) also reported inhibition of I_{to} in rat heart papillary myocytes. Tedisamil, another amiloride derivative, accelerates the inactivation of I_{to} in rat ventricular myocytes resulting in a prolongation of the action potential (Dukes and Morad, 1989). In guinea pig ventricular myocytes there is no dip during phase 1 of the action potential, which is related to the action of the transient outward potassium channels. These channels have not been reported in guinea pig ventricular myocytes hence we did not look at the effects of phenamil on this current.

I_{K1}

I_{K1} is the only outward current which inactivates at voltages above -30 mV and is involved in maintaining the resting membrane potential near the equilibrium potential for potassium (Surawicz, 1992) since it is not turned off at negative potentials (Sakmann and Trube, 1984). The current is outward above and negative below the reversal potential for potassium. In these studies the reversal potential was calculated and measured to be -83 mV. The inhibition of I_{K1} by phenamil was demonstrated using voltage ramp or step protocols. At potentials negative to -40 mV, I_{K1} is known to represent the dominant repolarizing current in guinea-pig ventricular myocytes (Hume, 1989). Slow voltage ramp

protocols have proven useful to investigate the voltage-dependence and pharmacological profile of I_{K1} (Harvey and Ten Eick, 1989a). Despite potential contamination by other dynamic current systems (I_{CaL}, I_K) at potentials positive to -50 mV, our data are consistent with the idea that the phenamil-sensitive current elicited during a voltage ramp in the range of -140 to -50 mV mainly reflects inhibition of the inwardly rectifying potassium current, I_{K1} (Guia *et al*, 1993). Since I_{K1} is not inactivated with time and is turned on almost instantly, the voltage ramp from -140 to -30 mV should reflect the true I_{K1} current. Sodium channels rapidly become inactivated during the slow ramp resulting in not enough sodium channels open at any one time to produce a measurable current over the 8-second voltage ramp protocol. L-type calcium channels remain open much longer and hence may result in an accumulation of calcium which may affect other calcium-dependent channels. The delayed outwardly rectifying potassium channels open slowly and remain open as long as the voltage is high. Both of these channels are prone to time-dependent run-down (Sanguinetti and Jurkiewicz, 1990; Matsuura *et al*, 1987; Korn and Horn, 1989). As a result, the quasi steady-state current is not reliable at voltages above -30 mV due to a small (due to inactivation) contribution from I_{CaL} above -30 mV, and by +60 mV there is little I_{CaL} but a noticeable contribution from I_{Ks}. Likewise, at very negative voltages there is interference with I_{K1} from sodium. The possibility that the phenamil-induced prolongation of the action potential could partially result from inhibition of I_K is not excluded by the data from the voltage ramp protocol because of the small inward deflection in the +60 mV range. In spite of the drawbacks, the ramp protocols provide useful information about the voltage-dependence of I_{K1}. The inhibition of I_{K1} by

phenamil was also confirmed with step protocols. The phenamil-induced suppression of outward K^+ flux through I_{K1} and positive shift of the "apparent" reversal potential of net current are mainly responsible for the observed lengthening of the action potential, and membrane depolarization (figures 26 to 30). The time-course of inhibition of I_{K1} by phenamil further supports the hypothesis that the inhibition of I_{K1} is responsible for the phenamil-induced prolongation of the action potential, both having a time-course of effect of around 10 to 15 minutes in our experiments.

The lengthening of the action potential, partial depolarization of resting membrane potential, and oscillatory potentials and afterdepolarizations are consistent with a block of I_{K1} (Surawicz, 1992). Some of the other pharmacological inhibitors of I_{K1} are not as potent, requiring much higher concentrations (Martin and Chinn, 1992), and are not as specific in cardiac tissue (Duan *et al*, 1993; Braun *et al*, 1992).

GENERAL DISCUSSION

Phenamil is among the more hydrophobic of the amiloride derivatives (Cragoe *et al*, 1967; Kleyman and Cragoe, 1988). This property allows it to enter the cell easily. Since it has a higher pKa than physiological pH, its protonated form would slowly accumulate in the cytosol where pH is lower than extracellular pH. It's hydrophobic nature would also result in accumulation into the sarcolemma. Phenamil-induced positive inotropy is slow to reach steady state, and higher concentrations eventually become toxic to the tissue before reaching steady state. It is possible that the cardiac effects of phenamil

described in this thesis require the accumulation of the drug in the cell. Although such an accumulation effect would explain the time required to produce positive inotropy, it is unlikely. The time required for the inhibition of I_{K1} and for prolonging the action potential are shorter than the time required to reach steady-state positive inotropy. Other mechanisms, such as the progressive filling of the sarcoplasmic reticulum may be responsible for the production of the delayed steady state positive inotropy.

Since phenamil has similar actions on both isolated myocytes and trabecular tissue, involvement of agents of neural origin appear to be unlikely. The release of norepinephrine was not required for the production of positive inotropy. Furthermore, the effects of phenamil on the tension profile do not resemble those of norepinephrine.

Amiloride and a few of its analogues have been shown to produce positive inotropy (Bielefeld *et al*, 1986; Siegl *et al*, 1984; Floreani *et al*, 1987). Kennedy *et al* (1986) attributed this to a combination of events, such as inhibition of the sodium pump, sodium-calcium exchange and prolongation of the action potential duration by amiloride. Indeed the use of rapid cooling contractures showed that phenamil did not inhibit sodium-calcium exchange at concentrations that prolong the action potential and produce positive inotropy.

Activation of protein kinase C could up-regulate the sodium-hydrogen exchange and produce cytosolic alkalization which can lead to positive inotropy. In our studies, phenamil produces positive inotropy without affecting intracellular pH. In cardiac tissue, where epithelial-type sodium channels have not been demonstrated, the predominant effect

of phenamil is to inhibit I_{K1} without significantly affecting I_K or I_{CaL}. The phenamil-induced prolongation of the action potential in the guinea-pig ventricular myocyte is adequately explained by a specific inhibition of inwardly rectifying potassium channels.

In our studies, phenamil produced negative inotropy in the rat. Some amiloride analogs have been shown to produce negative inotropy (Pierce *et al*, 1993), presumably by inhibiting calcium channels (Garcia *et al*, 1990). Fluorescence studies with fura-2 were performed showing decreased calcium entry into cardiac myocytes using amiloride and its analogs (Pierce *et al*, 1993). This interpretation may be flawed because these analogs have been shown to quench the fluorescence of fura-2 (Kraut *et al*, 1993). The negative inotropy found in the Pierce study was likely due to the sodium-hydrogen exchanger blocking effects of the analogs, in HEPES buffered media. By omitting bicarbonate from the bathing solution the bicarbonate-dependent pH buffering of the cells was disabled, making them dependent on the sodium-hydrogen exchanger to avoid acidosis. Intracellular acidosis is commonly known to produce negative inotropy (Gaskell, 1880; Fabiato and Fabiato, 1978; Orchard and Kentish, 1990). L-type calcium channels are not inhibited by phenamil in concentrations that produce positive inotropy (Guia *et al*, 1993). During the tail of the rat action potential, calcium is removed from the cells (Schouten and Ter Keurs, 1985). By prolonging the action potential, it is likely that phenamil causes further removal of calcium from the cells (Shattock and Bers, 1989), and this may be the cause of negative inotropy in the rat.

An interesting aspect in the data is that in smooth muscle phenamil inhibited the oscillations brought about by the absence of potassium from the bathing medium. In the absence of extracellular potassium, the sodium pump does not function hence there is a depolarization of the cell membrane. This causes voltage-gated calcium channels to open and produce the oscillation in tension. Inhibition of these oscillations may therefore be linked to calcium channel inhibition, however phenamil did not inhibit calcium channels in cardiac tissue.

Fast tetrodotoxin-sensitive sodium current was not measured, however prolongation of the action potential was evident before any noticeable changes in phase 0 of the action potential, which is sensitive to sodium channel activity. Considering that inhibition of sodium channels would produce negative inotropy, there was little reason to suspect inhibition of the tetrodotoxin-sensitive sodium channels as a primary effect of phenamil, a positive inotrope. Calcium and sodium channel openers are capable of producing positive inotropy (e.g.: BAY K-8644, Schouten *et al*, 1987; DPI 201-106, Hoey *et al*, 1994). Phenamil did not potentiate calcium current and it is not expected that sodium current is potentiated by phenamil. Potentiation of sodium current would be similar to inhibition of the sodium pump, resulting in positive inotropy via sodium-calcium exchange. Phenamil did not enhance or inhibit sodium-calcium exchange.

Dukes and Morad (1989) demonstrated that tedisamil, another amiloride analog, speeds up the inactivation of I_{to} in rat ventricular myocytes resulting in a prolongation of the action potential. The pharmacological profile of inhibitors of I_{to} includes positive

inotropy in the rat, as well as a prolongation of the action potential, predominantly at 50% repolarization as seen here and previously (Ruiz-Petrich and Leblanc, 1989). Phenamil had the opposite effects: positive inotropy, and a prolongation predominantly at 90% repolarization of the action potential. Any inhibitory effect of phenamil on I_{to} is not significant as compared to the inhibition of I_{K1}.

The amiloride-based compounds that produce positive inotropy appear to be stronger inhibitors of epithelial sodium channels than of the sodium-calcium exchanger (Kleyman and Cragoe, 1988). Compounds that produce positive inotropy appear to inhibit potassium channels. This implies a binding site on potassium channels similar in structure to the epithelial sodium channel binding site. The sequences of both the I_{K1} and the delayed rectifier channels have been reported. These channels are in the same family of genes as the epithelial sodium channel (described in figure 4). The structure of the I_{K1} channel (figure 36) is similar to that of the epithelial sodium channel, however it has a small extracellular loop (Kubo *et al*, 1993).

Block of I_{K1} occurred with as little as 10 μM phenamil in one cell, and reproducibly with 50 μM. Inhibitors of I_{K1} act as Class III antiarrhythmic agents according to the Vaughan Williams classification of antiarrhythmic drugs (Vaughan-Williams, 1984). Phenamil could be a potent antiarrhythmic compound with antifibrillatory actions at both the atria and the ventricles and would prolong refractory period without affecting conduction velocity (*c.f.*: terikalant, Escande *et al*, 1992). Unfortunately in zones that already have depressed conduction velocities, there may be a

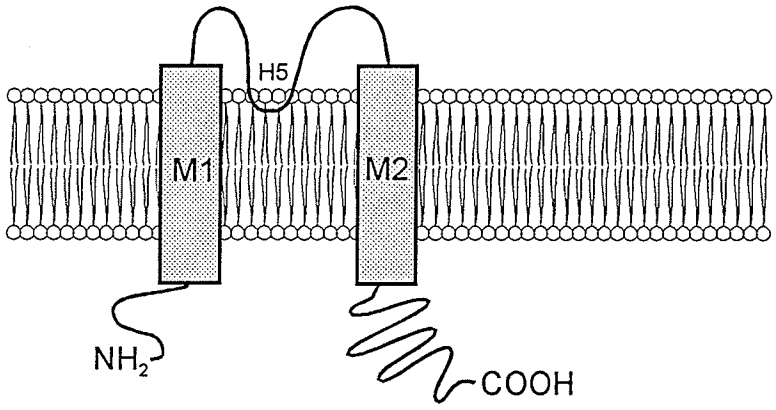

Figure 36

The structure of the I_{K1} channel (adapted from Valera *et al*, 1994 and Kubo *et al*, 1993) depicting the transmembrane topography of the protein. Amino acid sequence for I_{K1} is highly concerved between species and tissues (Ashen *et al*, 1995). The protein contains two transmembrane segments (M1 and M2) and one hydrophobic region (H5) in the extracellular loop. Both the C and N termini are cytoplasmic. The channel structure is similar to the epithelial sodium channel (see figure 1) however it has a smaller extracellular loop, and a single hydrophobic region. Based on sequence homology of the pore region (Valera *et al*, 1994), it is suggested that these channels are in the same superfamily of channels as the epithelial sodium channels.

conduction block due to the partial depolarization of the resting membrane potential. Although it has not been measured, amiloride has effects on the action potential that match the profile for an inhibitor of I_{K1} (Duff *et al*, 1991). A potentially dangerous situation would be an extreme lengthening of the action potential, partial depolarization of the resting membrane potential, and oscillatory potentials and afterdepolarizations that are consistent with a block of I_{K1} (Surawicz, 1992).

The I_{K1} channels do not allow passage of calcium into the cell (Sakmann and Trube, 1984), nor does inhibition of I_{K1} prolong the action potential in the region where calcium channels are active (Surawicz, 1992). However, the extra calcium to produce positive inotropy results from increased transsarcolemmal movement. Since I_{K1} becomes inactivated at voltages above -30 mV, it is difficult to implicate L-type calcium channels as being allowed to remain open longer, and a direct effect of phenamil on calcium channels has been ruled out. A weak inhibition of I_{K1} prolongs only the part of the action potential beyond the voltage range where calcium channels would be open. Stronger inhibition of I_{K1} results in membrane depolarization and inactivation of sodium channels, resulting in negative inotropy, and failure to respond to electrical stimulation. Transient calcium levels in the cytosol have been measured showing higher cytosolic calcium concentrations during the time of the twitch, corresponding to phases 2 to 4 of the action potential (Bers, 1987). The calcium channels close at the beginning of phase 3 of the action potential and calcium is removed from the cytosol by sodium-calcium exchange (Shattock and Bers, 1989) and into the SR by calcium ATP-ase (Baudet *et al*, 1993). The sodium-calcium exchanger is controlled by the ionic gradients for sodium and for calcium as well as by the difference

between the membrane potential and the reversal potential for the exchanger, or electrochemical driving force (Leblanc and Hume, 1990, Bers, 1991). Sodium-calcium exchange is electrogenic, exchanging 3 sodium molecules for each calcium (Reeves and Hale, 1984). The reversal potential for sodium-calcium exchange is more positive than the resting membrane potential, hence in resting state the exchanger removes calcium from the cytosol, but since there is very little calcium in the cytosol, the activity of the exchanger is low. At the end of the action potential, the repolarization of the membrane during phase 3 of the action potential increases the driving force for the removal of calcium by sodium-calcium exchange. These events are described by Shattock and Bers (1989), and are shown in figure 37. A depolarization of the membrane caused during phase 3 of the action potential would reduce the driving force for the exchanger. This would result in a decrease in activity of the exchanger and leave more calcium available for uptake into the SR. Integrated over many beats, this would eventually result in positive inotropy (Bers, 1991; Bridge *et al*, 1991). Figure 38 summarizes the proposed mechanism for the production of positive inotropy by phenamil.

Such a mechanism of positive inotropy could mimic inhibition of sodium-calcium exchange since the activity of the exchanger would decrease due to inhibition of I_{K1}. This provides a possible explanation for the finding that some amiloride analogs produce positive inotropy by inhibiting sodium-calcium exchange at concentrations known not to directly inhibit the exchanger (Brown *et al*, 1991). The prolongation of the action potential may result in some additional calcium entry through L-type channels. The sodium-calcium exchanger in rat ventricular myocytes functions in the direction opposite

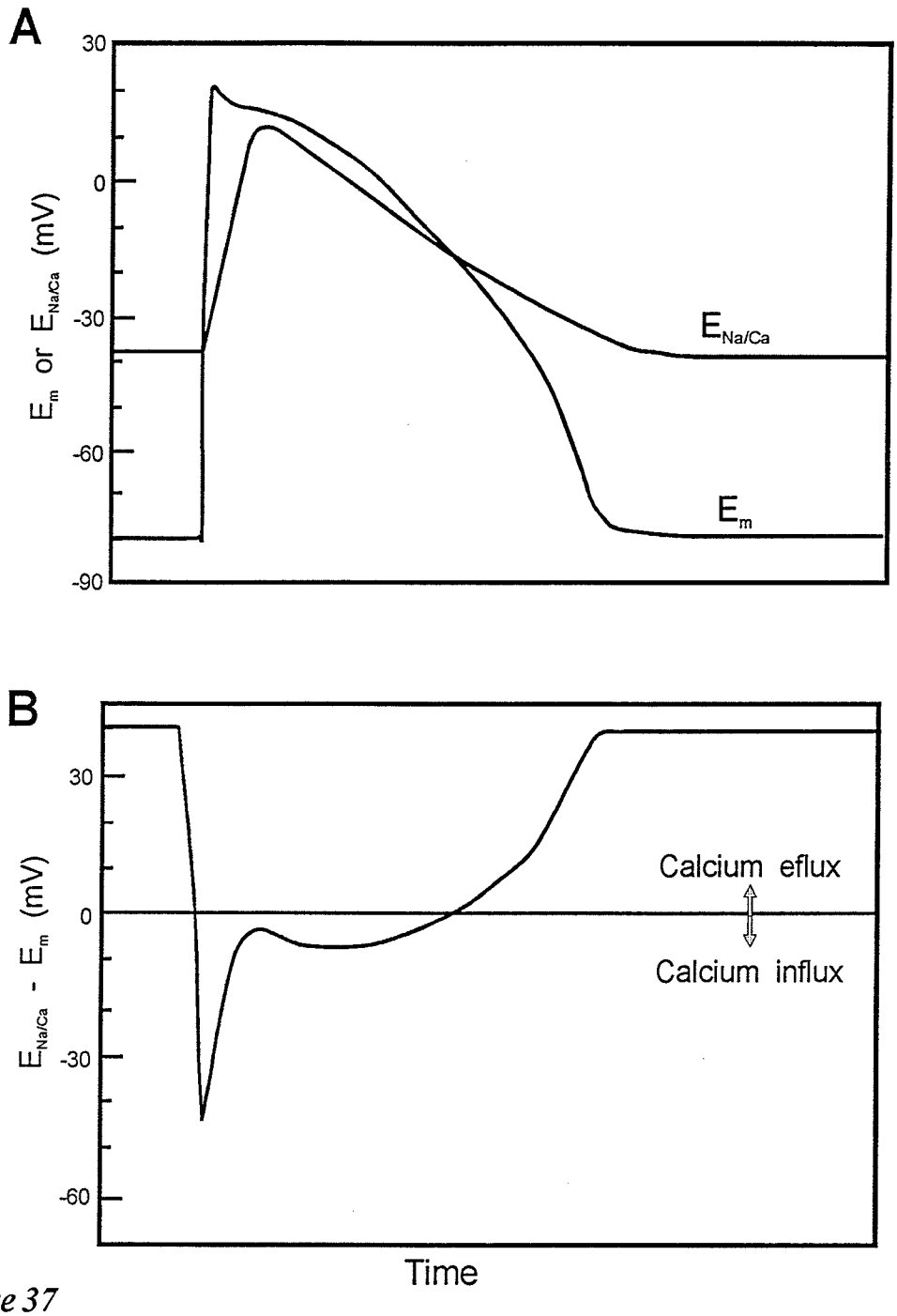

Figure 37

The driving force for the sodium-calcium exchanger (Shattock and Bers, 1989). **A**. An action potential from rabbit ventricle is superimposed on the calculated reversal potential for sodium-calcium exchange. **B**. The difference between the reversal potential of the exchanger and the membrane potential determines the driving force. Calcium influx occurs when the difference is less than 0 mV, or when the reversal potential of the exchanger is more negative than the membrane potential. Maximum calcium removal by the exchanger occurs during phase 3 of the action potential when cytosolic calcium levels are high, and the driving force for the exchanger in the forward mode is high. Maximum calcium entry through the exchanger occurs during phase 1 of the action potential when cytosolic calcium levels are low and cytosolic sodium levels are high.

The Model

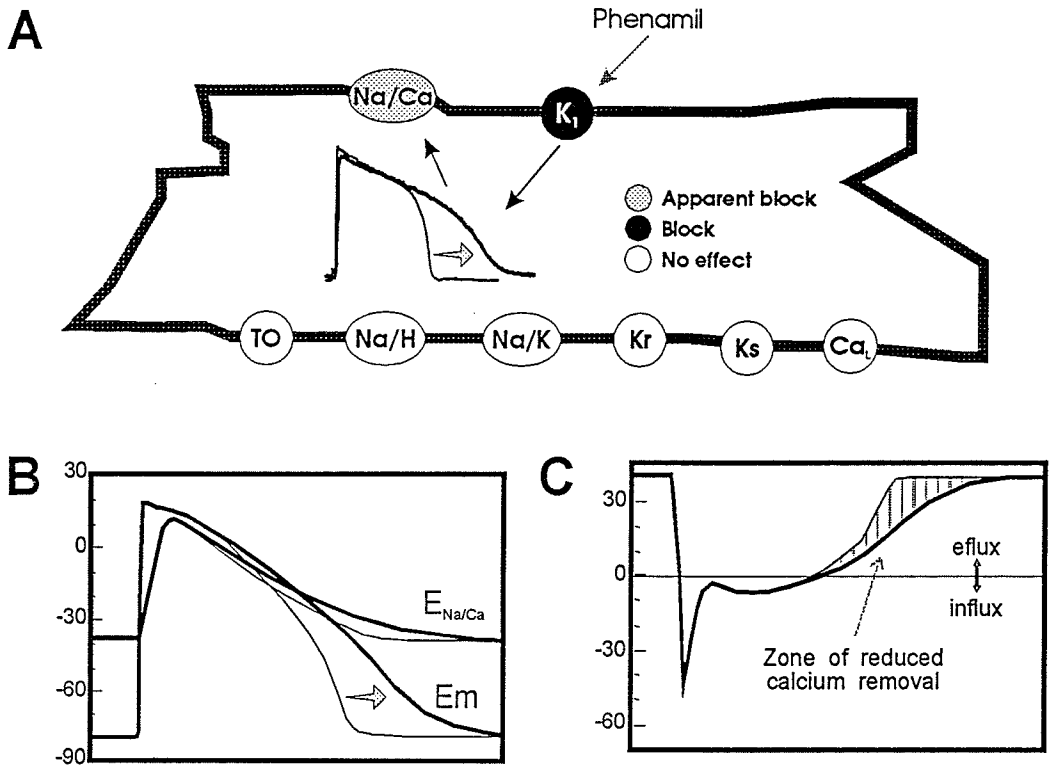

Figure 38

A proposed model for the inotropic effect of phenamil. Phenamil inhibits I_{K1} and prolongs the action potential. Sodium-calcium exchange during phase 3 of the action potential is maximally active. By maintaining the membrane potential depolarized for a longer time during the repolarization phase, the driving force for the exchanger is reduced. Calcium is also quickly taken up into the sarcoplasmic reticulum. The calcium that is not removed from the cell via sodium-calcium exchange is taken into the sarcoplasmic reticulum. Integrated over many beats, the gradual accumulation of calcium in the cell results in positive inotropy. **A.** A model cell illustrating the channels that are not affected by phenamil as measured in this study, as well as those affected by phenamil. Letters inside closed circles represent each of the channel types. Only one channel is shown to be inhibited by phenamil in concentrations that produce positive inotropy. Channel types not shown are not expected to produce positive inotropy if inhibited. When I_{K1} is inhibited, there is an apparent partial inhibition of sodium-calcium exchange. **B.** Same as in figure 37A, but showing the effect of inhibition of I_{K1}. The reversal potential of sodium-calcium exchange would follow the membrane potential, and prolong the time to remove calcium from the cytosol, however the calcium ATP-ase on the sarcoplasmic reticulum would still take up calcium from the cytosol during the prolonged presence of calcium at the end of the action potential. C. The driving force for sodium-calcium exchange would decrease due to the inhibition of IK1, resulting in decreased calcium removal from the cytosol.

to that of other species. During the tail of the action potential, calcium is removed from the cells by the exchanger, and during diastole, calcium is imported into the cells by sodium-calcium exchange (Bers, 1991). This peculiarity of rat ventricular tissue adequately explains the findings of negative inotropy in rat ventricular tissue in spite of a prolongation of the action potential by phenamil.

It is concluded therefore that phenamil, an epithelial sodium channel blocker, inhibits I_{K1} in cardiac tissue, a channel similar structurally to the epithelial sodium channel. The inhibition of I_{K1} prolongs phase 3 of the action potential thereby indirectly and transiently reducing the activity of sodium-calcium exchange, prolonging the time required for the exchanger to remove calcium from the cytosol during the repolarization of the action potential. It is during phase 3 of the action potential that the sodium-calcium exchanger is most effective in removing calcium from the cytosol. Since calcium uptake into the SR is not modified by phenamil, more calcium will be sequestered into the SR with each beat. Integrated over time, the resulting accumulation of calcium into the SR produces positive steady state inotropy.

CONCLUSIONS

This section summarizes the major findings included in this thesis.

•Phenamil is an effective smooth muscle relaxant by blocking sodium influx.

•Phenamil produces positive inotropy in cardiac tissue.

•Positive inotropy originates from a change in transmembrane calcium movement.

•Phenamil does not directly affect SR calcium content.

•Phenamil does not affect cytosolic pH.

•Inotropy does not require the release of neurotransmitters.

•Inotropy is concurrent with a prolongation of the action potential.

•Prolongation of the action potential is due to inhibition of I_{K1}

•Phenamil does not affect I_{CaL}, or I_K

•Phenamil has no direct effects on the sodium pump or on sodium-calcium exchange.

Inhibition of I_{K1} prolongs phase 3 of the action potential. Positive inotropy results from an indirect reduction in the activity of the sodium-calcium exchanger, secondary to the prolongation of the action potential during phase 3.

REFERENCES

Aalkjær, C., and E.J. Cragoe. Intracellular pH regulation in resting and contracting segments of rat mesenteric resistance vessels. *J. Physiol.*, **402**:391-410, 1988.

Akhtar-Khavari, F., M.A. Khoyi and E. Rezaei. Effects of amiloride on contractions and the release of tritium from rat vas deferens preloaded with [^{3}H]-noradrenaline. *Br. J. Pharmacol.*, **74**:123-127, 1981.

Allen, D.G., and C.H. Orchard. Myocardial contractile function during ischemia and hypoxia. *Circ. Res.*, **60**:153-168, 1987.

Altschuld, R.A., C.M. Hohl, K.G. Lamka, and G.P. Brierley. Effects of amiloride on calcium uptake by myocytes isolated from adult rat hearts. *Life Sci.*, **35**:865-870, 1984.

Anderson, S.E., E. Murphy, C. Steenbergen, R.E. London, and P.M. Cala. Na-H exchange in myocardium: effects of hypoxia and acidification on Na and Ca. *Am. J. Physiol.*, **259**:C940-C948, 1990.

Armstrong, J., T. Matainaho, E.J. Cragoe, G.J. Huxham, J.R. Bourke, and S.W. Manley. Bidirectional ion transport in thyroid: secretion of anions by monolayer cultures that absorb sodium. *Am. J. Physiol.*, **262**:E40-E45, 1992.

Ashen, M.D., B. O'Rourke, K.A. Kluge, D.C. Johns, and G.F. Tomaselli. Inward rectifier K^+ channel from human heart and brain: cloning and stable expression in a human cell line. *Am. J. Physiol.*, **268**:H506-H511, 1995.

Ashford, M.L.J., C.T. Bond, T.A. Blair, and J.P. Adelman. Cloning and functional expression of a rat heart K_{ATP} channel. *Nature*, **370**:456-459, 1994.

Atsumi, T., S. Sugiyama, E.J. Cragoe, and Y. Imae. Specific inhibition of the Na^+-driven flagellar motors of alkalophilic bacillus strains by the amiloride analog phenamil. *J. Bacteriol.*, **172**:1634-1639, 1990.

Barbry, P., O. Chassande, D. Duval, B. Rousseau, C. Frelin, and M. Lazdunski. Biochemical identification of two types of phenamil binding sites associated with amiloride-sensitive Na^+ channels. *Biochem.*, **28**:3744-3749, 1989.

Barbry, P., O. Chassande, R. Marsault, M. Lazdunski, and C. Frelin. [^{3}H]Phenamil binding protein of the renal epithelium Na^+ channel. Purification, affinity labeling, and functional reconstitution. *Biochem.*, **29**:1039-1045, 1990.

Baudet, S., R. Shaoulian, and D.M. Bers. Effects of thapsigargin and cyclopiazonic acid on twitch force and sarcoplasmic reticulum Ca^{2+} content of rabbit ventricular muscle. *Circ. Res.*, **73**:813-819, 1993.

Belles, B., C.O. Malecot, J. Hescheler, and W. Trautwein. "Run-down" of the Ca^{2+} current during long whole-cell recordings in guinea pig heart cells: role of phosphorylation and intracellular calcium. *Pflügers Arch.*, **411**:353-360, 1988.

Benos, D.J. Amiloride: a molecular probe of sodium transport in tissues and cells. *Am. J. Physiol.*, **242**:C131-C145, 1982.

Benos, D.J. "Amiloride: chemistry, kinetics and structure-activity relationships." **In** Na^+/H^+ exchange. ed.: S. Grinstein, CRC Press, 1988, pp. 121-136.

Benos, D.J., G. Saccomani, B.M. Brenner, and S. Sariban-Sohraby. Purification and characterization of the amiloride-sensitive sodium channel from A6 cultured cells and bovine renal papilla. *Proc. Natl. Acad. Sci.*, **83**:8525-8529, 1986.

Benos, D.J., G. Saccomani, and S. Sariban-Sohraby. The epithelial sodium channel. Subunit number and location of the amiloride binding site. *J. Biol. Chem.*, **262**:10613-10618, 1987.

Bers, D.M. Ca^{2+} influx and sarcoplasmic reticulum Ca^{2+} release in cardiac muscle activation during postrest recovery. *Am. J. Physiol.*, **248**:H366-H381, 1985.

Bers, D.M. SR Ca^{2+} loading in cardiac muscle preparations based on rapid-cooling contractures. *Am. J. Physiol.*, **256**:C109-C120, 1989.

Bers, D.M. Excitation-contraction coupling and cardiac contractile force. Kluwer Academic Publishers, Dordrecht, Netherlands, 1991.

Bers, D.M., J.W. Bassani, and R.A. Bassani. Competition and redistribution among calcium transport systems in rabbit cardiac myocytes. *Cardiovasc. Res.*, **27**:1772-1777, 1993.

Bers, D.M., J.H. Bridge, and K.T. MacLeod. The mechanism of ryanodine action in cardiac muscle assessed with Ca^{2+} selective microelectrodes and rapid cooling contractures. *Can. J. Physiol. Pharmacol.*, **65**:610-618, 1987.

Besterman, J.M., W.S. May, H. Le Vine, E.J. Cragoe, and P. Cuatrecasas. Amiloride inhibits phorbol ester-stimulated Na^+/H^+ exchange and protein kinase C. An amiloride analog selectively inhibits Na^+/H^+ exchange. *J. Biol. Chem.*, **260**:1155-1159, 1985.

Bielefeld, D.R., R.W. Hadley, P.M. Vassilev, and J.R. Hume. Membrane electrical properties of vesicular Na-Ca exchange inhibitors in single atrial myocytes. *Circ. Res.*, **59**:381-389, 1986.

Bielen, F.V., S. Bosteels, and F. Verdonck. Consequences of CO_2 acidosis for transmembrane Na^+ transport and membrane current in rabbit cardiac Purkinje fibers. *J. Physiol.*, **427**:325-345, 1990.

Biermans, G., J. Vereecke, and E. Carmeliet. The mechanism of the inactivation of the inward-rectifying K current during hyperpolarizing steps in guinea-pig ventricular myocytes. *Pflügers Arch.*, **410**:604-613, 1987.

Borzak, S., R.A. Kelly, B.K. Krämer, Y. Matoba, J.D. Marsh, and M. Reers. *In situ* calibration of fura-2 and BCECF fluorescence in adult rat ventricular myocytes. *Am. J. Physiol.*, **259**:H973-H981, 1990.

Bose, D., and I.R. Innes. The role of sodium pump in the inhibition of smooth muscle responsiveness to agonists during potassium restoration. *Br. J. Pharmacol.*, **49**:466-479, 1973.

Bose, D., L.V. Hryshko, B.W. King, and T. Chau. Control of interval-force relation in canine ventricular myocardium studied with ryanodine. *Br. J. Pharmacol.*, **95**:811-820, 1988.

Bose, R., J. Yu and E.J. Cragoe, Jr. Excitation-contraction coupling in tracheal smooth muscle studied with specific inhibitors of Na^+ channel and Na^+-H^+ antiporter. *Physiologist*, **32**:181, 1989.

Boyechko, G., and D. Bose. A versatile computer-controlled biological stimulus sequencer. *J. Pharmacol. Methods*, **12**:45-52, 1982.

Brading, A.F., M. Burnett and P. Sneddon. The effect of sodium removal on the contractile responses of the guinea-pig taenia coli to carbachol. *J. Physiol.*, **306**:411-429, 1980.

Brake, A.J., M.J. Wagenbach, and D. Julius. New structural motif for ligand-gated ion channels difined by an ionotropic ATP receptor. *Nature*, **371**:519-523, 1994.

Braun, A.P., D. Fedida, W.R. Giles. Activation of alpha 1-adrenoceptors modulates the inwardly rectifying potassium currents of mammalian atrial myocytes. *Pflügers Arch.*, **421**:431-439, 1992.

Bridge, J.H. Relationships between the sarcoplasmic reticulum and transarcolemmal Ca^{2+} transport revealed by rapidly cooling rabbit ventricular muscle. *J. Gen. Physiol.*, **88**:437-473, 1986.

Bridge, J.H., J. Smolley, K.W. Spitzer, and T.K. Chin. Voltage dependence of sodium-calcium exchange and the control of calcium extrusion in the heart. *Ann. N.Y. Acad. Sci.*, **639**:34-47, 1991.

Bridges, R.J., E.J. Cragoe, R.A. Frizzell, and D.J. Benos. Inhibition of colonic Na^+ transport by amiloride analogues. *Am. J. Physiol.*, **256**:C67-C74, 1989.

Bright, C.M., and D. Ellis. Intracellular pH changes induced by hypoxia and anoxia in isolated sheep heart Purkinje fibers. *Exp. Physiol.*, 77:165-175, 1992.

Brown, L., E.J. Cragoe, K.C. Abel, S.W. Manley, and J.R. Bourke. Amiloride analogues induce responses in isolated rat cardiovascular tissues by inhibition of Na^+/Ca^{2+} exchange. *Naunyn-Schmied. Arch. Pharmacol.*, **344**:220-224, 1991.

Canessa, C.M., J.D. Horisberger, and B.C. Rossier. Epithelial sodium channel related to proteins involved in neurodegeneration. *Nature*, **361**:467-470, 1993.

Cannell, M.B., H. Cheng, and W.J. Lederer. The control of calcium release in heart muscle. *Science*, **268**:1045-1049, 1995.

Cargnelli, Bova, G. S., and Luciani, S.: Effects of amiloride in guinea-pig and rat left atrial contraction as affected by frequency of stimulation and $[Ca^{2+}]_o$-$[Na^+]_o$ ratio: role of Na^+/Ca^{2+} exchange. *Br. J. Pharmacol.*, **97**:533-541, 1989.

Carter, G., and J.B. Gavin. Endocardial damage induced by lactate, lowered pH and lactic acid in non-ischemic beating hearts. *Pathol.*, **21**:125-130, 1989.

Chassande, O., S. Renard, P. Barbry, and M. Lazdunski. The human gene for diamine oxidase, an amiloride binding protein: Molecular cloning, sequencing, and characterization of the promoter. *J. Biochem.*, **216**:679-687, 1994.

Chilson, R.A., and L.D. Davis. Combined effects of ouabain and hypoxia on the transmembrane potential of canine cardiac Purkinje fibers. *J. Cardiovasc. Pharmacol.*, 7:368-376, 1985.

Chinn, K. Two delayed rectifiers in guinea pig ventricular myocytes distinguished by tail current kinetics. *J. Pharmacol. Exp. Ther.*, **264**:553-560, 1993.

Cobbe, S.M., and P.A. Poole-Wilson. The time of onset and severity of acidosis in myocardial ischaemia. *J. Mol. Cell. Cardiol.*, **12**:745-760, 1980.

Colatsky, T.J. Voltage clamp measurements of sodium channel properties in rabbit cardiac Purkinje fibers. *J. Physiol.*, **305**:215-234, 1980.

Collins, F.S. Cystic Fibrosis: molecular biology and therapeutic implications. *Science*, **256**:774-779, 1992.

Cragoe, E.J., J.R. Otto, W. Woltersdorf, J.B. Bicking, S.F. Kwong, and J.H. Jones. Pyrazine diuretics. II. N-amidino-3-amino-5-substituted 6-halopyrazine-carboxamides. *J. Med. Chem.*, **10**:66-75, 1967.

Cuthbert, A.W., and W.K. Shum. Characteristics of the entry process for sodium in transporting epithelia as revealed with amiloride. J. Physiol., **255**:587-604, 1976.

de Moraes, V.L. Opposite effects of amiloride and amiloride analogues on activation of natural killer cytotoxicity by the phorbol ester TPA and gamma interferon. *Immonol. Lett.*, **35**:119-123, 1993.

Driscoll, M. Molecular genetics of cell death in the nematode *Caenorbabditis elegans*. *J. Neurobiol.*, **23**:1327-1351, 1992.

Duan, D., B. Fermini, S. Nattel. Potassium channel blocking properties of propafenone in rabbit atrial myocytes. *J. Pharmacol. Exp. Ther.*, **264**:1113-23, 1993.

Dudeja, P.K., J.M. Harig, M.L. Baldwin, E.J. Cragoe, K. Ramaswamy, and T.A. Brasitus. Na^+ transport in human proximal colonic apical membrane vesicles. *Gastroenterol.*, **106**:125-133, 1994.

Duff, H.J., C.E. Brown, E.J. Cragoe, and M. Rahmberg. Antiarrhythmic activity of amiloride: Mechanisms. *J. Cardiovasc. Pharmacol.*, **17**:879-888, 1991.

Duff, H.J., W.M. Lester, and M. Rahmberg. Amiloride: antiarrhythmic and electrophysiological activity in the dog. *Circulation*, **78**:1469-1477, 1988.

Dukes, I.D. and M. Morad. Tedisamil inactivates transient outward K^+ current in rat ventricular myocytes. *Am. J. Physiol.*, **257**:H1746-1749, 1989.

Ebashi, S., and F. Lipmann. Adenosine triphosphate-linked concentration of calcium ions in a particulate fraction of rabbit muscle. *J. Cell. Biol.*, **14**:389-400, 1962.

Ehara, T., A. Noma, and K. Ono. Calcium-activated non-selective cation channel in ventricular cells isolated from adult guinea-pig hearts. *J. Physiol.*, **403**:117-133, 1988.

Eisner, D.A., C.G. Nichols, S.C. O'Neill, G.L. Smith, and M. Valdeolmillos. The effects of metabolic inhibition on intracellular calcium and pH in isolated rat ventricular cells. *J. Physiol.*, **411**:393-418, 1989.

Escande, D., M. Mestre, I. Cavero, J. Brugada, and C. Kirchhof. RP 58866 and its active enantiomer RP 62719 (Terikalant): blockers of the inward rectifier K^+ current acting as pure class III antiarrhythmic agents. *J. Cardiovasc. Pharmacol.*, **20**:S106-S113, 1992.

Fabiato, A. Calcium-induced release of calcium from the cardiac sarcoplasmic reticulum. *Am. J. Physiol.*, **245**:C1-C14, 1983.

Fabiato, A., and F. Fabiato. Effects of pH on the myofilaments and the sarcoplasmic reticulum of skinned cells from cardiac and skeletal muscles. *J. Physiol.*, **276**:233-255, 1978.

Farmer, S.G., J. S. Fedan, D.W.P. Hay, and D. Raeburn. The effects of epithelium removal on the sensitivity of guinea-pig isolated trachealis to bronchodilator drugs. *Br. J. Pharmacol.*, **89**:407-414, 1986.

Feher, J.J., and I.M. Rebeyka. Cooling and pH jump-induced calcium release from isolated cardiac sarcoplasmic reticulum. *Am. J. Physiol.*, **267**:H962-H969, 1994.

Floreani, M, and S. Luciani. Amiloride: Relationship between cardiac effects and inhibition of Na^+/Ca^{2+} exchange. *Eur. J. Pharmacol.*, **105**:317-322, 1984.

Floreani, M., M. Tessari, P. Debetto, S. Luciani, and F. Carpenedo. Effects of N-chlorobenzyl analogues of amiloride on myocardial contractility, Na-Ca-exchange carrier and other cardiac enzymatic activities. *Naunyn-Schmied. Arch. Pharmacol.*, **336**:661-669, 1987.

Fozzard, H.A., C.T. January, and J.C. Makielski. New studies of the excitatory sodium currents in heart muscle. *Circ. Res.*, **56**:475-485, 1985.

Frank, J.S., G. Mottino, D. Reid, R.S. Molday, and K.D. Philipson. Distribution of the Na^+-Ca^{2+} exchange protein in mammalian cardiac myocytes: an immunofluorescence and immunocolloidal gold-labeling study. *J. Cell. Biol.*, **117**:337-345, 1992.

Frelin, C., P. Barbry, P. Vigne, O. Chassande, E.J. Cragoe, and M. Lazdunski. Amiloride and its analogs as tools to inhibit Na^+ transport via the Na^+ channel, the Na^+/H^+ antiport and the Na^+/Ca^{2+} exchanger. *Biochimie*, **70**:1285-1290, 1988.

Frelin, C., P. Vigne, and M. Lazdunski. The role of the Na^+/H^+ exchange system in cardiac cells in relation to the control of the internal Na^+ concentration. *J. Biol. Chem.*, **259**:8880-8885, 1984.

Gallo, R.L. Aerosolized amiloride for the treatment of lung disease in Cystic Fibrosis. *N. Eng. J. Med.*, **323**:996-997, 1990.

Garcia, M.L., V.F. King, J.L. Shevell, R.S. Slaughter, G. Suarez-Kurtz, R.J. Winquist, and G.J. Kaczorowski. Amiloride analogs inhibit L-type calcium channels and display calcium entry blocker activity. *J. Biol. Chem.*, **265**:3763-3771, 1990.

Garty, H. Molecular properties of epithelial, amiloride-blockable Na^+ channels. *FASEB J.*, **8**:522-528, 1994.

Garty, H., and D.J. Benos. Characteristics and regulatory mechanisms of the amiloride-blockable Na^+ channel. *Physiol. Rev.*, **68**:309-372, 1988.

Gaskell, W.H. On the tonicity of the heart and blood vessels. *J. Physiol. Lond.*, **3**:48-75, 1880.

Gérard, C., J.A. Boudier, J. Mauchamp, and B. Verrier. Evidence for probenecid-sensitive organic anion transporters on polarized thyroid cells in culture. *J. Cell. Physiol.*, **144**:354:364, 1990.

Giles, W.R., and Y. Imaizumi. Comparison of potassium currents in rabbit atrial and ventricular cells. *J. Physiol.*, **405**:123-145, 1988.

Goegelein, H., and R. Greger. Na^+ selective channels in the apical membrane of rabbit proximal tubules (Pars Recta). *Pflügers Arch.*, **406**:198-203, 1986.

Goldstein, O., C. Asher, P. Barbry, E. Cragoe, W. Clauss, and H. Garty. An epithelial high-affinity amiloride-binding site, different from the Na^+ channel. *J. Biochem.*, **268**:7856-7862, 1993.

Guia A., and R. Bose. Effects of extracellular acidosis on the action of smooth muscle relaxants. *Proc. West. Pharmacol. Soc.*, **33**:77-84, 1990.

Guia A., and R. Bose. Simultaneous measurement of cytosolic pH and isometric tension in canine trabeculae: effect of inotropes. *FASEB J.*, 7:A326, 1993.

Guia, A., N. Leblanc, E.J. Cragoe, and R. Bose. Effects of phenamil on potassium channels of guinea-pig ventricular myocytes. *Biophys. J.*, **61**:306a, 1992.

Guia, A., N. Leblanc, and R. Bose. Effects of phenamil on potassium channels and calcium channels of guinea-pig ventricular myocytes. *J. Pharmacol. Exper. Ther.*, **274**:649-656, 1995.

Guiramand, J., M. Vignes, E. Mayat, F. Lebrun, I. Sassetti, and M. Recasens. A specific transduction mechanism for the glutamate action on phosphoinositide metabolism via the quisqualate metabotropic receptor in rat brain synaptoneurosomes: I. External Na+ requirement. *J. Neurochem.*, **57**:1488-500, 1991.

Haddy, F.J., M.B. Pamnani, B.T. Swindall, J. Johnston and E.J. Cragoe. Sodium channel blockers are vasodilators as well as natriuretic and diuretic agents. *Hypertension*, 7(suppl.I):I121-I126, 1985.

Hamill, O.P., A. Marty, E. Neher, B. Sakmann, and F.J. Sigworth. Improved patch clamp techniques for high-resolution current recording from cells and cell-free membrane patches. *Pflügers Arch.*, **391**:85-100, 1981.

Harrison, S.M., and M.K. Lancaster. The effects of NiCl on intracellular Ca^{2+}, Na^{+}, and H^{+}, during metabolic inhibition in rat ventricular cells. *Biophys. J.*, **66**:A95, 1994.

Harvey, R.D., and R.E. Ten Eick. On the role of sodium ions in the regulation of the inward rectifying potassium conductance in cat ventricular myocytes. *J. Gen. Physiol.*, **94**:329-348, 1989a.

Harvey, R.D., and R.E. Ten Eick. Voltage-dependent block of cardiac inward-rectifying potassium current by monovalent cations. *J. Gen. Physiol.*, **94**:349-361, 1989b.

Hayashi, H., H. Miyata, N. Noda, A. Kobayashi, M. Hirano, T. Kawai, and N. Yamazaki. Intracellular Ca^{2+} concentration and pH_i during metabolic inhibition. *Am. J. Physiol.*, **262**:C628-C634, 1992.

Hearse, D.J. The protection of the ischemic myocardium: surgical success v clinical failure? *Prog. Cardiovasc. Dis.*, **30**:381-402, 1988.

Henkin, J. Aerosolized amiloride for the treatment of lung disease in Cystic Fibrosis. N. Eng. J. Med., 323:997, 1990.

Hilgemann, D.W. Discrete stimulation of inotropic actions of ryanodine on guinea pig atrium in terms of a refined "one-way" model of E/C coupling. *J. Mol. Cell. Cardiol.*, **14**(suppl.1):39, 1982.

Hille, B. Ionic channels of excitable membranes. Pub. Sinauer Associates Inc., Sunderland, Massachusetts, 1992. pp. 1-82.

Hoey, H., G.J. Amos, and U. Ravens. Comparison of the action potential prolonging and positive inotropic activity of DPI 201-106 and BDF 9148 in human ventricular myocardium. *J. Mol. Cell. Cardiol.*, **26**:985-994, 1994.

Horisberger, J.D., C.M. Canessa and B.C. Rossier. The epithelial sodium channel: recent developments. *Cell. Physiol. Biochem.*, **3**:283-294, 1993.

Hryshko, L.V., and D.M. Bers. Ca current facilitation during post-rest recovery depends on Ca entry. *Am. J. Physiol.*, **259**:H951-H961, 1990.

Hryshko, L.V., R. Bouchard, T. Chau, and D. Bose. Inhibition of rest potentiation in canine ventricular muscle by BAY K 8644: Comparison with caffeine. *Am. J. Physiol.*, **257**:H399-H406, 1989.

Hullin, R., D. Singer-Lahat, M. Freichel, M. Biel, N. Dascal, F. Hofmann, and V. Flockerzi. Calcium channel beta subunit heterogeneity: functional expression of cloned cDNA from heart, aorta and brain. *EMBO J.*, **11**:885-890, 1992.

Hume, J.R. "Properties of myocardial K^+ channels and their pharmacological modulation." **In** Molecular and Cellular Mechanisms of Antiarrhythmic Agents. Ed..: Luc Hondeghem, Futura Publishing Co., Inc., pp 113-131, 1989.

Hume, J.R. and A. Uehara. Ionic basis of the different action potential configurations of single guinea-pig atrial and ventricular myocytes. *J. Physiol. Lond.*, **368**:525-544, 1985.

Hume, J.R., A. Uehara, R.W. Hadley, and R.D. Harvey. "Comparison of K^+ channels in mammalian atrial and ventricular myocytes." **In** Potassium channels, basic functions and therapeutic aspects. Ed.: Thomas J. Colatski, Wiley-Liss, New York, 1990, p 17.

Iafrate, R.P., K.L. Massey, and L. Mendeles. Current concepts in clinical and therapeutics: Asthma. *Clin. Pharmacy*, **5**:206-227, 1986.

Illingworth, J.A. A common source of error in pH measurements. *Biochem. J.*, **195**:259-262, 1981.

Imai, S., A-Y Shi, T. Ishibashi, and M. Nakazawa. Na^+/H^+ exchange is not operative under low-flow ischemic conditions. *J. Mol. Cell. Cardiol.*, **23**:505-517, 1991.

Irisawa, H., and R. Sato. Intra- and extracellular actions of proton on the calcium current of isolated guinea pig ventricular cells. *Circ. Res.*, **59**:348-355, 1986.

Ishizaka, K. Cellular events in the IgE antibody response. *Adv. Immunol.*, **23**:1-75, 1976.

James-Kracke, M.R. Quick and accurate method to convert BCECF fluorescence to pH_i: calibration in three different types of cell preparations. *J. Cell. Physiol.*, **151**:596-603, 1992.

Josephson, I.R., J. Sanchez-Chapula, and A.M. Brown. Early outward current in rat single ventricular cells. *Circ. Res.*, **54**:157-162, 1984.

Kaila, K., and R.D. Vaughan-Jones. Influence of sodium-hydrogen exchange on intracellular pH, sodium and tension in sheep cardiac Purkinje fibers. *J. Physiol.*, **390**:93-118, 1987.

Kaila, K., R.D. Vaughan-Jones, and C. Bountra. Regulation of intracellular pH in sheep cardiac Purkinje fiber: interactions among Na^+, H^+, and Ca^{2+}. *Can. J. Physiol. Pharmacol.*, **65**:963-969, 1987.

Karmazyn, M. Amiloride enhances postischemic ventricular recovery: possible role of Na^+-H^+ exchange. *Am. J. Physiol.*, **255**:H608-H615, 1988.

Kass, R.S., and M.C. Sanguinetti. Inactivation of calcium channel current in the calf cardiac purkinje fiber, evidence for voltage- and calcium-mediated mechanisms. *J. Gen. Physiol.*, **84**:705-726, 1984.

Katz, A. Physiology of the Heart. Raven Press, New York, 1977, p. 179.

Kennedy, R.H., J.R. Berlin, Y. Ng, T. Akera, and T.M. Brody. Amiloride: Effects on myocardial force of contraction, sodium pump, and Na^+/Ca^{2+} exchange. *J. Mol. Cell. Cardiol.*, **18**:177-188, 1986.

Kepron, W., J.M. James, B. Kirk, A.H. Sehon and K.S. Tse. A canine model for reaginic hypersensitivity and allergic bronchoconstriction. *J. Allergy Clin. Immunol.*, **59**:64-69, 1977.

Kerrick, W.G.L., D.A. Malencik, P.E. Hoar, J.D. Potter, R.L. Coby, S. Pocinwong, and E.H. Fischer. Ca^{2+} and Sr^{2+} activation: comparison of cardiac skeletal muscle contraction models. *Pflügers Arch.*, **386**:207-213, 1980.

Kijima, Y., E. Ogunbunmi, and S. Fleischer. Drug action of thapsigargin on the Ca^{2+} pump protein of sarcoplasmic reticulum. *J. Biol. Chem.*, **266**:22912-22918, 1991.

Kimura, M., K. Nakamura, J.W. Fenton, T.T. Andersen, J.P. Reeves, and A. Aviv. Role of external Na^+ and cytosolic pH in agonist-evoked cytosolic Ca^{2+} response in human platelets. *Am. J. Physiol.*, **267**:C1543-C1552, 1994.

King, B.W., and D. Bose. Mechanism of biphasic contractions in strontium-treated ventricular muscle. *Circ. Res.*, **52**:65-75, 1983.

King, B.W., Thesis: Contraction Patterns of Mammalian Myocardium: Influence of Strontium on Excitation-Contraction Coupling. University of Manitoba, Winnipeg, Manitoba, Canada, 1982.

Kleyman, T.R. and E.J. Cragoe. Amiloride and its analogs as tools in the study of ion transport. *J. Memb. Biol.*, **105**:1-21, 1988.

Knowles, M.R., N.L. Church, W.E. Waltner, J.R. Yankaskas, P. Gilligan, M. King, L.J. Edwards, R.W. Helms, and R.C. Boucher. Aerosolized amiloride for the treatment of lung disease in Cystic Fibrosis - Reply. N. Eng. J. Med., 323:997-998, 1990.

Kohmoto, O., K.W. Spitzer, M.A. Movsesian, and W.H. Barry. Effects of intracellular acidosis on $[Ca^{2+}]_i$ transients, transsarcolemmal Ca^{2+} fluxes, and contraction in ventricular myocytes. *Circ. Res.*, **66**:622-632, 1990.

Korn, S.J., and R. Horn. Influence of sodium-calcium exchange on calcium current rundown and the duration of calcium-dependent chloride currents in pituitary cells, studied with whole cell and perforated patch recording. *J. Gen. Physiol.*, **94**:789-812, 1989.

Krampetz, I., and R. Bose. Relaxant effect of amiloride on canine tracheal smooth muscle. *J. Pharmacol. Exp. Ther.*, **246**:641-648, 1988.

Krampetz, I., and R. Bose. Amiloride: a diuretic with bronchodilatory properties. *Clin. Invest. Med.*, **10**:B120, 1987.

Kraut, R.P., R. Bose, E.J. Cragoe, and A.H. Greenberg. The Na^+/Ca^{2+} exchanger regulates cytolysin/perforin-induced increases in intracellular Ca^{2+} and susceptibility to cytolysis. *J. Immunol.*, **148**:2489-2496, 1992.

Kraut, R.P., A.H. Greenberg, E.J. Cragoe, and R. Bose. Pyrazine compounds and the measurement of cytosolic Ca^{2+}. *Anal. Biochem.*, **214**:413-419, 1993.

Kubo, Y., T.J. Baldwin, Y.N. Jan, and L.Y. Jan. Primary structure and functional expression of a mouse inward rectifier potassium channel. *Nature*, **362**:127-133, 1993.

Lazdunski, M., C. Frelin, and P. Vigne. The sodium/hydrogen exchange system in cardiac cells: its biochemical and pharmacological properties and its role in regulating internal concentrations of sodium and internal pH. *J. Mol. Cell. Cardiol.*, **17**:1029-1042, 1985.

Leblanc, N., and J.R. Hume. Sodium current-induced release of calcium from cardiac sarcoplasmic reticulum. *Science*, **248**:372-376, 1990.

Lederer, W.J., E. Niggli, and R.W. Hadley. Sodium-calcium exchange in excitable cells: fuzzy space. *Science*, **248**:383, 1990.

Levesque, P.C., N. Leblanc, and J.R. Hume. Release of calcium from guinea pig cardiac sarcoplasmic reticulum induced by sodium-calcium exchange. *Cardiovasc. Res.*, **28**:370-378, 1994.

Levesque, P.C., N. Leblanc, and J.R. Hume. Role of reverse-mode Na^{+}-Ca^{2+} exchange in excitation-contraction coupling in the heart. *Ann. N.Y. Acad. Sci.*, **639**:386-397, 1991.

Lingueglia, E., S. Renard, N. Voilley, R. Waldmann, O. Chassande, M. Lazdunski, and P. Barbry. Molecular cloning and functional expression of different molecular forms of rat amiloride-binding proteins. *Eur. J. Biochem.*, **216**:679-687, 1993.

Lipp, P., and E. Niggli. Sodium current-induced calcium signals in isolated guinea-pig ventricular myocytes. *J. Physiol.*, **474**:439-446, 1994.

López-López, J.R., P.S. Shacklock, C.W. Balke, and W.G. Wier. Local calcium transients triggered by single L-type calcium channel currents in cardiac cells. *Science*, **268**:1042-1045, 1995.

Lukas, A., and C. Antzelevitch. Differences in the electrophysiological response of canine ventricular epicardium and endocardium to ischemia, role of the transient outward current. *Circulation*, **88**:2903-2915, 1993.

MacLeod, K.T., and S.E. Harding. Effects of phorbol ester on contraction, intracellular pH and intracellular Ca^{2+} in isolated mammalian ventricular myocytes. *J. Physiol.*, **444**:481-498, 1991.

Martin, C.L., and K. Chinn. Contribution of delayed rectifier and inward rectifier to repolarization of the action potential: pharmacologic separation. *J. Cardiovasc. Pharmacol.*, **19**:830-837, 1992.

Martin, R.L., S. Koumi, and R.E. Ten Eick. Comparison of the effects of internal $[Mg^{2+}]$ on I_{K1} in cat and guinea pig cardiac ventricular myocytes. *J. Mol. Cell. Cardiol.*, **27**:673-691, 1995.

Matsuda, H. Effects of intracellular calcium injection on steady-state membrane currents in isolated ventricular cells. *Pflügers Arch.*, **397**:81-83, 1983.

Matsuda, H. Open-state substructure of inwardly rectifying potassium channels revealed by magnesium block in guinea-pig heart cells. *J. Physiol.*, **397**:237-258, 1988.

Matsuura, H., T. Ehara, and Y. Imoto. An analysis of the delayed outward current in single ventricular cells of the guinea-pig. *Pflügers Arch.*, **410**:596-603, 1987.

McCord, J.M. Oxygen-derived free radicals in postischemic tissue injury. *N. Eng. J. Med.*, **312**:159-163, 1985.

Meng, H-P, and G.N. Pierce. Protective effects of 5-(N,N-dimethyl)amiloride on ischemia-reperfusion injury in hearts. *Am. J. Physiol.*, **258**:H1615-H1619, 1990.

Merot, J., M. Bidet, B. Gachot, S. le Maout, N. Koechlin, M. Tauc, and P. Poujeol. Electrical properties of rabbit early distal convoluted tubule in primary culture. *Am. J. Physiol.*, **257**:F288-F299, 1989.

Mitra, R., and M. Morad. Two types of calcium channels in guinea pig ventricular myocytes. *Proc. Natl. Acad. Sci.*, **83**:5340-5344, 1986.

Mohabir, R., H-C. Lee, R.W. Kurz, and W.T. Clusin. Effects of ischemia and hypercarbic acidosis on myocyte calcium transients, contraction, and pH_i in perfused rabbit hearts. *Circ. Res.*, **69**:1525-1537, 1991.

Moody, W.J., and S. Hagiwara. Block of inward rectifications by intracellular H^+ in immature oocytes of the starfish Mediaster aequalis. *J. Gen. Physiol.*, **79**:115-130, 1982.

Murphy, E., M. Perlman, R.E. London, and C. Steenbergen. Amiloride delays the ischemia-induced rise in cytosolic free calcium. *Circ. Res.*, **68**:1250-1258, 1991.

Noël, J., A. Tejedor, P. Vinay, and R. Laprade. Fluorescence measurement of intracellular pH on proximal tubule suspensions, the need for a BCECF sink. *Renal Physiol. Biochem.*, **12**:371-387, 1989.

Novotny, W.F., O. Chassande, M. Baker, M. Lazdunski, and P. Barbry. Diamine oxidase is the amiloride-binding protein and is inhibited by amiloride analogues. *J. Biochem.*, **269**:9921-9925, 1994.

O'Brodovich, H., V. Hannam, and B. Rafii. Sodium channel but neither Na^+-H^+ nor Na-glucose symport inhibitors slow neonatal lung water clearance. *Am. J. Respir. Cell. Mol. Biol.*, **5**:377-384, 1991.

Oh, Y.S., and D.J. Benos. Single-channel characteristics of a purified bovine renal amiloride-sensitive Na^+ channel in planar lipid bilayers. *Am. J. Physiol.*, **264**:C1489-C1499, 1993.

Orchard, C.H., and J.C. Kentish. Effects of changes of pH on the contractile function of cardiac muscle. *Am. J. Physiol.*, **258**:C967-C981, 1990.

Palmer, L.G. Epithelial Na channel: function and diversity. *Annu. Rev. Physiol.*, **54**:51-66, 1992.

Parenti, P., P. Ferrari, M. Ferrandi, G.M. Hanozeta, and G. Bianchi. Effect of amiloride analogues on sodium transport in renal brush border membrane vesicles from Milan hypertensive rats. *Biochem. Biophys. Res. Communic.*, **183**:55-61, 1992.

Pierce, G.N., W.C. Cole, K. Liu, H. Massaeli, T.G. Maddaford, Y.J. Chen, C.D. McPherson, S. Jain, and D. Sontag. Modulation of cardiac performance by amiloride and several selected derivatives of amiloride. *J. Pharmacol. Exp. Ther.*, **265**:1-12, 1993.

Pinon, J.F. and J. Fabre. Inhibition of potassium-induced contracture of the isolated rat aorta by amiloride. *Arzneim.-Forsch./Drug Res.*, **35**:421-423, 1985.

Pousti, A., and M.A. Khoyi. Effect of amiloride on isolated guinea-pig atrium. *Arch. Int. Pharmacodyn.*, **242**:222-229, 1979.

Putnam, R.W., and R.D. Grubbs. Steady-state pH_i, buffering power, and effect of CO_2 in a smooth muscle-like cell line. *Am. J. Physiol.*, **258**:C461-C469, 1990.

Rabkin, S.W. Comparison of the effect of amiloride and its analogue dichlorobenzamil on cardiac chronotropic responses to ouabain in myocardial cell aggregates in culture. *Pharmacol.*, **39**:230-239, 1989.

Raijman, I., E. Cragoe, and J. Sellin. Hormonal and pharmacologic regulation of sodium absorption in rabbit cecum *in vitro*. *Dig. Dis. Sci.*, **37**:1874-1881, 1992.

Reers, M., R.A. Kelly, and T.W. Smith. Calcium and proton activities in rat cardiac mitochondria: effect of matrix environment on behavior of fluorescent probes. *Biochem. J.*, **257**:131-142, 1989.

Reeves, J.P., and C.C. Hale. The stoichiometry of the cardiac sodium-calcium exchange system. *J. Biol. Chem.*, **259**:7733-7739, 1984.

Reuter, H. Properties of two inward membrane currents in the heart. *Ann. Rev. Physiol.*, **41**:413-424, 1979.

Rink, T.J., R.Y. Tsien, and T. Pozzan. Cytoplasmic pH and free Mg^{2+} in lymphocytes. *J. Cell Biol.*, **95**:189-196, 1982.

Robinson, H.K., S.E. Webber and J.G. Widdicombe. Electrolyte and other chemical concentrations in tracheal airway surface liquid and mucus. *J. Appl. Physiol.*, **66**:2129-2135, 1989.

Rosoff, D.M., "Phorbol esters and the regulation of sodium/hydrogen exchange" **in** Sodium/Hydrogen Exchange. S. Grinstein (ed.), CRC Press, Boca Raton, Florida, U.S.A., 1988. Pp. 235-242.

Rossier, B.C., C.M. Canessa, L. Schild, and J.D. Horisberger. Epithelial sodium channels. *Cur. Opin. Nephrol. Hypertens.*, **3**:487-496, 1994.

Rousseau, E., and J. Pinkos. PH modulates conducting and gating behaviour of single calcium release channels. *Pflügers Arch.*, **415**:645-647, 1990.

Ruiz-Petrich, E., and N. Leblanc. The mechanism of the rate-dependent changes of the conducted action potential in rabbit ventricle. *Can. J. Physiol. Pharmacol.*, **67**:780-787, 1989.

Sakmann, B., and G. Trube. Conductance properties of single inwardly rectifying potassium channels in ventricular cells from guinea-pig heart. *J. Physiol.*, **347**:641-657, 1984.

Sanguinetti, M.C., and N.K Jurkiewicz. Two components of cardiac delayed rectifier K^+ current: differential sensitivity to block by class III antiarrhythmic agents. *J. Gen. Physiol.*, **96**:195-215, 1990.

Sariban-Sohraby, S., and D.J. Benos. Detergent solubilization, functional reconstitution and partial purification of epithelial amiloride-binding protein. *Biochem.*, **25**:4639-4646, 1986.

Satoh, H., and K. Hashimoto. An electrophysiological study of amiloride on sino-atrial node cells and ventricular muscle of rabbit and dog. *Naunyn-Schmied. Arch. Pharmacol.*, **333**:83-90, 1986.

Schiffman, S.S., A.E. Frey, M.S. Suggs, E.J. Cragoe, and R.P. Erickson. The effect of amiloride analogs on taste responses in gerbil. *Physiol. Behav.*, **47**:435-441, 1990.

Schouten, V.J., H.E. ter Keurs. The slow repolarization phase of the action potential in rat heart. *J. Physiol. Lond.*, **360**:13-25, 1985.

Schouten, J.V., J.K. van Deen, P. de Tombe, and A.A. Verveen. Force-interval relationship in heart muscle of mammals, a calcium compartment model. *Biophys. J.*, **51**:13-26, 1987.

Seller, R.H., J. Greco, S. Banach, and R. Seth. Increasing the inotropic effect and toxic dose of digitalis by the administration of antikaliuretic drugs-further evidence for a cardiac effect of diuretic agents. *Am. Heart J.*, **90**:56-67, 1975.

Sellin, J.H., and W.P. Dubinsky. Apical nonspecific cation conductances in rabbit cecum. *Am. J. Physiol.*, **266**:G475-G484, 1994.

Sellin, J.H., H. Oyarzabal, E.J. Cragoe, and G.D. Potter. Phenamil inhibits electrogenic sodium absorption in rabbit ileum. *Gastroenterology*, **96**:997-1003, 1989.

Sham, J.S., L. Cleemann, and M. Morad. Gating of the cardiac Ca^{2+} release channel: the role of Na^{+} current and Na^{+}-Ca^{2+} exchange. Science, 255:850-853, 1992.

Shattock, M.J., and D.M. Bers. Rat vs. Rabbit ventricle: Ca^{2+} flux and intracellular Na^{+} assessed by ion-selective microelectrodes. *Am. J. Physiol.*, **256**:C813-C822, 1989.

Shi, A., Z.L. Wang, C.Y. Kwan, and E.E. Daniel. Inhibitory effects of amiloride on alpha adrenoceptors in canine vascular smooth muscle. *J. Pharmacol. Exp. Ther.*, **253**:791-797, 1990.

Shimoni, Y., R.B. Clark, and W.R. Giles. Role of an inwardly rectifying potassium current in rabbit ventricular action potential. *J. Physiol.*, **448**:709-727, 1992.

Shimoni, Y., and D.L. Severson. Thyroid status and potassium currents in rat ventricular myocytes. *Am. J. Physiol.*, **268**:H576-H583, 1995.

Siegl, P.K.S., E.J. Cragoe, M.J. Trumble, and G.J. Kaczorowski. Inhibition of Na^+/Ca^{2+} exchange in membrane vesicle and papillary muscle preparations from guinea pig heart by analogs of amiloride. *Proc. Natl. Acad. Sci.*, **81**:3238-3242, 1984.

Skou, J.C., and M. Esmann. The Na,K-ATPase. *J. Bioenerg. Biomembr.*, **24**:249-261, 1992.

Smith, P.R., and D.J. Benos. Epithelial Na^+ channels. *Annu. Rev. Physiol.*, **53**:509-530, 1991.

Smith, R.L., I.G. Macara, R. Levenson, D. Housman, and L. Cantley. Evidence that a Na^+/Ca^{2+} antiport system regulates murine erythroleukemia cell differentiation. *J. Biochem.*, **257**:773-780, 1982.

Soltoff, S.P., and L.J. Mandel. Amiloride directly inhibits the Na, K-ATPase activity of rabbit kidney proximal tubules. *Science*, **220**:957-959, 1983

Souhrada, M. and J.F. Souhrada. Specific reaginic antibody IgG_1-induced changes of airway smooth muscle cells. *J. Appl. Physiol.*, **65**:767-775, 1988.

Souhrada, M., M.H. Souhrada and J.F. Souhrada. The inhibition of sodium influx attenuates airway response to a specific antigen challenge. *Br. J. Pharmacol.*, **93**:884-892, 1988.

Spurgeon, H.A., M.D. Stern, G. Baartz, S. Raffaeli, R.G. Hansford, A. Talo, E.G. Lakatta, and M.C. Capogrossi. Simultaneous measurement of Ca^{2+}, contraction and potential in cardiac myocytes. *Am. J. Physiol.*, **258**:H574-H586, 1990.

Stjarne, L., J. Bao, F.G. Gonon, C. Mermet, M. Msghina, E. Stjarne, and P. Astrand. Presynaptic receptors and modulation of noradrenaline and ATP secretion from sympathetic nerve varicosities. *Ann. NY Acad. Sci.*, **604**:250-265, 1990.

Stuart-Smith, K. and P.M. Vanhoutte: Heterogeneity in the effects of epithelium removal in the canine bronchial tree. *J. Appl. Physiol.*, **63**:2510-2515, 1987.

Stühmer, W., F. Conti, H. Suzuki, X.D. Wang, M. Noda, N. Yahagi, H. Kubo, and S. Numa. Structural parts involved in activation and inactivation of the sodium channel. *Nature*, **339**:597-603, 1989.

Stys, P.K., S.G. Waxman, and B.R. Ransom. Na(+)-Ca2+ exchanger mediates Ca2+ influx during anoxia in mammalian central nervous system white matter. *Ann. Neurol.*, **30**:375-80, 1991.

Surawicz, B. Role of potassium channels in cycle length dependent regulation of action potential duration in mammalian cardiac Purkinje and ventricular muscle fibers. *Cardiovasc. Res.*, **26**:1021-1029, 1992.

Takahashi, N., K. Morishige, A. Jahangir, M. Yamada, I. Findlay, H. Koyama, and Y. Kurachi. Molecular cloning and functional expression of cDNA encoding a second class of inward rectifier potassium channels in the mouse brain. *J. Biol. Chem.*, **269**:23274-23279, 1994.

Tande, P.M., E. Mortensen, and H. Refsum. Rate-dependent differences in dog epi- and endocardial monophasic action potential configuration *in vivo*. *Am. J. Physiol.*, **261**:H1387-H1391, 1991.

Tang, C.M., F. Presser, and M. Morad. Amiloride selectively blocks the low threshold (T) calcium channel. *Science*, **240**: 213-215, 1988.

Thomas, J.A., R.N. Buchsbaum, A. Zimniak, and E. Racker. Intracellular pH measurements in Ehrlich Ascites tumor cells using spectroscopic probes generated in situ. *Biochemistry*, **18**:2210-2218, 1979.

Tohse, N. Calcium-sensitive delayed rectifier potassium current in guinea pig ventricular cells. *Am. J. Physiol.*, **258**:H1200-H1207, 1990.

Trautwein, W. Membrane currents in cardiac fibres. *Physiol. Rev.*, **5**:793-835, 1973.

Tytgat, J., J. Vereecke, and E. Carmeliet. Mechanism of cardiac T-type Ca^{2+} channel blockade by amiloride. *J. Pharmacol. Exp. Therap.*, **254**:546-551, 1990.

Valera, S., N. Hussy, R.J. Evans, N. Adami, R.A. North, A. Surprenant, and G. Buell. A new class of ligand-gated ion channel defined by P2X receptor for extracellular ATP. *Nature*, **371**:516-519, 1994.

Van Renterghem, C., and M. Lazdunski. A new non-voltage-dependent, epithelial-like Na^+ channel in vascular smooth muscle cells. *Pflügers Arch.*, **419**:401-408, 1991.

Vanhoutte, P.M. Epithelium-derived relaxing factor(s) and bronchial reactivity. *J. Allergy Clin. Immunol.*, **83**:855-861, 1989.

Vassalle, M., J. Karis, and B.F. Hoffman. Toxic effects of ouabain on Purkinje fibers and ventricular muscle fibers. *Am. J. Physiol.*, **203**:433-439, 1962.

Vaughan-Jones, R.D., and M-L Wu. Extracellular H^+ inactivation of Na^+-H^+ exchange in the sheep cardiac Purkinje fiber. *J. Physiol.*, **428**:441-466, 1990.

Vaughan-Jones, R.D., D.A. Eisner, and W.J. Lederer. Effects of changes of intracellular pH on contraction in sheep cardiac Purkinje fibers. *J. Gen. Physiol.*, **89**:1015-1032, 1987.

Vaughan-Williams, E.M. A classification of antiarrhythmic actions reassessed after a decade of new drugs. *J. Clin. Pharmacol.*, **24**:129-147, 1984.

Verrier, B., G. Champigny, P. Barbry, C. Gerard, J. Mauchamp, and M. Lazdunski. Identification and properties of a novel type of Na^+-permeable amiloride-sensitive channel in thyroid cells. *Eur. J. Biochem.*, **183**:499-505, 1989.

Vigne, P., G. Champigny, R. Marsault, P. Barbry, C. Frelin, and M. Lazdunski. A new type of amiloride-sensitive cationic channel in endothelial cells of brain microvessels. *J. Biochem.*, **264**:7663-7668, 1989.

Voilley, N., E. Lingueglia, G. Champigny, M.G. Mattéi, R. Waldmann, M. Lazdunski, and P. Barbry. The lung amiloride-sensitive Na^+ channel: Biophysical properties, pharmacology, ontogenesis, and molecular cloning. *Proc. Nat. Acad. Sci.*, **91**:247-251, 1994.

Wahler, G.M., S.J. Dollinger, J.M. Smith, and K.L. Flemal. Time course of postnatal changes in rat heart action potential and in transient outward current is different. *Am. J. Physiol.*, **267**:H1157-H1166, 1994.

Waldorff, S., P.B. Hansen, H. Kjærgård, J. Buch, H. Egeblad, and E. Steiness. Amiloride-induced changes in digoxin dynamics and kinetics: abolition of digoxin-induced inotropism with amiloride. *Clin. Pharmacol. Ther.*, **30**:172-176, 1981.

Wallert, M.A. and O. Frohlich. Na^+-H^+ exchange in isolated myocytes from adult rat heart. *Am. J. Physiol.*, **257**:C207-C213, 1989.

Walker, K.E., E.G. Lakatta, and S.R. Houser. Age associated changes in membrane currents in rat ventricular myocytes. *Cardiovasc. Res.*, **27**:1968-1977, 1993.

Waltner, W.E., R.C. Boucher, J.T. Gatzy and M.R. Knowles. Pharmacotherapy of airway disease in cystic fibrosis. *Trends in Pharmacol. Sci.*, **8**:316-320, 1987.

Wang, Z.G., B. Fermini, and S. Nattel. Repolarization differences between guinea pig atrial endocardium and epicardium: evidence for a role of I_{to}. *Am. J. Physiol.*, **260**:H1501-H1506, 1991.

Wang, Z., B. Fermini, and S. Nattel. Mechanism of flecainide's rate-dependent actions on action potential duration in canine atrial tissue. *J. Pharmacol. Exp. Ther.*, **267**:575-581, 1993.

Weiner, I.M., and G.H. Mudge. "Diuretics and other agents employed in the mobilization of edema fluid." **In** The Pharmacological Basis of Therapeutics, 7th ed., ed.: A. Goodman Gilman, L.S. Goodman, T.W. Rall, and F. Murad, McMillan Publishing Co., New York, 1985, pp 887-907.

Wendt, I.R., and D.G. Stephenson. Effects of caffeine on Ca-activated force production in skinned cardiac and skeletal muscle fibres of the rat. *Pflügers Arch.*, **398**:210-216, 1983.

Wettwer, E., G. Amos, J. Gath, H.R. Zerkowski, J.C. Reidemeister, and U. Ravens. Transient outward current in human and rat ventricular myocytes. *Cardiovasc. Res.*, **27**:1662-1669, 1993.

Wible, B.A., M. deBiasi, K. Majumbder, M. Taglialatela, and A.M. Brown. Cloning and functional expression of an inwardly rectifying K^+ channel from human atrium. *Circ. Res.*, **76**:343-350, 1995.

Wier, W.G., and P. Hess. Excitation-contraction coupling in cardiac Purkinje Fibers: effects of cardiotonic steroids on the intracellular [Calcium2+] transient, membrane potential, and contraction. *J. Gen. Physiol.*, **83**:395-415, 1984.

Yamashita, S., s. Motomura, and N. Taira. Cardiac effects of amiloride in the dog. *J. Cardiovasc. Pharmacol.*, **3**:704-715, 1981.

Yap, A.S., J.W. Armstrong, E.J. Cragoe, J.R. Bourke, G.J. Huxham, and S.W. Manley. Activation of sodium transport mediates regulation of thyroid follicle volume in response to hypotonic media. *Am. J. Physiol.*, **264**:E644-E649, 1993.

Yu, J., A. Guia, R. Bose, S. Mink, W. Kepron and E.J. Cragoe. Sodium role in antigen-induced contraction of tracheal smooth muscle in dogs. *FASEB J.*, 1990.

Yu, J., E.J. Cragoe and R. Bose. Excitation-contraction coupling in tracheal smooth muscle studied with specific inhibitors of Na^+ channel and Na^+-H^+ antiporter. *The Physiologist*, **32**:189, 1989.

Yu, J., A. Guia, S. Mink, W. Kepron, E.J. Cragoe, S. Sharma, and R. Bose. Role of sodium in antigen-induced contraction of tracheal smooth muscle in dogs. *Resp. Physiol.*, **91**:111-24, 1993.

Yu, J., J.J. Zheng, B.Y. Ong, and R. Bose. Intracellular pH measurement with fluorescent dye in canine basilar arteries. *Blood Vessels*, **28**:464-474, 1991.

Zhou, H., S.S. Tate, L.G. Palmer. Primary structure and functional properties of an epithelial K channel. *Am. J. Physiol.*, **266**:C809-824, 1994.